IZMIR KATIP CELEBI UNIVERSITY
GRADUATE SCHOOL OF NATURAL AND APPLIED
SCIENCES

SURFACE MODIFICATION OF MICRONIZED QUARTZ
POWDERS AND INVESTIGATION OF ADDITIVES AS FILLING
MATERIAL IN POLYMER MATRIX COMPOSITE MATERIALS

PhD THESIS
Orhan AKYÜZ

Department of Materials Science and Engineering

Thesis Advisor: Prof.Dr. Şerafettin DEMİÇ

JULY 2020

IZMIR KATIP CELEBI UNIVERSITY

GRADUATE SCHOOL OF NATURAL AND APPLIED SCIENCES

SURFACE MODIFICATION OF MICRONIZED QUARTZ POWDERS AND INVESTIGATION OF ADDITIVES AS FILLING MATERIAL IN POLYMER MATRIX COMPOSITE MATERIALS

PhD THESIS

Orhan AKYÜZ

(D130111004)

0000-0003-3490-5695

Department of Materials Science and Engineering

Thesis Advisor: Prof.Dr. Şerafettin DEMİÇ

JULY 2020

İZMİR KATİP CELEBİ ÜNİVERSİTESİ
FEN BİLİMLERİ ENSTİTÜSÜ

MİKRONİZE KUVARS TOZLARININ YÜZEY MODİFİKASYONUNUN YAPILMASI VE POLİMER MATRİSLİ KOMPOZİT MALZEMELERDE DOLGU MALZEMESİ OLARAK İNCELENMESİ

DOKTORA TEZİ

Orhan AKYÜZ

(D130111004)

0000-0003-3490-5695

Malzeme Bilimi ve Mühendisliği Ana Bilim Dalı

Tez Danışmanı: Prof. Dr. Şerafettin DEMİÇ

TEMMUZ 2020

Orhan AKYÜZ, a **PhD** student of **IKCU Graduate School Of Natural And Applied Sciences,** successfully defended the thesis entitled **"SURFACE MODIFICATION OF MICRONIZED QUARTZ POWDERS AND INVESTIGATION OF ADDITIVES AS FILLING MATERIAL IN POLYMER MATRIX COMPOSITE MATERIALS",** which he prepared after fulfilling the requirements specified in the associated legislations, before the jury whose signatures are below.

Thesis Advisor :

        Prof. Dr. Şerafettin DEMİÇ

        İzmir Kâtip Çelebi University

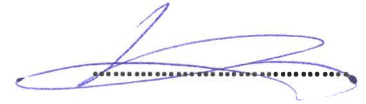**Jury Members :**

        Assoc. Prof. Dr. Mücahit SÜTÇÜ

        İzmir Kâtip Çelebi University
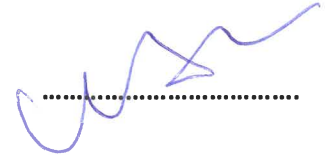
        Assoc. Prof. Dr. Cem TOZLU

        İzmir Kâtip Çelebi University

        Assoc. Prof. Dr. Ayhan ORAL

        Çanakkale Onsekiz Mart University

        Assoc. Prof. Dr. Mustafa EROL

        Dokuz Eylül Universsity

Date of Submission   : **12.06.2020**
Date of Defense   : **16.07.2020**

To my family

FOREWORD

undergraduate education and postgraduate education life both scientifically and mentally and I have always seen their contributions to be a good scientist and felt his friendship.

July 2020   Orhan AKYÜZ

TABLE OF CONTENTS

LIST OF TABLES

LIST OF FIGURES

ABBREVIATIONS

PP	**:**	Polypropylene
MQ	**:**	Micronized Quartz
SQ	**:**	Silanized Quartz
SiC	**:**	Silicon Carbide
PMC	**:**	Polymer Matrix Composite
MMC	**:**	Metal Matrix Composite
CMC	**:**	Ceramic Matrix Composite
LDPE	**:**	Low-Density Polyethylene
HDPE	**:**	*High-Density Polyethylene*
PVC	**:**	Polyvinyl Chloride
PS	**:**	Polystyrene
SAN	**:**	Styrene Acrylonitrile
PTFE	**:**	Polytetrafluoroethylene
PET	**:**	Polyethylene Terephthalate
ABS	**:**	Acrylonitrile Butadiene Styrene
PBT	**:**	Polybutylene Terephthalate
PBS	**:**	Polybutylene Succinate
PLA	**:**	Polylactic Acid
PE	**:**	Polyethylene
EPDM	**:**	Ethylene-Propylene-Diene Rubber
VTMS	**:**	Vinyltrimethoxysilane
EVA	:	Ethylene vinyl acetate
LLDPE	**:**	Linear Low-Density Polyethylene
MA-PE	**:**	Maleic Anhydride Polyethylene
MA-PP	**:**	Maleic Anhydride Polypropylene
PA	**:**	Polyamide
bis-GMA	**:**	Bis-Phenol-A-Diglycidyldimethacrylate
FRC	**:**	Fiber-Reinforced Composite
CAG	**:**	Contact Angle Goniometry
PAA	**:**	Polyacrylic Acid
IGC	**:**	Inverse Gas Chromatography
SC1	**:**	Standard Cleaning Solution 1
HMDS	**:**	Hexamethyldisilazane
FA	**:**	Fly Ash
SLS	**:**	Sodium Lauryl Sulphate
PVA	**:**	Polyvinyl Alcohol
FR	**:**	Flame Retardancy

APP	:	Ammonium Persulfate
PER	:	Pentaerythritol
LOI	:	Limited Oxygen Index
CS	:	Carbon Steel
TEOS	:	Tetraethoxysilane
CE	:	Cyanate Esters
MPTS	:	γ- Methacryloxypropyltrimethoxysilane
CP/MAS NMR	:	Cross Polarization/Magic Angle Spinning Nuclear Magnetic Resonance
BMN	:	$Ba(Mg_{1/3}Nb_{2/3})O_3$
SBS	:	Shear Bond Strength
AO	:	Atomic Oxygen
CF	:	Carbon Fiber
EP	:	Epoxy
IFSS	:	Interface Shear Strength
SCA	:	Silane Coupling Agents
KH570	:	γ-(methacryloyloxy) propyltrimethoxysilane
HTs-P	:	$P_3O_{10}^{5-}$ pillared Mg/Al hydrotalcite
WOT	:	Rare-Earth Coupling Agent
APTES	:	γ-Aminopropyltriethoxysilane
ALK	:	Alkanolamide
RBDPS	:	Refined Bleached Deodorized PalmStearin
MFC	:	Microfibrillated Cellulose
SG-Si171	:	Vinyltrimethoxysilane
NDZ-311	:	Di(Dioctylpyrophosphato) Ethylene Titanate
HGM	:	Hollow Glass Microsphere
EDAX	:	Energy Dispersive X-Ray Spectroscopy
FE-SEM	:	Field Emission Scanning Electron Microscopy
SBR	:	Styrene-Butadiene Rubber
p-NS	:	Pristine Nanosilica
m-NS	:	Modified Nanosilica
WF	:	Wood Fiber
KH550	:	γ--Aminopropyl Triethoxy Silane
A171	:	Trimethoxy Vinyl Silane
DCP	:	Dicumyl Peroxide
PAN	:	Polyacrylonitrile
CF	:	Carbon Fiber
ILSS	:	Interlaminar Shear Strength
P-MQ	:	Micronized Quartz Powders
P-SQ	:	Silanized Quartz Powders
P-2287	:	COATOSIL- 2287 Modified Micronized Quartz Powders
P-MP200	:	COATOSIL-MP 200 Modified Micronized Quartz Powders
P-A187	:	SILQUEST A-187 Modified Micronized Quartz Powders
P-A110	:	VEMAB A-110 Modified Micronized Quartz Powders
MQ-PP	:	Micronized Quartz Added Polypropylene Matrix Composites
SQ-PP	:	Silanized Quartz Added Polypropylene Matrix Composites
10MQ	:	10% Micronized Quartz + 90% PP Composite

20MQ	**:** 20% Micronized Quartz + 80% PP Composite
30MQ	**:** 30% Micronized Quartz + 70% PP Composite
10SQ	**:** 10% Silanized Quartz + 90% PP Composite
20SQ	**:** 20% Silanized Quartz + 80% PP Composite
30SQ	**:** 30% Silanized Quartz + 70% PP Composite
40SQ	**:** 40% Silanized Quartz + 60% PP Composite
2287	**:** COATOSIL-2287 Modified 10% Quartz + 90% PP Composite
MP200	**:** COATOSIL-MP 200 Modified 10% Quartz + 90% PP Composite
A187	**:** SILQUEST A-187 Modified 10% Quartz + 90% PP Composite
A110	**:** VEMAB A-110 Modified 10% Quartz + 90% PP Composite
TGA	**:** Thermogravimetric Analysis
XRD	**:** X-Ray Diffraction
DMA	**:** Dynamic Mechanical Analysis
SEM	**:** Scanning Electron Microscopy
DSC	**:** Differential Scanning Calorimetry
XPS	**:** X-Ray Photoelectron Spectroscopy
FTIR	**:** Fourier Transformed Infrared Spectroscopy
TC	**:** Thermal Conductivity
Tg	**:** Glass Transition Temperature
Tm	**:** Melting Temperature
E″	**:** Storage Modulus
E′	**:** Loss Modulus
eV	**:** Electronvolt
ΔH_c	**:** Enthalpy Change
ΔH_m	**:** Enthalpy of Melting
X_c	**:** Percentage Crystallinity
T_c	**:** Crystallization Temperature
kV	**:** Kilovolt
cm	**:** Centimeter
MPa	**:** Mega Pascal
GPa	**:** Giga Pascal
mg	**:** Milligram
min	**:** Minute
°C	**:** Centigrade Celsius
mL	**:** Milliliter
rpm	**:** Return Per Minute
mm	**:** Millimeter
mK	**:** Millikelvin
W	**:** Watt
T_{Onset}	**:** Onset Temperature
ASTM	**:** American Society for Testing and Materials
pH	**:** Power of Hydrogen

SURFACE MODIFICATION OF MICRONIZED QUARTZ POWDERS AND INVESTIGATION OF ADDITIVES AS FILLING MATERIAL IN POLYMER MATRIX COMPOSITE MATERIALS

ABSTRACT

The interfacing compatibility of the matrix material with the filler material in composite materials is one of the most important factors affecting the performance of the composite. A wide variety of chemical methods are applied to increase the interfacial compatibility of the matrix material with the filler material. The most important of all is the surface modification technique, in which surface-active agents are used to reinforce the matrix-filler bond and where a chemical process is applied to the surface of the filler material.This technique is based on the chemical treatment of the filler material with surface active agents to increase the compatibility of the matrix-filler materials by forming chemical bond(s) between the matrix material and the filler as well as a physical strength in their interactions. In this study, micronized quartz (MQ) powders, in order to be used as filling material, were first modified with four different surface modification agents. Then, micronized quartz, commercially available as silanized quartz (SQ) and surface modified micronized quartz powders were mixed with Polypropylene (PP) being used as matrix material by high-speed thermokinetic mixer in order to produce composite materials. The effect of surface modification of filler material on the mechanical, viscoelastic, thermal and morphological properties of the produced polymer-based quartz added composite materials was investigated. Tensile and three point bending tests were performed on the universal mechanical testing machine to determine the mechanical properties of the produced composites. Viscoelastic behavior of composites were tested by dynamic mechanical analysis (DMA) system. Filling material-matrix interface compatibility of the produced materials was visualized by scanning electron microscopy (SEM) technique. Thermogravimetric analysis (TGA), differential scanning calorimetry (DSC) and thermal conductivity (TC) tests were performed to determine the thermal properties of composites. Fourier transform infrared spectroscopy (FTIR) was used to determine the bonding types and spectral properties of the produced composites.

As a result of these investigations, it is clear that addition of micronized quartz develops tensile modulus, thermal conductivity and viscoelastic properties of the

matrix material, PP. It was also observed that mechanical and thermal properties of samples are improved after the surface modification when compared to non-modified samples.

Keywords: Polymer Matrix Composites, Polypropylene, Quartz, Surface Modification, Mechanical Properties

MİKRONİZE KUVARS TOZLARININ YÜZEY MODİFİKASYONUNUN YAPILMASI VE POLİMER MATRİSLİ KOMPOZİT MALZEMELERDE DOLGU MALZEMESİ OLARAK İNCELENMESİ

ÖZET

Kompozit malzemelerin performansına etki eden en önemli etkenlerden birisi, dolgu ve matris malzemelerinin arayüzey uyumudur. Her iki malzemenin arayüzey uyumunu artırmak için çeşitli kimyasal yöntemler uygulanmaktadır. Bunların en başında matris-dolgu malzemesi bağını/etkileşimini güçlendirmek için yüzey aktif ajanların kullanıldığı ve dolgu malzemesinin yüzeyine kimyasal bir işlemin uygulandığı yüzey modifikasyon tekniğidir. Bu tekniğin temeli, yüzey aktif ajanlarla kimyasal işleme tabi tutulan dolgu malzemesi ile matris malzemesi arasında fiziksel bir bağ kuvvetinin yanında kimyasal bağ oluşturularak matris-dolgu malzemesi uyumunun artırılmasına dayanmaktadır. Bu çalışmada ilk olarak dolgu malzemesi olarak kullanılan mikronize kuvars (MQ) tozları, 4 farklı yüzey modifikasyon ajanı ile muamele edilerek yüzey modifikasyon işlemi yapılmıştır. Daha sonra mikronize kuvars, ticari olarak temin edilen silanize kuvars (SQ) ve yüzey modifikasyonu yapılmış mikronize kuvars tozları ve matris malzemesi (Polipropilen, PP) birlikte yüksek hızlı termokinetik karıştırıcı ile karıştırılarak kompozit malzeme üretimleri gerçekleştirilmiştir. Yüzey modifikasyonu işlemine tabi tutulan kuvars katkılandırmanın, üretilen polimer esaslı, kompozitlerin mekanik, viskoelastik, termal ve morfolojik özelliklerine olan etkisi incelenmiştir. Katkılandırma ile üretilen kompozitlerin mekanik özelliklerini belirlemek için mekanik test makinesinde çekme ve 3 nokta eğme testleri yapılmıştır. Bu kompozitlerin viskoelastik davranışları, dinamik mekanik analiz (DMA) sistemi ile test edilmiştir. Dolgu malzemesi-matris arayüzey uyumu taramalı elektron mikroskobu (SEM) tekniği ile görüntülenmiştir. Kompozitlerin termal özelliklerini belirlemek için termogravimetrik analiz (TGA), diferansiyel taramalı kalorimetri (DSC) ve termal iletkenlik (TC) testleri yapılmıştır.

Üretilen kompozitlerin kimyasal bağ ve spektroskopik özelliklerinin belirlenmesi için fourier dönüşümlü kızılötesi spektroskopisi (FTIR) tekniği kullanılmıştır.

İncelemeler sonucunda mikronize kuvars katkısının PP'nin çekme modulü, eğilme modülü, termal iletkenliği ve viskoelastik özellikleri geliştirdiği görülmüştür. Yüzey modifikasyonlu örneklerin modifikasyonsuz örneklerle karşılaştırıldığında mekanik ve termal özellikleri geliştirdiği görülmüştür.

Anahtar Kelimeler: Polimer Esaslı Kompozitler, Polipropilen, Kuvars, Yüzey Modifikasyonu, Mekanik Özellikler

1. INTRODUCTION

1.1 Definition and Properties of Composites

In today's world, the ever-evolving technology and the endless desires of people increase the demand for innovative materials. In this respect, composite materials seem to be one of the most preferred options as new materials due to their superior properties compared to traditional materials such as metal and wood [1-4].

A composite material is called a new type of material that has the desired properties by bringing together with the visible levels of materials at least two or more of the same or different groups within each other without dissolution, without atomic exchange and by combining the superior properties of materials in its components. Composite materials have many superior properties compared to other conventional materials [5-8].

The superior properties of composite materials are as follows;

1. High strength / density ratio

2. High stiffness / density ratio

3. High corrosion resistance

4. High wear resistance

5. High temperature resistance

6. High chemical resistance

7. Weather and UV Resistance

8. Good thermal conductivity

9. Very good electrical and thermal insulation

10. Lightness

11. Vibration absorption [7, 9, 10].

There are some disadvantages as well as advantages of composite materials depending on the production methods and materials used.

The disadvantages of composite materials are;

1. The ideal properties cannot always be obtained in relation to the quality of the production methods used when manufacturing composite materials. Different strength properties can be observed even for the same composite material,

2. Difficult to produce,

3. Difficulty in processing,

4. Many of the composite materials exhibit different resistance properties to forces from different directions in terms of mechanical properties,

5. Many polymer based composites lose their matrix properties due to the solvent and abrasive liquids in the working environment,

6. Materials used in the production of composites are expensive,

7. They are not suitable for all kinds of assembly methods, limited welded joints,

8. The methods used in their production are laborious, time consuming and expensive,

9. Post-production forming processes are limited and difficult to be shaped by conventional machining due to the abrasives contained within them,

10. It is not possible to produce most composites with renovation [11-14]

1.2 Classification of Composites

Although it is not possible to draw definite limits in the grouping of composites which can be used in many materials in their structure, it consists of three main classes according to the type of matrix components and the shapes of the filling components. Composites are divided into three classes as metal, ceramic and polymer matrix composites according to matrix materials [15, 16].

1.3 Metal Matrix Composites

Metal matrix composites (MMC) have high elastic modulus, high tensile compression and shear strength, high service temperature. In addition, they become extremely important engineering materials because they combine ductility and toughness of metals, high strength and high elastic modulus properties of ceramics. Besides these advantages, they have gained more importance in terms of having reproducible microstructure, mechanical properties and low density values [8, 17].

The most commonly used matrix materials are aluminum, titanium, copper and magnesium. As can be seen in Figure 1.1, aluminum, copper and titanium are generally reinforced with boron and silicon carbides and can operate smoothly up to 300 ℃ and 800 ℃ respectively. Graphite is the most commonly used reinforcing material for magnesium and especially copper, which is preferred in terms of thermal conductivity. As all the metals begin to lose their properties at very high temperatures, although they are reinforced with reinforcement materials, the operating temperatures should also be considered in metal matrix composites [18, 19].
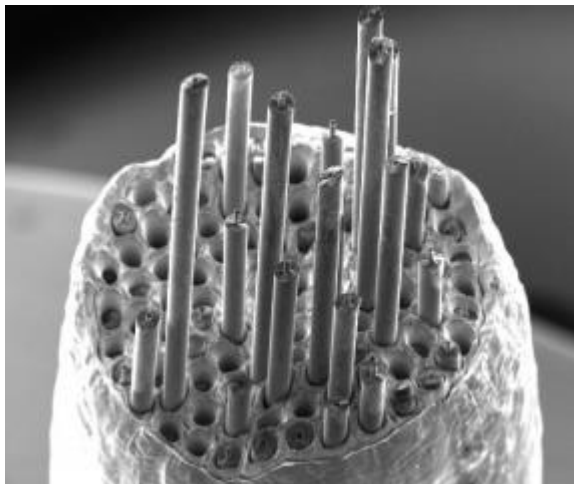
Figure 1.1 Microscopic view of the fracture surface for SiC reinforced copper matrix composite [20].

1.4 Ceramic Matrix Composites

Ceramic materials are very hard and brittle. They also have low density features. Ceramic materials are the materials in which thermal shock resistance and toughness are low. Therefore, they can cause high destruction as they exhibit sudden damage during use. In the case of reinforcement of ceramic materials with ceramic fibers, it is aimed to increase their resistance against sudden fractures while increasing their toughness. Therefore, if fragility is checked; they are excellent materials for hot zone parts of car and aircraft gas turbines such as knives, discs and pistons.

Reinforcement of ceramics with reinforcing materials increases their usage. In ceramic matrix composites (CMC), reinforcement materials are divided into two groups as continuous and discontinuous. Ceramics reinforced with continuous fibers are more preferred due to their higher toughness [21, 22].

Commonly used ceramic matrix composites can be grouped as follows:

- Carbides (e.g. Silicon Carbide, SiC)
- Nitrides (e.g. Silicon Nitride, Si_3N_4)
- Oxides (e.g. Alumina Mullite, $Al_6Si_2O_{13}$)
- Glass ceramics (e.g. Lithium Aluminasilicate) [8, 23]
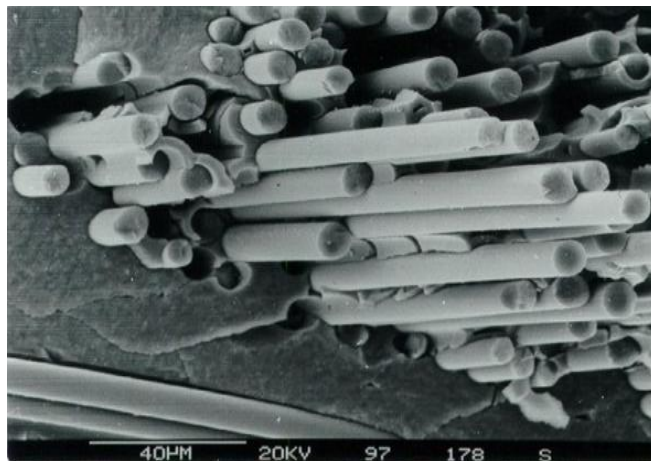
Figure 1.2 Fracture surface of a fiber-reinforced ceramic composed of SiC fibers and SiC matrix [24].

In ceramic matrix composites, it is also useful to examine the carbon matrix ones seperately. Carbon is generally reinforced with carbon in composite materials to

4

form carbon/carbon composite structures. Carbon / carbon composite structures stand out among other ceramic matrix composites with their resistance to temperatures above 2200 ℃ and the extra resistance they gain at these temperatures. Carbon/carbon composites also have high fatigue strength and dimensional stability. Because carbon element is chemically and biologically inert and can remain sterile in the human body, it is used in many medical fields. Today, many medical implants are preferred as these material because their resistance to corrosion and chemicals is much better than stainless steel and similar alloys. However, the material and production costs of carbon/carbon composites are unfortunately too high [8, 18, 25].

1.5 Polymer Matrix Composites

Since the beginning of the production of polymer matrix composites (PMC), composite materials started to attract the interest of the industry since the 1960s. For the last 50 years, PMChave become common engineering materials and are actively used in many areas such as sports goods, consumer goods, automotive, aerospace, marine, electrical and defense industries. PMC are important in both traditional and high-tech applications due to their high specific strength, low cost, wear resistance and high dimensional stability [26].

In its simplest definition, a polymer is defined as a long chain, high molecular weight compound formed by more or less regular bonding of identical or different atomic groups by chemical bonds. Polymers are formed by the formation of long chains by combining multiple molecules under heat and pressure (21, 27).

In polymeric composites, reinforcing materials provide strength and stiffness to composite, while matrix material assumes roles such as increasing corrosion resistance, distributing incoming load, and integrity of the structure. Especially in PMC, the strength is directly related to the reinforcing material. Currently, studies are being carried out on optimizing the stiffness of the PMC and increasing the strength of the fibers [28].

Polymers are divided into two groups as thermoset and thermoplastic. Thermoset polymers consist of long hydrocarbon molecules and primary bonds of atoms held within the molecules. However, the polymer molecules are also linked by covelent

bonds together with crosslinking. The arrangement of thermoset molecules is random and has an amorphous structure. On the other hand, they do not show any signs of heat softening as they form cross-links during the production of thermoset matrix composites. They have a covalently bonded, insoluble and fuze three-dimensional network structure. They can be softened at certain temperatures if the cross-link number is low [29]. Table 1.1 shows the mechanical and thermal properties of commonly used polymeric matrices. The low cost of thermosets and the long history of their use are important advantages. They have therefore dominated the space and construction sectors [30, 31].

Table 1.1 Mechanical and thermal properties of commonly used polymeric matrices [30].

Thermoset	Density (g/cm^3)	Young's Modulus (GPa)	Tensile Strength (MPa)	K (W/m^{0}C)	C$_p$ (Kj/kg°C)	T$_g$ (°C)
Polyester	1.10-1.23	3.1-4.6	50-75	0.17-0.22	1.3-2.3	70
Epoxy	1.10-1.20	2.6-3.8	60-85	0.17-0.20	1.05	65-175
Phenolic	1.00-1.25	3.0-4.0	60-80	0.12-0.24	1.4-1.8	300
Maleimide	1.20-1.32	3.2-5.0	48-110	-	-	230-345
Vinyl ester	1.12-1.13	3.1-3.3	70-81	-	-	70

The most commonly used thermosets are unsaturated polyester and epoxies. Polyesters are in the form of syrup consisting of polymer chains dissolved in a reactive organic solvent (monomer). With the addition of a suitable catalyst and accelerator, the syrup undergoes a chemical reaction in the cold state, causing a solid and three-dimensional structure without pressure. The main starting materials for forming polyester resins are dibasic organic acids (saturated and unsaturated both) and dihydric alcohols (glycols). By eliminating water between acids and glycols, ester bonds form, forming a long chain molecule of alternative acid and glycol units. The polymer chain of polyester is shown in Figure 1.3 [32].
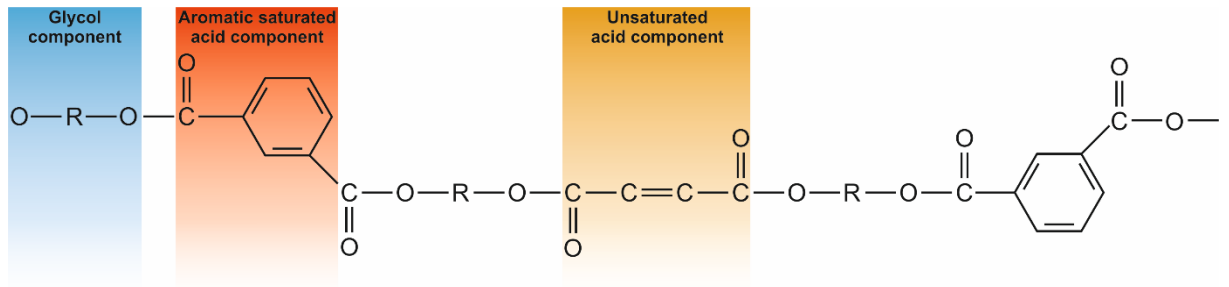
Figure 1.3 The polymer chain structure of polyester [32].

Polyesters are polymers of low density and cost which are generally reinforced with glass fibers and can be used up to temperatures of 100°C. They are the most commonly used thermoset matrix composites in automotive, aerospace and structural parts. They are not preferred in places where high performance is expected due to their mechanical properties falling with humidity and temperature, limited shelf life and high shrinkage during polymerization [19, 33].

Epoxy resins are generally produced by reacting epichlorohydrin with bisphenol A. The polymer chain of the epoxy is shown in Figure 1.4. Epoxy resins are substantially different from polyester and vinyl ester resins since they do not contain volatile monomeric components. Different resins are formed by varying the proportions of epichlorohydrin and bisphenol A [32].

Epoxies are more expensive than polyesters but have the advantage of less shrinkage during polymerization. It has dimensional stability, mechanical properties under heat and humidity and good bonding to many reinforcing materials as well as higher operating temperatures (170 °C). Therefore, many of the high-performance polymeric composites have an epoxy matrix [19, 33].

Figure 1.4 Epoxy polymer chain [32].

Figure 1.5 shows the structure of another epoxy resin with glycidyl ester resins. Here the viscosity and reactivity are ideal for vacuum impregnation, lamination and casting applications [32].

Figure 1.5 Another epoxy with a glycidyl ester [32].

In thermoplastic polymers, molecules are not chemically combined. The molecules are individual and held together by weak secondary bonds such as van Der Waals bonds and hydrogen bonds, or by intermolecular forces. When heat is applied, these weak secondary bonds in the solid thermoplastic break, and under pressure the molecules can move and flow in a new configuration. During cooling, the molecules

form a new solid structure by restoreting in a new configuration and new secondary bonds. Therefore, thermoplastic polymers can repeat the softening, melting and re-solidification processes by heating several times in desired cases [29, 34].

The thermoplastic polymeric composites soften due to the characteristic glass transition temperature (Tg) in the polymers when heated to certain temperatures. Therefore, they can be reshaped under heat and pressure, but their use is limited because they cannot rise to high temperatures. Composites having thermoplastic polymer structure with high toughness properties can be produced easily by conventional plastic production techniques such as injection and extrusion with low cost and high production quantities compared to other composites. The main drawback of using thermoplastic polymer as a matrix material is the relatively high thermal expansion values. These high expansion values may create a mismatch between the fiber and matrix materials, and may also be highly influenced by environmental factors [33, 35].

Table 1.2 Some physical properties of commonly used polymers.

Material	Density (g/cm³)	Yield Strength (MPa)	Tensile Modulus (MPa)	Melting Temperature (℃)
High Density Polyethylene (HDPE)	0.95-0.96	23-30	900-1550	126-135
Low Density Polyethylene (LDPE)	0.90-0.92	7-16	120-550	105-123
Polyvinyl Chloride (PVC)	1.30-1.48	40-55	2450-4700	199-204
Polypropylene (PP)	0.90-0.91	31-45	1950	16-163
Polystyrene (PS)	1.04-1.05	44-52	3100-3170	180-260
Polytetrafluoroethylene (PTFE)	1.80-2.41	12-14	480-630	327-346
Polycarbonate	1.19-1.22	61-67	2235-2500	310-220
Polyethylene Terephthalate (PET)	1.35-1.40	60-85	2800-3170	255-
Polybutylene Terephthalate (PBT)	1.30-1.31	58-60	1600-2700	220-225

1.6 Polypropylene

PP is one of the widely used polymeric materials due to its advanced mechanical, physical and thermal properties. It has a high melting point, low density and good impact resistance [36]. PP can be used in many fields such as automotive, aviation, electronics, health [37-40].

PP is a simple vinyl polymer to which methyl groups are attached to the second carbon atom on the backbone chain in different layouts that determine the tacticity (regularity) of the chain. In other words, the symmetry or orientation of each methyl group relative to the methyl group of the neighboring monomer has a strong effect on the main property of propylene polymerization [41]. In Figure 1.6, the propylene monomer has been shown to convert to a PP polymer [42].

Propylene Monomer

Polypropylene Polymer
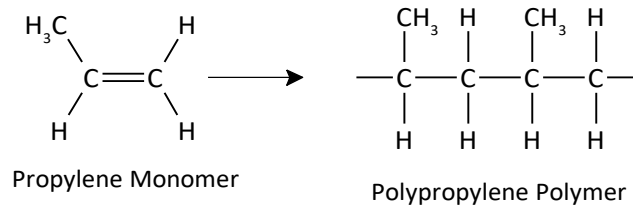
Figure 1.6 Polypropylene production from ethylene monomer [42].

PP is a semi-crystalline thermoplastic formed by the polymerization of propylene monomer with the use of Ziegler-Natta catalyst [43]. It is semi-transparent, white and solid at room temperature. Its melting temperature is approximately 160 °C. The density of the PP without addition is between 0.90 and 0.91 g/cm^3, which may vary depending on whether the matrix contains additive. By way of example, the density value of PP containing 30% glass fiber additive is 1.125 g/cm^3. PP is the most commonly used commercial-purpose thermoplastic and is often referred to as a low-cost engineering polymer [44].

Since it is not chemically polar, it has high corrosion resistance against many solvents and chemicals. It is one of the most effective thermoplastic materials in resistance to organic chemicalsas well as to inorganic environments. It is resistant to most solvents up to 60 °C, but aromatic and halogenated hydrocarbons can cause swelling in the structure [45]. It is resistant to acidic and alkaline environmental conditions, salt solution, alcohol, petrolium, various fruit juices and many oils. PP based materials have high chemical resistance due to their high crystallinity [45].

Table 1.3 PP polymer material properties and test standarts [46].

Properties	Unit	Value	Test Method
Density	g/cm^3	0.90-0.91	ASTM-D-1501
Yield Strength	Kg/cm^2 (23°C)	300-350	ASTM-D-638
Elongation	%	600-700	ASTM-D-638

Flexural Strength	Kg/cm^2 (°C)	7500-8000	ASTM-D-747
Hardness (Rockwell)	R-Scale (°C)	90-94	ASTM-D-785
Ratio of Water Absorption	%	<0.03	ASTM-D-570
Dielectric constant	X 10^6 CS (10°C)	2.2-2.3	ASTM-D-150
Dielectric Loss	X 10^6 CS (18°C)	0.0003-0.001	ASTM-D-150
Resistance of Voltage	kV/mm	30.32	ASTM-D-149
Resistance of Specific Volume	Ohm-cm	<10^{16}	ASTM-D-257
Thermal Conductivity	Kcl/cm/cm^2/s/°C	2.7 10^{-7}	…………………..
Specific Heat	Gcal/g°C	0.46	…………………..
Thermal Coefficient of Expansion	mm/mm/°C	110-106	ASTM-D-695
Deformation Temperature	°C	120-130	ASTM-D-648
Softening Temperature	°C	165-172	ASTM-D-648

1.7 Quartz

Quartz is a non-toxic, inert material which is the most common mineral in the Earth's surface [169]. Because of this harmless properties, quartz can be used in foods and agriculture and does not cause toxicological consequences [170]. Archaeological findings, geological formations, even meteorites and rocks from Moon and Mars contains natural quartz [171, 172]. From research to commercial, there is wide usage area in many fields.

The temperature range that quartz and its polymorphs, tridymite and cristobalite present is smaller than 870°C, between 870 and 1470°C and bigger than 1470°C, respectively. Both tridymite and cristobalite are metastable at ambient temperatures. All three minerals have α and β modifications which refers to stability below 573°C and between 573°C and 870°C, respectively. The α -β transition is reversible by causing a change in atomic positions without any rapturing or bonding. The α form is rhombohedral and the β form has a hexagonal structure. The silicones share the oxygen atoms in a tetrahedral shape for both forms. While the angle between Si―O bonds is 66º with the optic axis, the angle is 44º between two others. Hence, oxygens are existed in two equivalent pairs. The nature of the Si―O bond in SiO_2 is described as ~40% ionic and ~60% covalent [173, 174]. This covalent component provides rigidity for the materials and prevent macroscopic diffusions such as lattice atoms. The structure of quartz is uneven and dislocate. Even it has a complex structure, identification of conformation is poor. Misplaced lattice atoms tend to be located near impurities. Si―O bond rupture and direct "knock-on" collisions are two

11

damage mechanism as a result of SiO_2 has both ionic and covalent nature and consequently creates vacancy and interstitial creation. This second mechanism requires energetic nuclear particle which radiation induce substansional damage by displacement of lettuce atom in quartz and change the characteristics of material. In a large number of literature investigated the permanent damage effects in quartz major studies can be given for SiO_2 structure [175, 176].

1.8 Surface Modification of Fillers

Polymeric materials are doped with inorganic or organic fillers to improve properties such as mechanical and thermal. Fillers are used to reduce the cost as well as improve the properties of polymeric materials [47]. The filler in ASTM D 1566 is defined as "a solid compound, usually finely divided, which is added to a polymer in relatively large proportions for technical or economic reasons [48].

The most commonly used fillers in the production of polymeric composite materials are;

1. Calcium carbonate
2. Talk
3. Mica
4. Silica
5. Barium sulfate
6. Magnesium hydroxide
7. Aluminum trihydroxide
8. Carbon black
9. Titanium dioxide
10. Metal powder

Fillers can be defined as organic or inorganic according to chemical composition, spherical, cubic, irregular, block, plate, flake, fiber and mixtures thereof according to particul shapes, nano, micro and macro according to particle size, thermal conductor according to thermal properties, conductor or insulator acoording to thermal expansion coefficient, electrical properties.

In composite materials, the structure of the filler-matrix interface plays an important role in the properties of the composite. Especially when it comes to mechanical properties, one of the most important events in polymeric composites is the interaction between the filler material and the polymer matrix [49,50]. The interaction determines the mechanical properties of polymeric composites. In general, a better matrix-filler interface will provide high modulus, tensile strength and hardness properties as well as fatigue, cracking and corrosion resistance [51, 52].

In order to increase the interaction between the filler and polymer matrix, processes can be applied on the surface of the filler material. The treatment of the filler surface increases the adhesion between matrix and filler [53, 54].

Surface treatment processes are applied to additives in order to change the morphological and chemical properties of additives. Thanks to these applied processes, compatibility of filling material-matrix material is increased and the properties of the composite are improved [55, 56]. In order to increase the adhesion between the filler and polymer matrix, surface modification processes are applied to the filler surface [57, 58, 59]. Surface modifications can be applied to additives by physical and chemical methods. Physical methods do not change the chemical composition of additives. On the other hand, an intermediate layer is formed on the additive surface to increase matrix-filling material compatibility in the chemical method [60, 61]. In addition to increasing the matrix-filling material compatibility in the composite, the surface modifications also show a protective feature against the moisture and the chemical [62]. In polymeric composite materials, various chemical modification methods such as acetylation, benzoylation, and addition of alkaline, silane, peroxide, isocyanate, permanganate are applied to additives to increase matrix-filling material interface compatibility and provide good adhesion [63, 64].

Alkali treatment is one of the most common methods used to increase matrix-filling material compatibility [65]. This method increases the roughness of the surface of the additive in addition to reducing the diameter of the additive. Most of the hemicellulose, lignin, pectin, wax and oils found in the outer surfaces of natural additives are removed after the application of this process. In this way, surface of the natural fiber becomes cleaner. In addition to increased surface area and removal of

dirt on the surface, the appearance of more hydroxyl groups on the surface means more possible number of reactions between the matrix-filling materials. All these situations are factors that increase interface compatibility [66-68]. Alkoxide ionization of the hydroxyl group after the reaction of sodium hydroxide with the fiber cell is represented in Scheme 1.1.

Fiber—OH + NaOH → Fiber—O$^-$Na$^+$ + H$_2$O + impurities
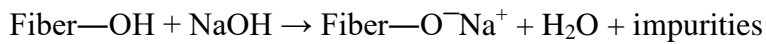
Scheme 1. 1 The chemical reaction of sodium hydroxide with fiber cell.

Current studies on alkali treatment are frequently encountered in the literature. Huda et al. examined the effect of alkaline treatment on pineapple leaf fiber on the performance of pineapple leaf fiber/PLA composite materials in their study. In the study, they demonstrated that the mechanical properties of the alkali-treated fiber reinforced composite exhibit superior mechanical properties compared to the untreated fiber reinforced composite [69]. Koichi Goda et al. studied the effect of alkylation on ramie fiber on tensile properties. The load application technique was used during alkali treatment to improve the mechanical properties of the fibers. Ramie fibers were treated alkaline with a solution containing 15% NaOH and exposed to a load of 0.049 and 0.098 N. When the results were examined, they observed that the tensile strength was increased in the range of 4-18% for the alkali-treated ramie fibers compared to the untreated ramie fibers [70]. Wanjun Liu et al. investigated the effect of fiber surface treatment on Indian grass-doped biocomposite material. In order to decrease the cementing force between fibrils, it is needed to eliminate hemicellulose and lignin and it results decreasing inter-fibrillar region of the fiber with alkali solution treatment for grass fibers. This process causes both homogeneous dispersion of the biofiber and higher aspect ratio of the fiber in the composite. As a result, fiber reinforcement efficiency is improved and mechanical properties such as tensile, flexural and impact strengths are increased at the end [71]. Ray et al. treated the jute fibers in 5% NaOH solution at 30 °C for 0, 2, 4, 6, and 8 hours alkaline treatment. They observed that the modules of fibers treated for 4, 6 and 8 hours increased by 12%, 68% and 79%, respectively. They demonstrated that the flexural strength of the fibers treated with alkaline treatment for 4 hours in 35%

added composite sample increased approximately 20% from 199.1 to 238.9 MPa [72].

Although there are many studies done, it is clear that alkaline treatment is an application that increases fiber / matrix interface compatibility and is widely used. Apart from this technique, which is commonly used in composite samples with organic fiber, different techniques are used to increase interface compatibility in composites with inorganic filler materials.

Another common application that improves the polymer matrix and filler interface is the use of silane coupling agents. Coupling agents indicate a class of additives that can improve the properties of the interface between polymer materials and fillers. The coupling agents contain two types of groups with different properties presented in the molecular structure. The first group coupling agents chemically react with the polymer matrix or can have good compatibility. The second group of coupling agents can form chemical bonds with the inorganic material or filler. It can improve the interface adhesion of the two materials and significantly improve the performance of the filler or strengthen the polymer materials. The most commonly used coupling agents are silanes. This applied process is often called *silanization*.

Silanization is a low cost and effective covalent coating method that makes the material surface rich in terms of hydroxyl groups [73-75]. Silanization is the process of functionalization of silicone or borosilicate backings with a silane solution that results in the formation of a silane mono layer, which acts as a binding agent between the matrix and the filler material and improves the adhesion of the matrix to the filler material [76, 77]. A silane compound is a monomeric silicon-based molecule that contains four components. Since silicon is in the same family as the carbon in the periodic table, it can form covalent bonds with the other four neighboring atoms. However, it is less electronegative than carbon and more prone to chemical reactions than typical organic compounds.

Silanes containing at least one silicon-carbon bonding are called organosilanes. Organosilanes can also have hydrogen, oxygen, or halogen atoms directly attached to the silicon atomic nucleus. Some of these derivatives are highly reactive and can be used to form covalent bonds with other molecules or surfaces [78, 79].

15

The general structure of a functional silane coupling agent is shown in Figure 1.7. The organic arm typically has a structure called *functional group* or *reactive component* that facilitates covalent bonding with the other molecule. The other part consists of silane-reactive groups directly attached to silicon atoms and can be of various types. These molecules can simply contain a hydrogen atom (called a silicon hydride), a halogen-silicon derivative such as a chlorine atom (called chlorosilane), an ―OH group (silano) or methyl ether (methoxysilane) or ethyl ether organic components (ethoxysilane) [80].

Functional or reactive group

Silicon atom

R — (CH$_2$)$_n$ — Si — X
          X
          X

Alkyl chain

Hydrolyzable groups
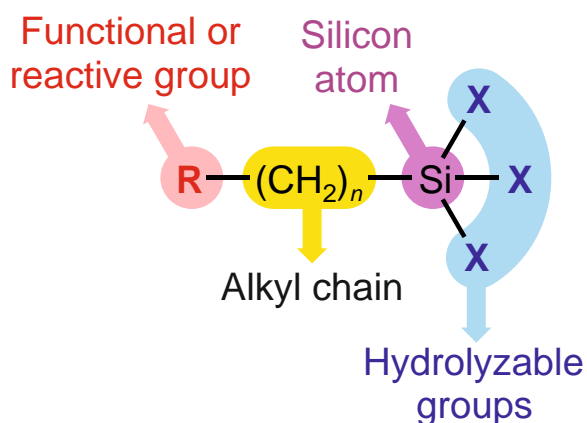
Silane coupling agent

Figure 1.7 The general structure of a silane coupling agent includes a functional group or reactive group at the end of an organic spacer [80].

General reactions of silane coupling agents to inorganic backing materials are shown schematically in Figure 1.8. The reaction mechanism and the formation of a reactive interconnection may differ from those usually encountered with organic reactive groups. Unlike most other reactive groups, the most common silane coupling group (alkoxy) should generally be hydrolyzed first to form a reactive intermediate and then bound to the substrate. Hydrolysis of an alkoxysilane It produces a highly reactive form of silanol, which is necessary for binding to inorganic surface hydroxyls [80].
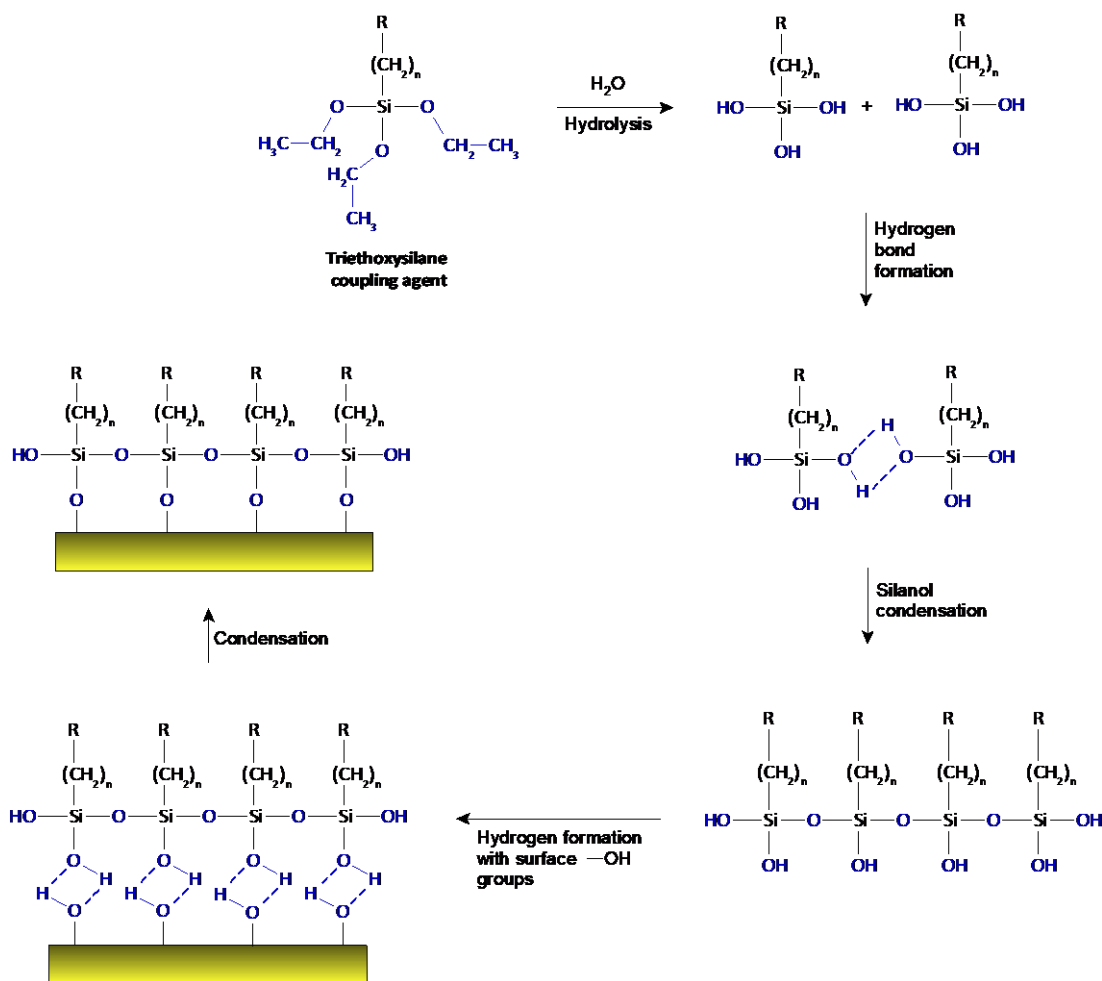
Figure 1.8 The reactions involved with the coupling of an organosilane compound to an inorganic surface containing available —OH groups [80].

The initial reaction in solution or near an inorganic substrate is the condensation of the silane coupling agents to form a polymer matrix that is bonded together by —Si—O—Si— bonds. Simultaneously growing silane network interacts with the inorganic substrate by forming a hydrogen bond network with —OH groups on its surface. Then another condensation reaction occurs. Heat or vacuum is usually required to remove water formed as by-product in this reaction. The resulting reaction eventuates in formation of organosilane polymer-surface with covalently bounded stable siloxane-linking [80, 81].

Many studies have been carried out by using silanization technique to increase matrix-filler interface compatibility in polymer based composite materials. For example, Chen et al. reported processing Cloisite 25A organoclays with trimethoxysilane (3-glycidoxypropyl). This silanized clay has been found to function

17

as an effective binder in poly lactic acid (PLA) / poly butylene succinate (PBS) blends. As the content of silane treated clay increased by up to 10% by weight, the tensile strength and elongation of PLA/PBS mixtures increased [82].

Kole et al. suggested that polyethylene grafted with silane can be used in ethylene-propylene-diene rubber (EPDM)/silicon blends as a coupling agent [83]. Later, vinyltrimethoxysilane (VTMS)-grafted ethylen vinyl acetate (EVA) was used by Zhang et al. As a coupling agent for EPDM/methyl vinyl silicone rubber blends, they stated that 10 phr of VTES-grafted EVA that added to blend gives significant improvements for both mechanical properties and thermal stability [84].

Demir and Tinçer performed compatibilization principle of composite materials in order to harmonize poly(ethylene terephthalate) (PET)/high density polyethylene (HDPE) blends [85]. In this study, PET powder which was treated with vinyl tris-(2-methoxyethoxy) silane, g-lycidoxypropyltrimethoxysilane and g-methacryloxypropyltrimethoxysilane coupling agents and silane were mixed with HDPE under the melting point of PET. The chemical structures of silanes are shown in Figure 1.9. As a result of this process, it was reported that the silane treatment has a substantial effect on tensile strength. At a PET loading of 40% (wt), silane treatment allowed an increase in tensile strength up to 32 MPa, whereas unmodified silane parts showed only a tensile strength of 21 MPa. The compatibilization between PET and HDPE was also revealed by means of scanning electron microscopy (SEM) analysis. In another study, Oyman and Tinçer investigated the use of a polybutadiene group contained silane coupling agent in melted PET/PP blends [86]. According to the results of SEM analysis, tubular-type fibrillary extensions in silane-modified blends was observed. In the meantime, it can be said that silane coupling agent showed harmonizing effect on blends due to improved tensile strength and impact properties.
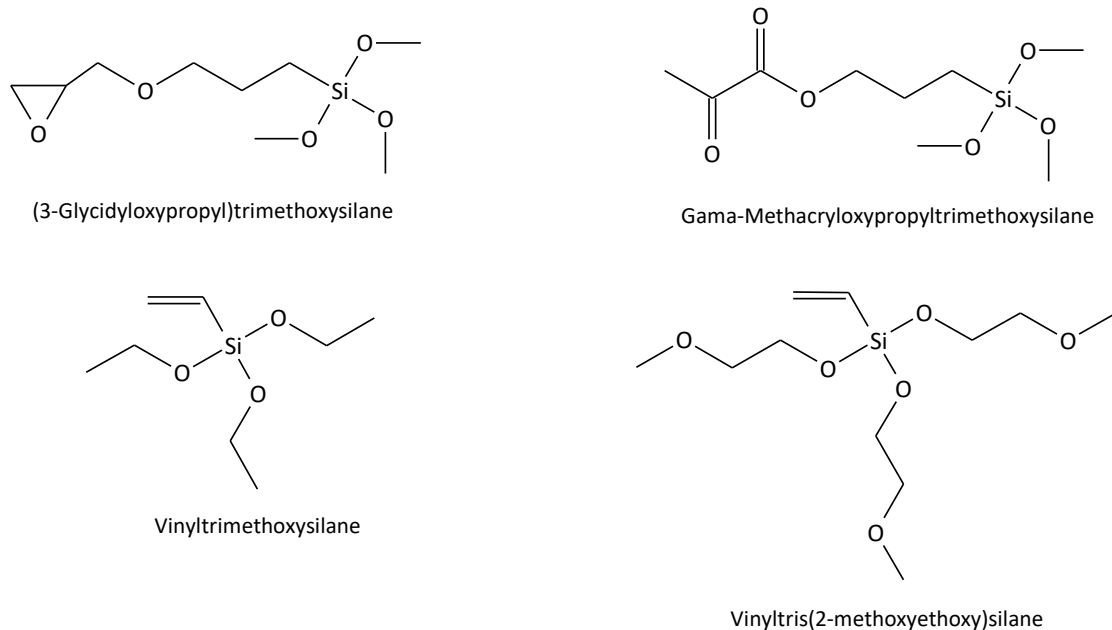
Figure 1.9 Chemical structure of silanes before grafting onto intermediate compounds [85].

Shien and Chuang examined the thermal properties of VTES compatibilized low-density polyethylene (LDPE)/linear low-density polyethylene (LLDPE) blends [87]. LDPE and LLDPE were grafted by silane with free-radical grafting method and the blend of LDPE/LLDPE was melt extruded and cross linking reacted with the help of water. It was observed that activated silane enhance the thermal behavior by creating a new layer between LDPE and LLDPE.

Gan et al. worked on combining silane coupling agent and MA-PE in the compatibilization of LLDPE/epoxy resin [88]. In this study, VTES was added into LLDPE via melt grafting method. General mechanical properties were improved at the end of crosslinking of polyethylene formed by the hydrolysis of functional groups of silanes. Similarly, Nachtigall et al. investigated the difference between VTES-grafted PP with MA-PP and PP-PA mixtures [89]. The findings show that silane coupling agent has a lower compatibility effect than MA-PP. The addition of MA-PP provides a finer dispersion of the PA phase in PP, higher flow stress and longer breaking elongation.

Zhang et al. has studied on increasing the friction resistance and moisture stability of asphalt concrete mixtures by adding silane coupling agents [90]. Min et al. was used

the basalt aggregates on asphalt mixture with surface treating method in order to improve moisture damage resistance. This work showed that the silane coupling agent had a significant impact on basalt-asphalt interface performance [91]. Likewise, Xie et al. investigated that perfect moisture stability in terms of higher indirect tensile strength and tensile strength ratio during the freeze-thaw process can be obtained by surface treating with silane coupling agent in asphalt mixture [92].

Matinlinna et al. examined the effect of novel silane system on the bending properties of the composite in glass fiber reinforced composites for dental applications. Three functional coupling agent and their crosslinking blends was used for bonding continuous E-glass fibers to a bis-GMA resin system and flexural strength and modulus were measured. Two subgroups were randomly selected. 3-Acryloxypropyltrimethoxysilane, 3-isocyanatopropyltriethoxysilane and 3-methacryloxypropyl-trimethoxysilane were used for the first subgroup and a cross-linker silane mixed, 1,2-bis-(triethoxysilyl)ethane with these functional silanes in the second subgroup. Silanized fibers were introduced to bis-phenol-A-diglycidyldimethacrylate (bis-GMA)-based monomer system and light polymerization occurs in order to form fiber-reinforced composite (FRC) test specimens. E-glass which contains FRCs that coated with original silane coupling agent was the control group and stored in dry storage, 30 days and 6 months immersion in water. Flexural strengths and moduli of test specimens were measured and fracture surfaces were imaged with SEM. Control sample coated with original silane and stored in water for 6 months showed the highest flexural strength while the sample with 3-isocyanatopropyltriethoxysilane performed the lowest. Matinlinna et al. suggested that other trialkoxysilanes or some blends can reveals equal or slightly better flexural properties for fiber-reinforced composite using the experimental bis-GMA resin system [93].

Thomason and Jones investigated the concentration of hydroxyl groups on glass surfaces with contact angle goniometry (CAG) on their work called "The Concentration of Hydroxyl Groups on Glass Surfaces and their Effect on the Structure of Silane". In this work, the densities of hydroxyl groups were measured with the help of measuring the contact angle with water of differing pH in octane. The maximum contact angle was determined at the point of zero charge and was

used in calculating the density of hydroxyl groups on boron-free E-glass and E-glass surfaces. Boron-free E-glass surface had a slightly higher hydroxyl group density than the E-glass surface. It was investigated that the surface concentration of hydroxyl groups is sensitive for both glass formulation and heat treatment history. Hydroxyl group glass surface concentration was significantly decreased after 600 oC heat treatment. Re-hydrolysisat a humidityof 80 % only led to a partial recovery in the density of OH groups on the surface [94].

Miao Shui investigated the surface modification of ultra-fine calcium carbonate filling materials with different proportions of polyacrylic acid (PAA) and examined its properties in his study published in 2003. In the study, binding amount, binding efficiency, X-ray photoelectron spectroscopy (XPS) and reverse gas chromatography (IGC) tests were performed for characterization of PAA coated filling materials. As a result of IGC test, it was observed that the surface tension of PAA modified by filling materials was decreased in comparison with the reference material. He observed that 4% PAA was the highest surface energy in modified filling materials [95].

Jay W. Grate et al. investigated silane modifications on glass and silica surfaces in their study. In this work, they examined the effects of surface treatments before modification and revealed that the contact angle changes in air-water and oil-water environments after modification. They observed that the wetting angles of the borosilicate glass surfaces and silica surfaces cleaned with standard cleaning solution 1 (SC1) and silanized with hexamethyldisilazane (HMDS) differ. However, they obtained an oil-wet surface by modifying the glass surface cleaned with boiling concentrated nitric acid (HNO_3) solution with HMDS. Thus, equal oil-wet surfaces were obtained in silica and glass silanized with HMDS. As a result, they showed that pretreatment and silanization is possible in silicone-silica/glass micromodels previously combined with anodic bonding, and the change in wettability has an important and observable effect on the immiscible liquid displacements in the pore web [96].

D.C.D. Nath et al. modified the fly ash (FA) surface with sodium lauryl sulphate (SLS) surfactant and used it in the production of composite film with polyvinyl

alcohol (PVA). They examined both unmodified FA and modified FA samples by using XRF, SEM, TEM, FTIR and XPS. As a result of oxide-based chemical analysis using XRF, it has been observed that the chemical composition is almost unchanged. Although SEM and TEM analyzes were not possible to display the unmodified and modified shapes of the same particles, it was observed that the particles were mostly irregular in spherical morphology. They revealed that SLS-FA doped composite films have 33% higher in strength compared to unmodified FA doped composite films. They commented that this increase in tensile strength was due to the level of the physical valve between the SLS-FA and PVA surfaces [97].

H. Demir et al. used ammonium polyphosphate (APP) as an acid source and blowing of the PP material, pentaerythritol (PER) as a carbon active substance, and natural zeolite for increasing flame retardancy agent in order to improve the flame retardant (FR) properties. Zeolite was added to the flame retardant formulation in four different concentrations (1, 2, 5 and 10% by weight) to investigate synergy with flame retardant materials. Zeolite and APP were treated with two different surface coupling agents, three (trimethoxysilyl) -1-propanetiol and (3-aminopropyl) - tritoxysilane in order to investigate the effect of both mechanical properties and flame retardant performance of composites. Maleic anhydride grafted polypropylene (MAPP) was used to make the PP hydrophilic. The flammability of FR-PP composites was measured by determining the limiting oxygen index (LOI). The LOI value was found to reach a maximum of 41% for APP:PER (2: 1) PP composite treated with mercapto silane containing 5% by weight of zeolite. It was revealed that the tensile strengths of the composites were increased with the addition of MAPP, and the breaking elongations of the composites were increased with silane treatments [98].

In the study conducted in 2017, Jing Sang et al. examined the adhesion properties between uncured natural rubber and carbon steel (CS) modified with silane binding agent. It was determined that the effect of silane binding agents on adhesion behavior between CS and uncured natural rubber by using XPS, FTIR, AFM and regional nanoscale thermal analysis techniques. High amount of silicon content was confirmed with FTIR and XPS analyzes in all surface treated samples [99].

In their study, Hu Yan et al. tried to obtain a super hydrophilic surface by using tetraethoxysilane (TEOS) silane as coupling agent to improve the self-cleaning and anti-dust properties of photovoltaic cells. In the study, many Si—OH bonds were formed on the first layer of glass using TEOS, and then the second layer was attached to the special silane-binding agent TEOS layer. At the end of the reaction, it was obtained a super hydrophilic surface on the glass based surface [100].

In the study published in 2018, Wang Chuang et al. modified the nano-silicon dioxide (nano-SiO_2) surface with the KH-560 small molecular coupling agent and the SEA-171 macromolecular coupling agent. Modified nano-SiO_2 particles were used as additives in cyanate ester resin (CE). They investigated the effect of nano-SiO_2 content and matrix-filler material interface properties on nano-SiO_2/CE composite materials. In experimental studies, it has been observed that the binding between the nano-SiO_2 particles and the CE resin has increased with the addition of the coupling agent. Thanks to this interface compatibility, it has been demonstrated that the heat resistance and friction properties of the composite material are improved. It was indicated that the thermal decomposition temperature increases by 75℃ and the friction coefficient decreases by 25%, as a result of this, the wearing resistance increases by 77% in the 3.0wt% nano-SiO_2/CE composite modified with SEA-171 when compared to approximately pure CE material [101].
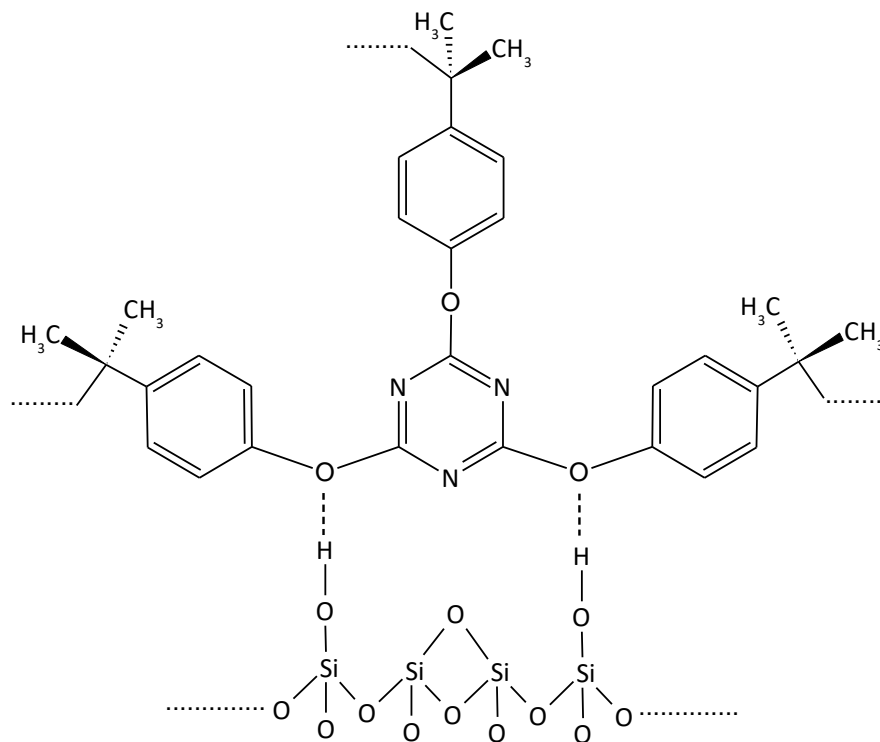
Figure 1.10 Shematic illustration of hhydrogen bonding between nano SiO_2 and CE [101].

Jun Jiang et al. examined the effect of silanization with γ-methacryloxypropyltrimethoxysilane (MPTS) on the agglomeration and moisture absorption behavior of silica particles in their study in 2018. They observed that MPTS additive with different rates (2, 46 and 8%) changed the amount of ─OH group and accordingly the silica agglomerations were different. It was seen that large pores in unmodified silica agglomerates disappeared by shrinking from MPTS modification. It was investigated that ─OH groups decreased with increasing MPTS concentration above 6% MPTS concentration. At low relative humidity and MPTS concentrations, adsorption retardation occurred on silanized silica in terms of moisture sorption and it is said that a synergistic effect between the surface ─OH group content and pore characteristics can set off [102].

N. M. Bravaya et al. produced hybrid material by modifying Al_2O_3 nanofiber with various silane coupling agents and using these for ethylene and propylene copolymers as additives in their study in 2019. Trialkoxysilane with alkenyl and alky functional groups was used for modifications. As a result of CP, MAS, NMR analysis applied on all modified nanoparticles, it was observed that there were no

alkoxy groups and the formation of any type of siloxane groups was identifiable. Results of the study revealed that the selection of the silane coupling agent was critical for the mechanical properties of the nanoparticle-polyolefin nanocomposites. 150% increase in tensile strength and a 50% increase in breaking elongation were observed in octylsilane-functionalized nanocomposite samples with 0.63wt% filler additive [103].

Yanyuan Qi et al. investigated the effect of the surface modification of the ceramic material in polymer-ceramic dielectric composite materials. In the study, surface modification was performed with vinyltrimethoxysilane (VTMS) in order to increase the interface compatibility of $Ba(Mg_{1/3}Nb_{2/3})O_3$ (BMN) ceramic material, which is incorporated into the PTFE polymer matrix material. It was observed that VTMS modified BMN ceramic materials did not make any change in the crystal structure, and VTMS modified BMN/PTFE composites had a low cavity and a sufficiently uniform structure. As a result, it has been revealed that the modification of ceramic filling materials with silane coupling agent is an effective method to improve the structure and microwave dielectric properties of the PTFE-based composite [104].

In 2020, Yuya Komagata et al. aimed to investigate the effect of interfacial adaptation between feldspar porcelain modified with silane coupling agent using corona discharge technique and resin cement. The schematic representation of the corona discharge technique is given in Figure 1.11. The shear bond strength (SBS) of the produced composites was measured. As a result of surface characterization studies, it was observed that corona discharge treatment forms silanol groups on the porcelain surface and this surface exhibits hydrophilic property without increasing the roughness. With the help of these silanol groups on the porcelain surface created by the corona discharge technique, it was seen that SBS increased. According to experimental studies, it was demonstrated that corona discharge treatment can be used in modification of glass-ceramic surfaces in order to increase bonding strength [105].

a)

$$OH$$
$$|$$
$$—Si—O—Si—O—Si—O—Si—O—Si—$$

b)

HO   OH HO   OH---OH HO   OH HO

$$—Si—O—Si—O—Si—O—Si—O—Si—$$

c)

HO   OH   OH

$$—Si—O—Si—O—Si—O—Si—O—Si—$$
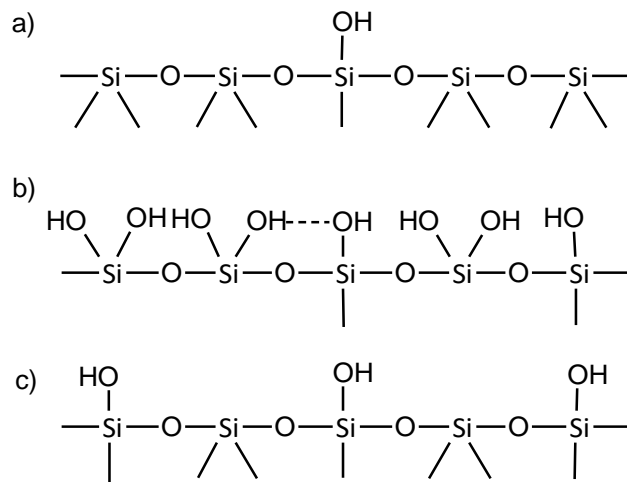
Figure 1.11 Schematic illustrations a) non-treated surface, (b) corona-discharge-treated surface, and (c) corona-post-heated Surface [105].

Nan Zheng et al. used silane coupling agent in order to increase the atomic oxygen (AO) erosion resistance and interface shear strength (IFSS) of the carbon fiber/epoxy (CF/EP) composite material. In the study, carbon fiber surfaces were modified by using silane coupling agent (SCA) and then CF/EP composite materials were produced. When AFM images were examined, a relatively smoother surface was observed in SCA treated CFs samples compared to CFs with untreated rough surface. It was indicated that the compatibility of SCA-coated CFs and CF/EP composite interfaces increased thanks to the silica (SiO_2) layer verified by XPS in SCA-treated CFs samples, thereby improving IFSS and AO erosion resistance [106].

Yahong Min et al. synthesized a new silane coupling agent in silane γ-(methacryloyloxy) propyltrimethoxysilane (KH570). They were investigated the interface compatibility of silane coupling agents and basalt rocks by modifying the basalt surface with KH570 and the newly synthesized silane coupling agent (Figure 1.12). As a result of XPS and FTIR analyses, it was observed that silane coupling agents bind strongly to basalt rocks. In the SEM study, it was seen that silane coupling agents formed in the form of thin films on the surface of modified basalt rocks. In the Marshall test conducted, it was found that the sensibility of moisture varies more in the samples that were modified with the new silane coupling agent, compared with those that were not modified and modified with the KH570. As a result of the study, it was clear that the new silane coupling agent plays an important role in increasing the basalt and asphalt interface performance [107].
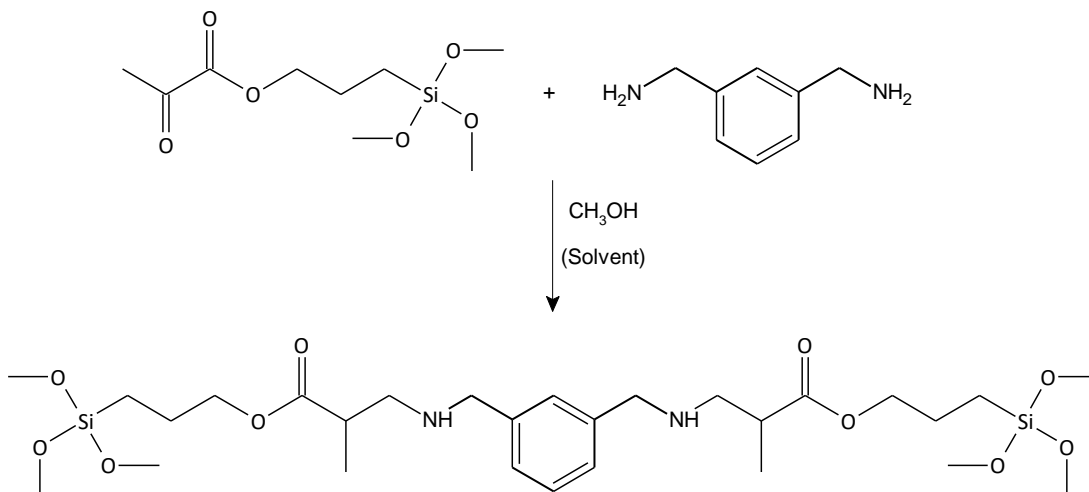
Figure 1.12 Synthesis of the new coupling agent from KH570 coupling agent [107].

In 2019, Sheng Xu et al. used phosphor containing hydrotalcite modified with rare soil coupling agent in PP matrix composite production in order to improve the flame retardant properties. $P_3O_{10}^{5-}$ columnar Mg/Al hydrotalcite (HTs-P) was used as filling material in the study. PP/W-HTs-P composite productions were conducted by adding rare earth coupling agents (WOT) modified HTs-P into the PP matrix. The produced composite samples were characterized by XRD, FTIR, contact angle measurement, SEM and TGA analysis. It was found that HTs-P samples modified with WOT have become exhibiting hydrophobic behavior other than hydrophilic after modification. From the XRD and SEM analyzes, it was observed that the interface compatibility between W-HTs-P filling material and PP matrix has improved. As a result of TGA analysis, it was investigated that PP/HTs-P samples with a char residue rate of 5.3% increased to 12.5% in W-HTs-P doped PP/W-HTs-P composite samples and based on these results, it was interpreted that the thermal stability of the matrix material improves. When considering the HTs-P and modified WOT, W-HTs-P samples have similar layered structure and chemical composition, and it was thought that change in the dimensional distribution of W-HTs-P samples after the modification affect the development of physical and mechanical properties [108].

Bing Qiao et al. modified nano silica particles using γ-aminopropyltriethoxysilane (APTES). In the study, it was developed a new and effective method for high density silanization of nano silica particles using APTES. The method was performed in

three stages through solution mixing, spray drying and thermal treatment. The solution was occurred fast and very limited during the mixing phase. In the spray drying phase, APTES silanization agent adhered to the surface of nano silica particles with physical and chemical absorption. At the thermal treatment stage, ATPES sprayed nano silica particles were processed at certain temperatures and times. It was observed that the reverse reaction was dominant at temperatures below 300°C and APTES inoculation intensity decreased, while the foreward reaction was dominant at temperatures above 300°C and the inoculation intensity increased. It was determined that the optimum temperature was 360°C and the optimum duration was approximately 30 minutes for high vaccination intensity [109].

Indra Surya et al. investigated the effect of alkanolamide (ALK) and silane coupling agent in silica-added natural rubber composite material. Standard malaysian rubber grade natural rubber was used in the study. APTES was used as the silane coupling agent. ALK was synthesized from Refined Bleached Deodorized Palm Stearin (RBDPS) and diethanolamine. Molecular structure of ALK and APTES are given Figure 1.13. ALK and APTES were added separately at 1.0, 3.0, 5.0 and 7.0 pH ratios. Curing conditions improved, better filling material distribution was obtained and better filled material-matrix compatibility was observed in samples using both additives. Optimum properties were obtained at pH = 5.0 with both ALK and APTES doped samples. When ALK and APTES doped samples are compared, it was observed that ALK doped samples show better distribution and show more effective filling material-matrix interface compatibility [110].
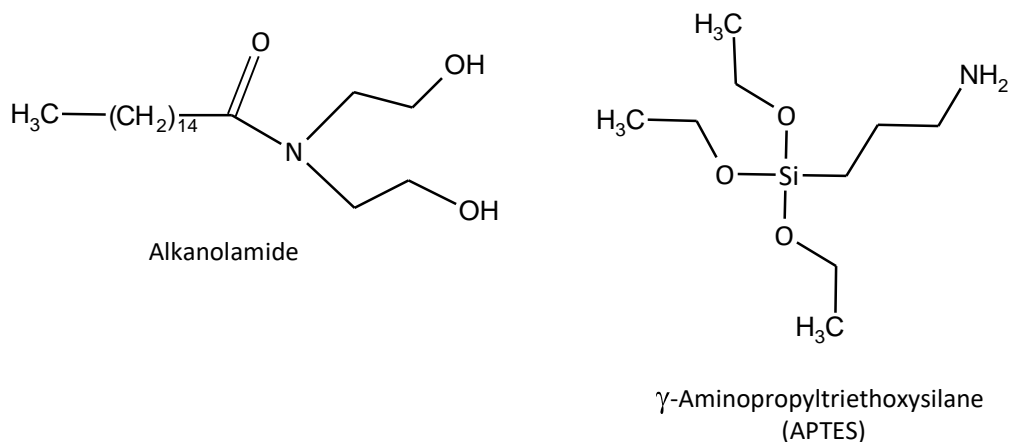
Figure 1.13 Molecular structure of Alkanolamide and APTES [110].

28

Shinsuke Ifuku and Hiroyuki Yano examined the effect of silane binding agent on the mechanical properties of microfibrillated cellulose (MFC) added composites. The molecular structures of the silane coupling agent and acrylic resin used in the study are shown in Figure 1.14. Composites with MFC fiber additives are preferred due to their mechanical properties. In the study, MFC fiber surfaces were modified with a silane coupling agent which has amino (—NH$_2$) functional group in order to improve the fiber-matrix interface. According to mechanical tests, Young's modulus value of the composite increased by 70%. As a result of these studies, it has been observed that in composite applications where the unique structure MFC is used as additive material, mechanical properties can be improved by using silane coupling agent [111].
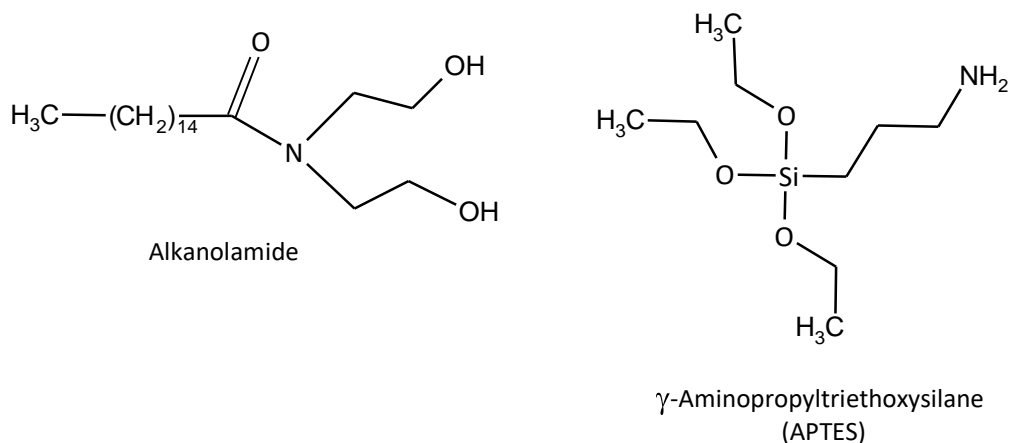
Figure 1.14 Molecular structure of γ-aminopropyltriethoxysilane and acrylic resin [111].

Guojun Cheng et al. examined their properties by modifying the surface of coal powders with different coupling agents for potential inorganic material applications. In the study, γ-methacryloxypropyltrimethoxysilane (KH-570), vinyltrimethoxysilane (SG-Si171) and di(dioctylpyrophosphato) ethylene titanate (NDZ-311) coupling agents were used in order to increase the surface activity of coal powders. The molecular structure of coal powder and coupling agents is shown in Figure 1.15. Both modified coal powders and unmodified coal powders were added into anhydrous ethanol and their dispersions were examined. In the study, it is found that unmodified coal powders show poor dispersion in anhydrous ethanol, and especially coal powders modified with NDZ-311 have better dispersion in anhydrous

ethanol. It is commented that this was due to the formation of a coupling agent coating layer on the surface of coal powders after modification, and as a result, the surface properties of coal powders did not change and exhibit higher hydrophobic properties. As a result of the study, it is suggested that coal powders modified with NDZ-311 can be used for better performance and long product life cycle in rubber and plastic materials [112].
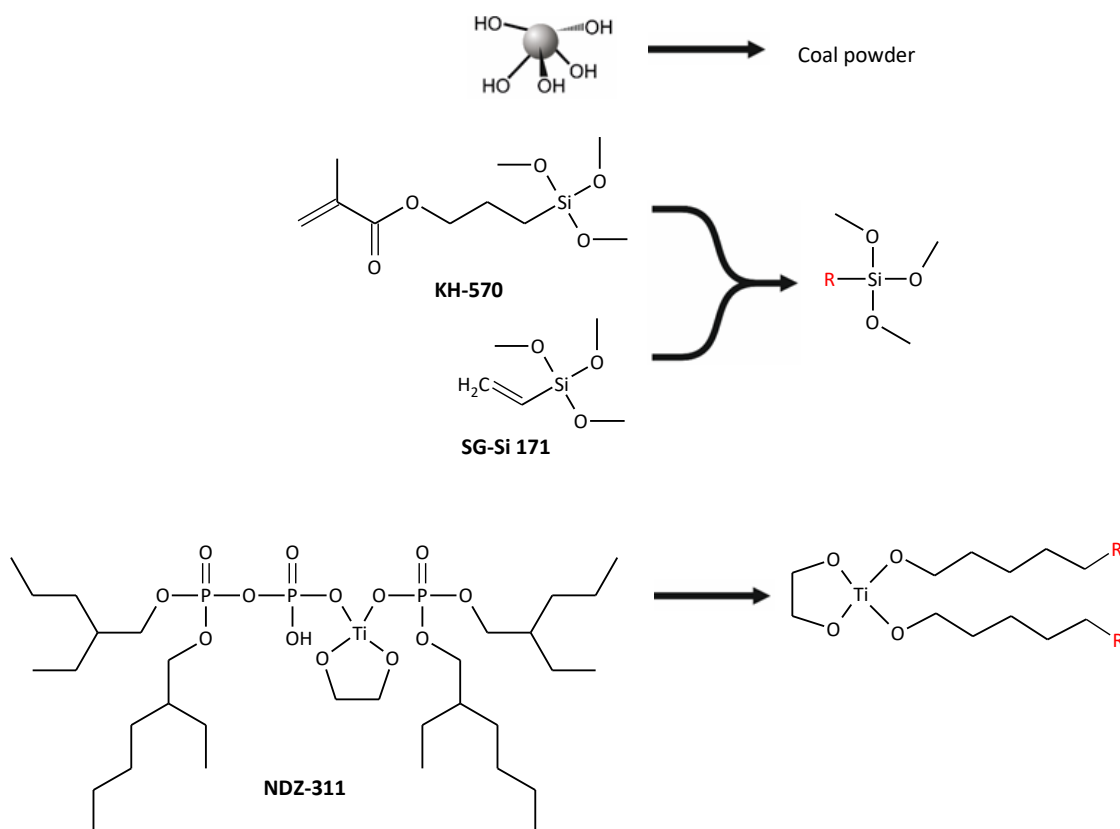
Figure 1.15 The molecular formulas of coal powder, KH-570, SG-Si171 and NDZ-311 [112].

B. L. Zhu et al. prepared LDPE matrix composites with hollow glass sphere (HGM) additives. In the study, it is examined the effect of density, quantity and modification on thermal and dielectric properties. The surface modification mechanism of HGM with KH570 is given schematically in Figure 1.16. It is found that thermal conductivity is reduced by increasing the amount of HGM in the composite or by decreasing the density of HGM. In samples with the same amount of HGM and density in the composite, it is investigated that the samples with HGM additive modified with the appropriate amount of KH570 silane coupling agent had higher

thermal conductivity than unmodified HGM added samples. It is observed that the dielectric constant of composites at 1 MHz frequency decreased with increasing amount of HGM or decreasing density of HGM, but dielectric loss increased with increasing amount of HGM or increasing density of HGM. In composites produced with HGM modified with the appropriate amount of KH570, the dielectric constant and loss at the frequency of 1 MHz decreased simultaneously. As a result of the improvement of the surface-modified HGM and LDPE matrix interface contact properties which was validated with SEM screening, it is revealed that the thermal conductivity and dielectric properties at low frequencies have been developed. The results obtained at the end of the experimental studies are presented that it is correlative when compared with the different models developed specifically for particle additive composites and hollow sphere added composites [113].
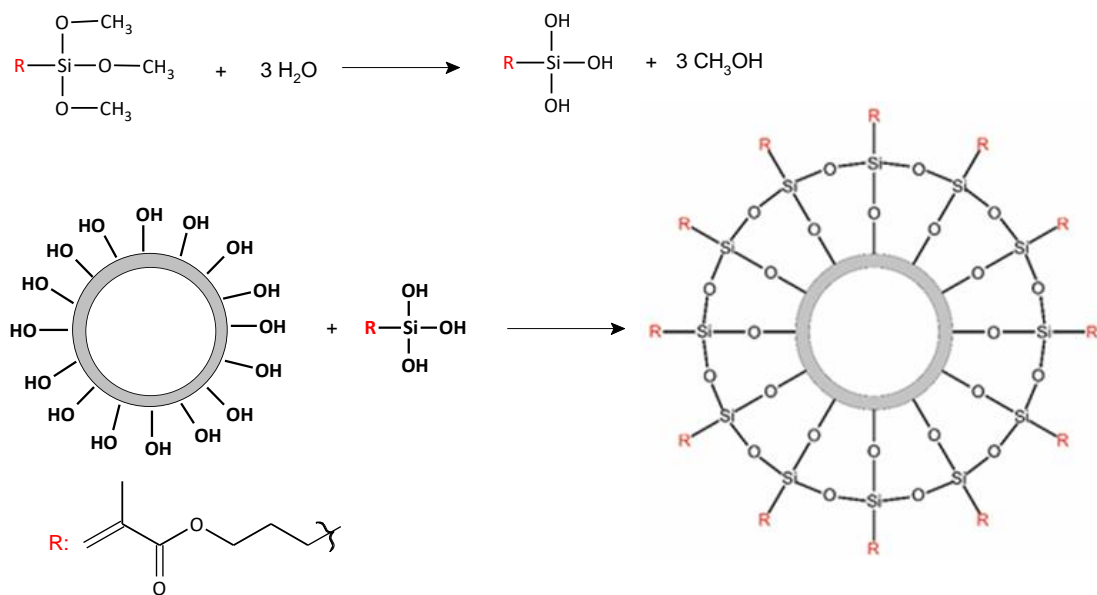
Figure 1.16 The mechanism of surface modification of HGM with KH570 [113].

In a study conducted by F.R. Lamastra et al. in 2017, diatomite surface having hydrophobic properties was silanized in a basic and ecologist way with sulfur-containing organosilanes in order to exhibit hydrophilic properties for rubber applications. Chemical modifications were carried out at 85 °C in H_2O:NaOH:H_2O_2 solution. The modified diatomic toxic solvent-free bis(triethoxysilylpropyl) were silanized with disulphite. Morphological properties and chemical composition of the diatomite were investigated in Energy Dispersive X-ray Spectroscopy (EDAX) and

31

Field Emission Scanning Electron Microscopy (FE-SEM). Surface modification and silanization effect was evaluated with FTIR and XPS. The diatomite pore size was chosen from different diatom types ranging from 25 nm to 1 μm. Spectroscopic characterization studies have confirmed the occurence of silanization reactions with some silanols. Silanized diatomite and untreated diatomite were used as filling material in uncured vulcanized solvent casting Styrene-Butadiene Rubber (SBR) films to verify that the modification did not negatively affect the polymer/filler material interface. In films with 10% diatomite additives (silanized or untreated), the elastic modulus was increased by 50% without significantly affecting the tensile strength. When the rupture surfaces obtained from the tensile test were examined with SEM, it was observed that both silanized and untreated diatomites dispersed well in the polymer matrix, resulting in good SBR/filler interface adhesion [114].

Iyer and Torkelson examined the effect of nano silica additive and the effect of modification of the silica surface in PP based hybrid nanocomposites with nano silica additive. In the study, pristine nano silica (p-NS) or HMDS modified nano silica (m-NS) added nanocomposites produced by solid-state shear pulverization technique. In microscopic examination, it was seen that 10-100 nm sized nano filling materials dispersed well in the composite. PP/p-NS hybrids have been shown to have superior Young's modulus and tensile strength. Compared to PP matrix material in PP/p-NS composites, the highest Young's modulus was seen in samples containing 8% p-NS by weight with increase of 46% and the highest tensile strength was observed with increase of 22% in samples containing 6% p-NS by weight. The thermal stability and nucleating efficiency in PP/p-NS hybrid increased significantly for PP crystallization. As a result of the study, it is revealed that the compatibility of polymer-nano filling material interface can be improved with the modification of additives with the effect of good dispersion [115].

In 2019, Liu et al. investigated the effect of modification of wood veneer with silane coupling agent in HDPE matrix composite materials with wood fiber (WF) additives for decorative applications. In the study, two different KH550 production number APTES and A171 production number trimethoxy vinyl silane were used as coupling agents. The schematic representation of the reaction that takes place on the wood veneer surface is given in Figure 1.17. The WF/HDPE composite was subjected to

dicumyl peroxide (DCP) surface treatment in order to increase the compatibility before coating with the wood veneer. When the reduced total reflection-FTIR spectroscopy curve was examined, it was seen that two different silane coupling agents were grafted on the surface of the wood veneer. The contact angle between distilled water and wood veneer after silanization increased from 46º to 120º after modification. It has been found that the bond strength between the modified wood veneer and the WF/HDPE composite has increased significantly, and the samples modified with A171 exhibit higher bond strength than those modified with the KH550. It was observed that as the amount of WF in the WF/HDPE composite increases, bond strength with wood veneer decreases and water resistance decreases. When SEM images are analyzed, it is obtained that the wood veneer and HF/HDPE composite interface are more intense in samples modified with A171 [116].
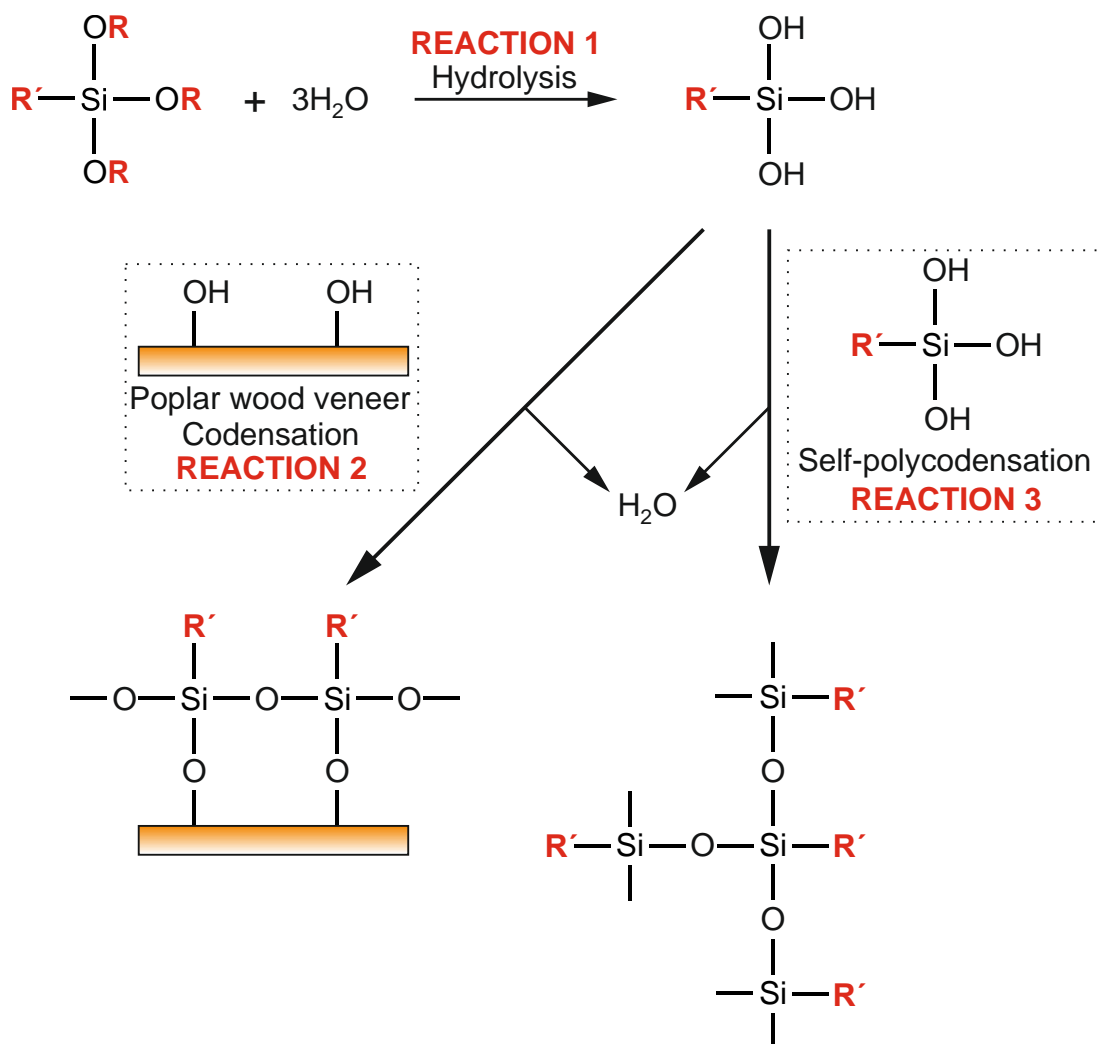
Figure 1.17 The reaction mechanism of silane Reaction 1 mechanism of hydrolysis; Reaction 2 bonding with wood; Reaction 3 self-condensation. R' represents the radical ''CH$_2$@CHA" of A171 and the radical ''NH$_2$(CH$_2$)3A" of KH550 [117, 118].

Wen et al. made a two-stage surface treatment on carbon fiber in their study in 2019 and examined the interface properties in CF/EP composites. After the electrochemical oxidation process, polyacrylonitrile (PAN) based carbon fibers (CFs) were grafted with KH550 silane coupling agent and two-stage surface modification was performed (Figure 1.18). FTIR, XPS, Raman spectroscopy and surface contact angle measurement analyzes were conducted to examine the physicochemical properties of modified CFs surfaces. When the CF surfaces are examined, the crystal structure slightly changes after KH550 silane coupling agent grafting, while the number of functional groups containing oxygen increased relatively after the surface treatment. The effects of the treatments applied on the CF surface on the interfacial shear strength (IFSS) and interlaminar shear strength (ILSS) properties of CF/EP composite materials were investigated in detail. Compared with untreated CF-added composite samples, it was seen that both electrochemical oxidant and KH550 silane grafting increased the IFSS and ILSS values of CF/EP composites. It has been concluded that in particular KH550 grafting with electrochemical oxidation to the CF surface exhibits maximum interface properties in CF/EP composites [119].
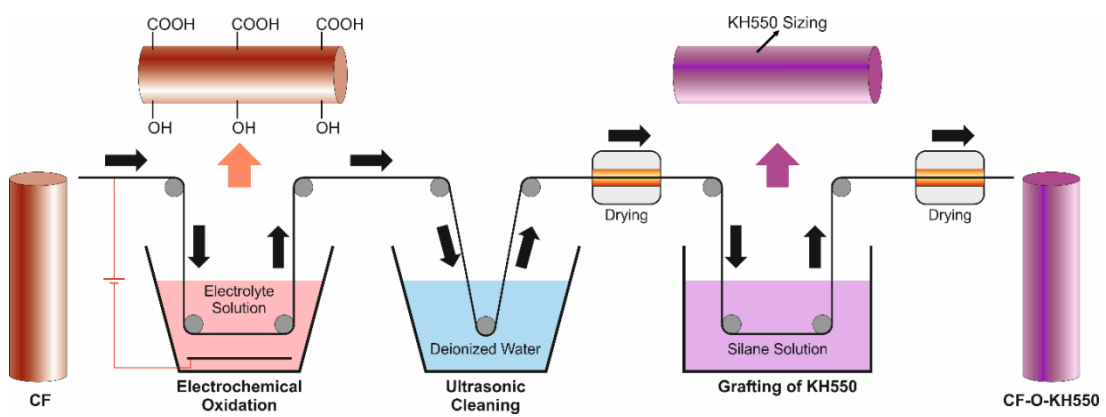
Figure 1.18 The schematic illustration of two-step surface treatment [119].

Su and Shi investigated the effect of mechanical properties on the polydimethylsiloxane (PDMS) composite matrix by modifying the hydrophilic fumed nano silica filling material with four different silane coupling agents with different non-hydrolytic groups. In the study, four different silane coupling agents

were used with similar hydrolytic groups such as ethyl triethoxysilane (ETES), octyl triethoxysilane (OTES), phenyl triethoxysilane (PTES) and APTES agents. Nano silica modifications containing six different amounts of agents were made in each coupling agent, and PDMS matrix composites were prepared with all these examples. Compared with the pure PDMS membrane, the modified nano silica composite added to the PDMS increases the tensile strength. When Hansen Solubility Parameter is accepted as characterizer which defines the miscibility between the non-hydrolytic groups of the four coupling agents and the solvent (n-hexane), it is showed that the miscibility has a significant impact on the tensile modulus of the composite membranes. When the length of the non-hydrolytic groups is greater than the distance between the two adjacent hydroxyl groups, the combination of the protected hydroxyl groups of the non-hydrolytic groups with other coupling agent molecules was blocked, thereby number of available hydroxyl groups reduced. When all of the potential hydroxyl groups on the nano silica surface react with the coupling agent molecules, the composite's tensile modulus will have reached the maximum value. In addition, according to the results of equilibrium swelling in ethanol and water, it is observed that the membrane with large tensile modulus has strong resistance to swelling [120].

In 2019, Luis Quiles-Carrillo et al. used slate fibers (SFs) modified with glycidyl- and amino-silane coupling agents in bio-based polyamide 1010 (PA1010) reinforcement. In the study, firstly, slate fibers were obtained from the tile sector wastes and surface modification was made with glycidyl- and amino-silane coupling agents to the surface of these fibers in order to improve the interface adhesion properties of the composite. The molecular structures of the silane coupling agents used in the study are given schematically in Figure 1.19. Compared with PA1010 material, it was observed that the mechanical properties of composite samples with both glycidyl-silane modified slate fibers (G-SF) and amino-silane modified slate fibers (A-SF) improved. A threefold increase was observed in the tensile modulus. Composite samples prepared with silanized SFs additives have been demonstrated to exhibit high thermal stability and improved thermo-mechanical resistance properties. In PA1010/SF composites, water uptake has fallen below 1% by weight, which has been evaluated to positively affect the mechanical performance of PA1010/SF

composites; this means PA1010/SF composites are less affected by atmospheric moisture. This improved property was attributed to the higher reactivity of the cyclic anhydride that were take place in the coupled silane and terminal hydroxyl groups of the biopolymer [121].
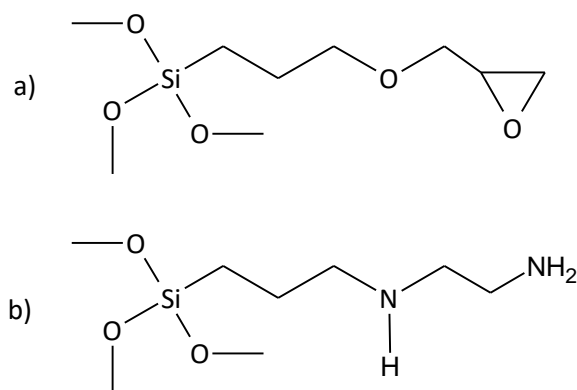
Figure 1.19 Chemical structure of the silane coupling agents: (a) (3-glycidyloxypropyl) trimethoxysilane (GPTMS); (b) [3-(2-aminoethylamino)propyl] trimethoxysilane (AEAPTMS).

In 2020, Karnati et al. modified the surface of silica nanoparticles (SNPs) with dual silane coupling agents in order to improve the performance of bitumen. In the study, the surface of SNPs was modified with 3-(trihydroxysilyl)propyl methylphosphonate (THPMP) and (3-glycidyloxypropyl) trimethoxysilane (GPTMS). Dual silane combinations were successfully performed in the form of APTES with THPMP and GPTMS with APTES. The surface-modified SNPs were added to the bitumen (PG 64-22) at a rate of 4% by weight. Mixing was carried out at a relatively low mixing temperature (135 °C) at low mixing speed (900 rpm) and short mixing time (30 min). When the samples prepared with all silane and silane combinations are examined, the best results in terms of the development of stability, agglomeration, distribution in the bitumen and the property of bitumen were found in the samples where APTES and GPTMS were combined. Compared to APTES-SNPs added bitumen composites reported before, APTES and GPTMS co-modified SNPs added bitumen composites show improved aging, fatigue cracking and low temperature cracking performance characteristics. Compared to APTES-SNPs, the APTES-GPTMS-SNPs combination decreased average particle size by 19% and increased particle mean zeta potential by 123%. As a result of the study, it has been demonstrated that the surface modified

36

SNPs added bitumen can be used in asphalt coating applications due to the improved properties [122].

As a result of technological developments and limited raw material resources, it is a situation that it has become more prominent in recent years to produce more advanced products with existing raw materials. Many studies have been carried out in the past century regarding composite materials in combining various types of materials in different proportions and in different geometric shapes. In the last situation that has been reached today, composite material productions that can exhibit higher properties come to the forefront. Matrix-filling material interface compatibility, which is one of the most important parameters affecting the performance of composite material, is a very actively studied subject. Especially in polymer-based composite materials, the surface properties of the filling material are critically important for interface compatibility. For this reason, in polymer based composite materials, it is desired to increase the compatibility with the matrix by adding additional processes to the surface of the additive material. The most important issue is the properties expected to be exhibited from the composite material to be produced. Scientists who are working in the field of material engineering design the most ideal composite material needed for the application by determining the matrix material selection, filling material and its proportions as well as the processes that can be applied to the matrix/filling material interface.

In this thesis, micronized quartz powders are incorporated into the PP matrix material, then the changed mechanical, thermal, viscoelastic and morphological properties of the modified PP material were investigated. The thesis study was shaped in three stages:

- In the first stage, high purity micronized quartz-doped PP matrix composite materials and silanized quartz doped PP matrix composite materials are produced. Micronized quartz used in the process is extracted from an important mine in our country and do not contain iron compounds that are one of the most important ore characteristics for the electricity sector. On the other hand, silanized quartz powders are supplied from foreign countries and are widely used commercially in the electrical industry.

- In the second stage of the study, surface modification was carried out by treating micronized quartz powders with four different silane coupling agents.

- In the third stage of the study, surface-modified micronized quartz added into PP matrix in order to produce the composite materials. Tensile strength and three point bending tests in order to determine the mechanical properties, Dynamic Mechanical Analysis (DMA) to determine viscoelastic properties, Scanning Electron Microscopy (SEM) analysis to observe matrix/filling material interface compatibility, Thermogravimetric Analysis (TGA) in order to determine thermal properties, Differential Scanning Calorimetry (DSC) analysis and Thermal Conductivity (TC) tests, X-Ray Diffraction (XRD) Analysis to determine crystallographic properties, and Fourier Transform Infrared Spectroscopy (FTIR) analysis to determine spectroscopic properties were applied for the composite materials produced in the first and third stages.

In the second stage, XRD, XPS, TGA and SEM analyzes were performed in order to determine the surface properties of the micronized quartz powders that were surface modified and to observe the effect of the modification.

In this study, PP granule material is preferred as polymeric matrix material considering that it can easy melted with high speed thermo kinetic mixer, it can be supplied easily and the common usage criteria in the industry. The reasons for selected micronized quartz as filling material can be listed as;

- Having high quality ore in our country,
- Using preferred material as additive in many sectors, especially in medium and high voltage switchgear devices,
- Not producing the surface-modified quartz powders commercially in our country as a result of this we are dependent on abroad.

The commercial silanized quartz is included in this study for a reason. It provides a comparison of the surface modification effect between the commercial silanized quartz and high purity micronized quartz powders with the samples under the same conditions and it creates the idea of starting point for commercial production. The materials used in this study, modification processes, composite material production

processes, test and analysis processes, results obtained and discussion sections are given in detail below.

2. MATERİALS AND METHOD

2.1 Materials

2.1.1 Polymer

In this research, Petoplen MH 418 polypropylene that was supplied from Petkim with 25 kg polyethylene sacks was used. Material properties of Petoplen MH 418 used in the study are given in Table 2.1.

Table 2.1 Properties of petoplen MH 418 polymer matrix.

Properties	Unit	Value
Melt Flow Index	g/10 minute	4.0-6.0
Density (23°C)	g/cm^3	0.905
Melting Point (DSC)	°C	163
Tensile Strength at Yield	MPa	34
Tensile Strength at Break	MPa	42
Flexural Modulus	MPa	1450
Color B 10 D 65	-	1.8

2.1.2 Powders

In this study, micronized quartz powder obtained from quartz that extracted from the mines of Pomza Export Mining Industry and Trade Co. in the region of Salihli Kaletepe and the silanized quartz with surface modification obtained from Quarzwerke Group was applied. Also, micronized quartz powder taken from Pomza was used as filling material in polymer matrix composite materials after it has been modified with four different surface agents. The result of particle size analysis of micronized quartz powder is indicated in Table 2.2.

Particle size distribution graphs of micronized quartz and commercial silanized quartz powders supplied are given in figures 2.1. D10, D50 and D90 values of micronized quartz powders were obtained as 2.50, 24.12 and 75.53 μm, respectively. D10, D50 and D90 values of commercial silanized quartz powders were obtained as 2.02, 13.48 and 36.81 μm, respectively. Particle size distribution of commercial silanized quartz powders is lower and homogeneous than micronized quartz.
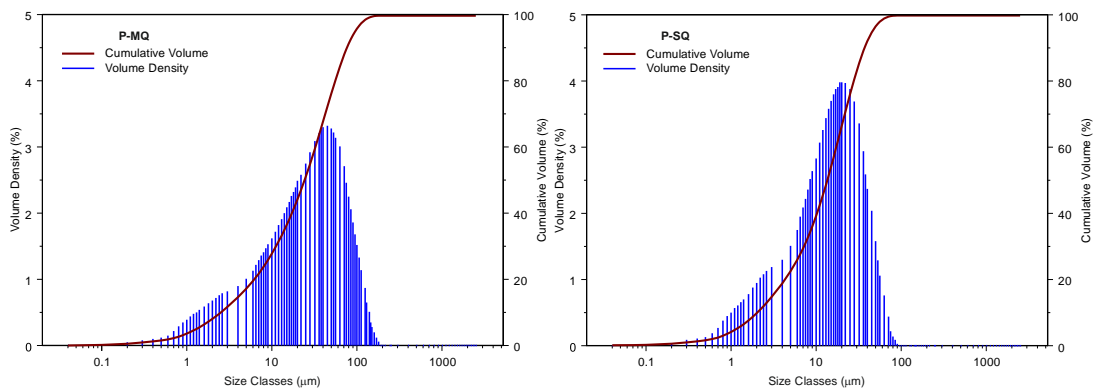
Figure 2.1 Particle size distrubiton analysis of P-MQ and P-SQ samples

Table 2.2 Particle size analysis result of micronized quartz and silanized quartz powders

Samples	D_{10} (μm)	D_{50} (μm)	D_{90} (μm)
P-MQ	2.50	24.12	75.53
P-SQ	2.02	13.46	36.81

Micronized quartz powder is widely used as filling material for insulation applications in electricity sector because of its low electrical conductivity, high abrasion and corrosion resistance. The most important feature that should be considered while it is used as Epoxy filling material because of the insulating property is the amount of iron and iron compounds in impurity atoms. Chemical analysis of micronized quartz powders used in this study is given in Table 2.3.

Table 2.3 Chemical analysis of micronized quartz powders.

SiO_2	Fe_2O_3	Al_2O_3	TiO_2	CaO	K_2O	Others
%	%	%	%	%	%	%
99.410	0.040	0.200	0.002	0.160	0.020	0.080

2.1.3 Surface Modifying Agents

Four different agents were selected for surface modification process of micronized quartz powder. The common properties of selected agents are advanced adhesive characteristics, be used in wide range of epoxy application and easily available in the market. Surface modification agents and their properties are given below.

2.1.3.1 Silquest A-187

Silquest A-187 is epoxy functional silane that may be suitable for urethane, epoxy, polysulphide, silicone and acrylic caulk, coatings, sealants and adhesives in terms of adhesive properties. Its chemical name is γ-glycidoxypropyltrimethoxysilane and molecular formula is $C_9H_{20}O_5Si$ and the chemical structure is shown in Figure 2.2 below. Some physical properties of Silquest A-187 surface modification agent is indicated in Table 2.4.
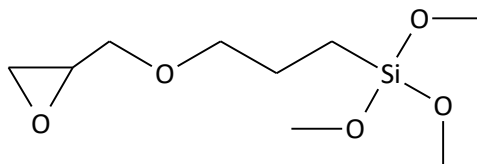
Figure 2.2 Moleculer structure of γ-glycidoxypropyltrimethoxysilane.

Table 2.4 Typical physical properties of Silquest A-187.

Properties	Unit	Value
Apperance	-	Clear, Pale
Moleculer Weight	g/mol	236.1
Density	g/mL	1.070
Specific Gravity at 25/25℃	-	1.069
Refractive Index nD 25℃	-	1.427
Flash Point	℃	110
Boiling Point	℃	120

2.1.3.2 Coatosil MP 200

Coatosil MP 200 is an oligomeric functional epoxy silane that is used as adhesion enhancer or binder in polysulfide, urethane, epoxy and acrylic caulk, filling pastes, adhesives and coatings. Its chemical name is 3-glycidyl-oxypropyl-trimethoxy-silane and the molecular structure is given in Figure 2.3 below. Some physical properties of Coatosil MP 200 surface modification agent is indicated in Table 2.5.
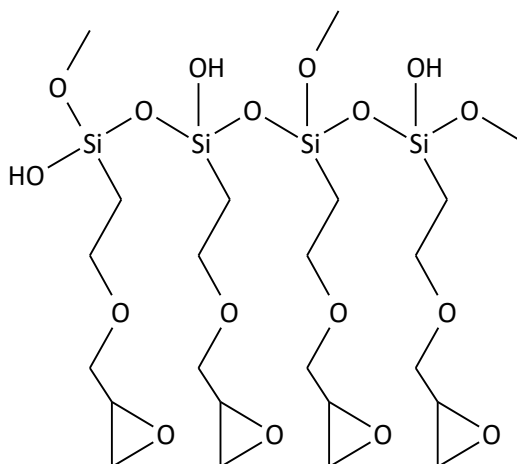
Figure 2.3 Moleculer structure of 3-glycidyl-oxypropyl-trimethoxy-silane (Coatosil MP 200).

Table 2.5 Typical physical properties of Coatosil MP 200.

Properties	Unit	Value
Apperance	-	Pale yellow
Density	g/mL	1.166
Vapor Pressure	20°C	<1.33 hPa
Refractive Index nD 25°C	-	1.429
Flash Point	°C	122
Boiling Point	°C	290

2.1.3.3 Coatosil 2287

Coatosil 2287 silane is used for improvement of cross-linking performance against to yellowing of waterbased dispersion of polymers such as polyurethane and acrylic. It may provide water absorption resistance and adhesive enhancing properties when it is applied for cross-linker. Its chemical name is 3-glycidoxypropylmethyldiethoxysilane and molecular formula is $C_{11}H_{24}O_4Si$. Its molecular structure is given in Figure 2.4 below. Some Physical properties of Coatosil 2287 surface modification agent are summarized in Table 2.6.

42
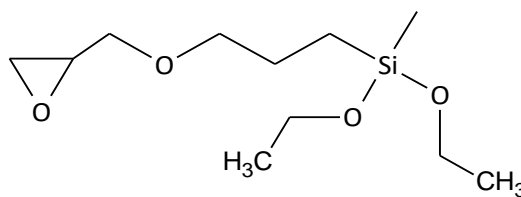
Figure 2.4 Moleculer structure of 3-glycidoxypropylmethyldiethoxysilane (Coatosil 2287).

Table 2.6 Typical physical properties of Coatosil 2287.

Properties	Unit	Value
Apperance	-	Clear, Pale
Moleculer Weight	g/mol	428.39
Density	g/mL	0.978
Refractive Index nD 25℃	-	1.431
Flash Point	℃	110
Boiling Point	℃	122

2.1.3.4 Vemab A-110

While Vemab A-110 silane is used for combining organic polymers and inorganic filling materials, it improves the mechanical, electrical, and resistance properties of materials into water and anti-aging characteristics. During the usage in thermoplastic and thermosetting resin, it increases considerably compression strength, sliding strength and the other physical properties as well as dry and wet bending strength. Vemab A-110 silane provides adhesion and anti-wetting properties when used in resin-casting. Its chemical name is 3-aminopropyltriethoxysilane and the molecular formula is $C_9H_{23}NO_3Si$. Its molecular structure is given in Figure 2.5 below. Some physical properties of Vemab A-110 surface modification agent are summarized in Table 2.7.
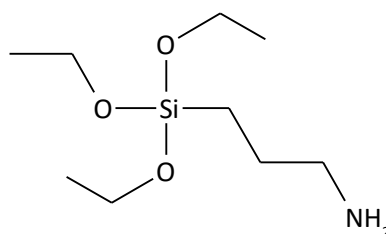
Figure 2.5 Moleculer structure of 3-aminopropyltriethoxysilane (Vemab A-110).

43

Table 2.7 Typical physical properties of Vemab A-110.

Properties	Unit	Value
Apperance	-	Clear, Pale
Moleculer Weight	g/mol	221.37
Density	g/mL	0.946
Refractive Index nD 25℃	-	1.422
Flash Point	℃	96
Boiling Point	℃	217

2.2 Quartz Surface Modification Process

Firstly, a liter of aqueous solution containing 5% alcohol in mass was prepared in the plastic beaker. The plastic beaker was placed on a magnetic stirrer and the pH value was recorded. Acetic acid was slowly added to the beaker. Once the pH value remained at the ideal level (3-3.5), 1.5 mL of the modification agent was added to the aqueous solution and stirred for 60 minutes at 500 rpm.

At the end of 60 minutes, 150 grams micronized quartz powders were added into the solution. The magnetic stirrer speed was increased to 800 rpm and the quartz was mixed in the solution during 90 minutes. At the end of 90 minutes, the magnetic stirrer was stopped and the solution was passed through a filter paper to obtain surface modified quartz powders. These powders were dried at 110℃ during 4 hours. A schematic representation of surface modification process flow is given in Figure 2.6.
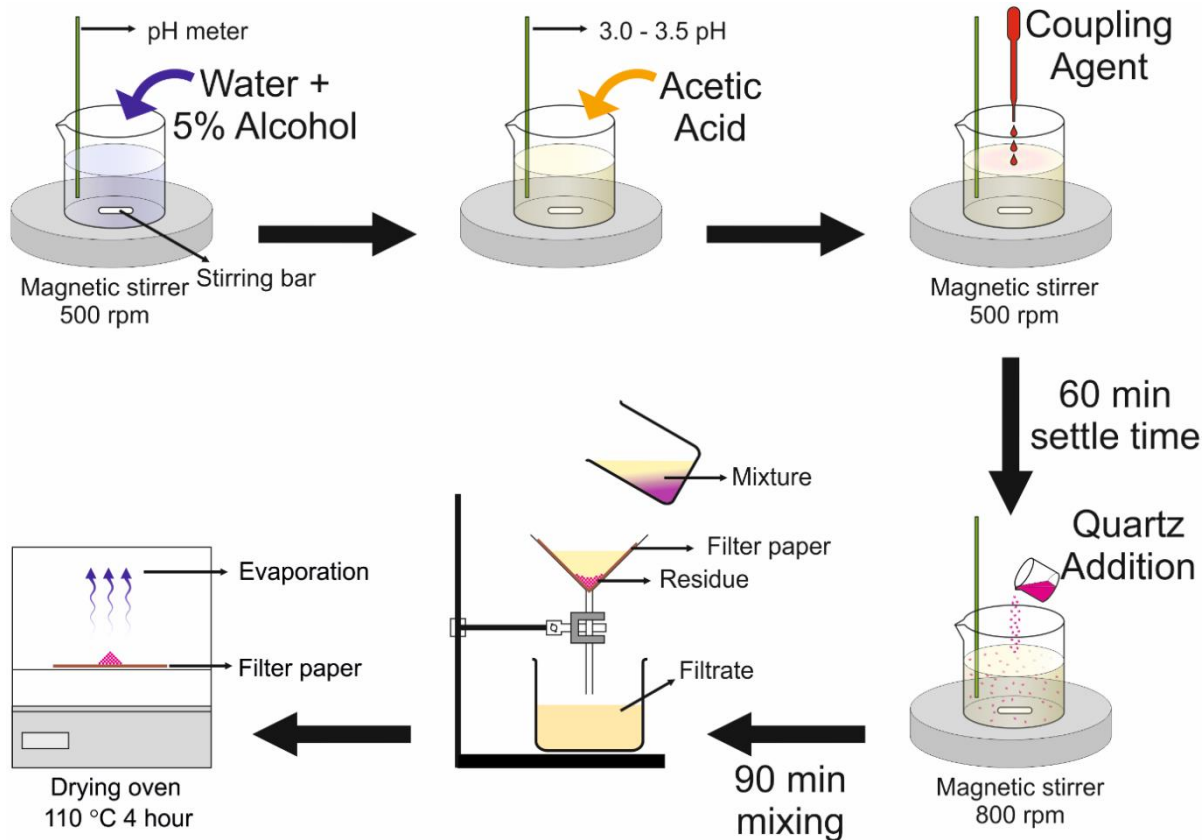
Figure 2.6 Shematic illustration of quartz surface modification process.

Table 2.8 Additive powders materials names.

Samples	Name
Micronized Quartz Powders	P-MQ
Silanized Quartz Powders	P-SQ
COATOSIL- 2287 Modified Micronized Quartz Powders	P-2287
COATOSIL-MP 200 Modified Micronized Quartz Powders	P-MP200
SILQUEST A-187 Modified Micronized Quartz Powders	P-A187
VEMAB A-110 Modified Micronized Quartz Powders	P-A110

2.3 Composite Production Process

High speed thermo-kinetic mixer (Mixer) was used to produce PP based composite materials. In this mixer rotating at a speed of 2000 rpm, the materials can reach a temperature of approximately 190 ℃. The resulting polymer pulps are cooled in the desired form to provide preparation of test samples for various tests. Its application is

simple and fast, so it is widely used in preliminary tests in the plastic industry [123, 124].

The most important advantage of the mixer is that it allows for the production of composite materials with ideal dispersed additive material in short periods [125]. The materials melted as a result of the mixing in the mixer were taken to the plates with the dimensions of 200X200 mm and molded in temperature and time controlled hot cold press (Gülnar hot press, Turkey). In order to produce composites in a high speed thermo kinetic mixer, composite mixtures of 70 grams were prepared. After mixtures containing 10%, 20, 30 and 40% micronized quartz amount were prepared with the help of precision scales, productions were made. It was observed that quartz was agglomerated in the composite plates produced in the 40% micronized quartz-containing composite samples. Accordingly, 40% of products with micronized quartz added products were not taken to the tests because they would be misleading in reflecting the current situation.

Composites containing 10%, 20 and 30% quartz were produced. They all were prepared and produced in silanized quartz added composite production. Mixtures of fixed 10% additive ratio were prepared in the production of surface modified quartz doped products. The path followed in production; 70 grams mixtures are prepared at the desired particle/polymer ratio in the precision scales. Then these mixtures were placed in the mixer's tank and the machine was started. After 20 seconds, the machine was stopped to open the tank and place the melted mixture in 2 metal plates measuring 200X200 mm. The melted material in the plate was molded by pressure molding technique in heating and cooling control press. The molded composite samples were cut into special molds for standard testing. A schematic representation of all this production flow is given in Figure 2.7. The names of the PP based composite samples produced are given in Table 2.9.
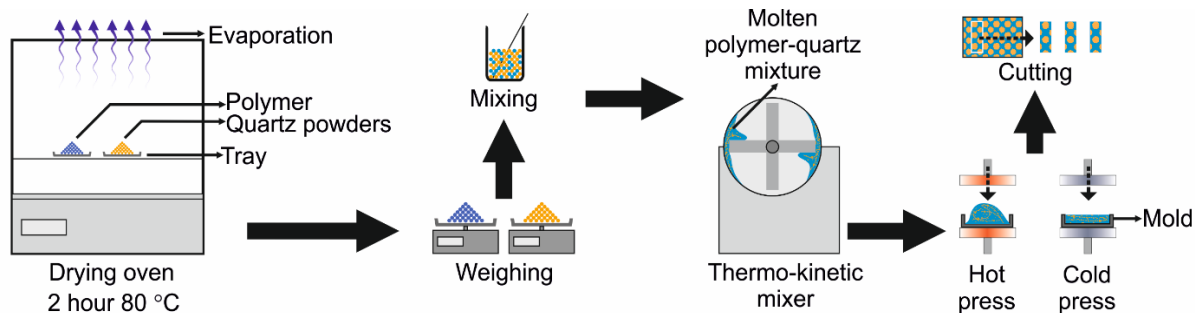
Figure 2.7 Schematic illustration of PP-based composite manufacturing process.

Table 2.9 PP based composites mixing ratios and samples names.

Samples (wt%)	Short Name
Micronized Quartz Reinforced PP Composites	
10% Micronized Quartz + 90% PP Composite	**10MQ**
20% Micronized Quartz + 80% PP Composite	**20MQ**
30% Micronized Quartz + 70% PP Composite	**30MQ**
Silanized Quartz Reinforced PP Composites	
10% Silanized Quartz + 90% PP Composite	**10SQ**
20% Silanized Quartz + 80% PP Composite	**20SQ**
30% Silanized Quartz + 70% PP Composite	**30SQ**
40% Silanized Quartz + 60% PP Composite	**40SQ**
Surface Modified Quartz Reinforced PP Composites	
COATOSIL - 2287 Modified 10% Quartz + 90% PP Composite	**2287**
COATOSIL-MP 200 Modified 10% Quartz + 90% PP Composite	**MP200**
SILQUEST A-187 Modified 10% Quartz + 90% PP Composite	**A187**
VEMAB A-110 Modified 10% Quartz + 90% PP Composite	**A110**

2.4 Characterization

2.4.1 Tensile Testing

The tensile properties of PP and quartz powder reinforced PP composite specimens were tested at room temperature using a Shimadzu Autograph AG-IS Series universal testing machine at a crosshead speed of 50 mm/min according to ASTM standard D638 [126]. The average values of five tests for tensile strength and Young's modulus were reported for each specimen.

2.4.2 Three-Point Bending Test

Three-point bending tests were conducted to characterize the flexural properties of the PP and quartz powder reinforced PP composite plates by following the ASTM D790 standard [127]. The tests were performed using a Shimadzu Autograph AG-IS

Series universal testing machine at room temperature. The tests were carried out at a constant crosshead speed of 2 mm/min and span length of 32 mm.

2.4.3 Dynamic Mechanical Analysis (DMA)

The storage modulus and loss modulus of PP and quartz powder reinforced composites were evaluated using a dynamic mechanical analyzer (TA Instruments, DMA Q800) [128]. Single cantilever was used and multi frequency-strain modulus mode was selected to analyze all specimens between the temperatures of 25 and 130 °C at ambient condition.

2.4.4 Thermogravimetric Analysis (TGA)

Thermogravimetric analyses of the quartz powders, PP and quartz powders reinforced PP composites were conducted by using thermogravimetric analyzer (TA Instruments, TGAQ500). at a heating rate of 10°C/ min and the flow rate of 50 mL/min in the range of 30–600°C under nitrogen atmosphere [129].

2.4.5 Differential Scanning Calorimetry (DSC) Analysis

Measurements of crystallinity percentage, phase change temperatures and specific heat capacities of composite neat PP were performed in a differential scanning calorimetry (DSC) instrument. TA instrument trademark, Q2000 model DSC was used for each analysis. Before all measurements, the DSC instrument was calibrated with certified Indium standard. Measurement method was designed as a heat/cool/heat procedure. Heating and cooling rate of DSC was set up 10 °C/min at 20-200 °C. End of the first heating cycle, 5 min isothermal step was applied to DSC oven for relaxation and for removing all mechanical stress on to the samples [129]. Then the samples were cooled at a constant cooling rate from 200 to 20°C. At the second heating cycle, again samples were started to heat from 20 to 200 °C. 20 ml/min nitrogen atmosphere was applied for preventing degradation and oxidation of samples in the DSC chamber. Samples were weighted 10±1 mg and hermetic standard aluminum pans were used for all analysis.

2.4.6 Thermal Conductivity Analysis

The thermal conductivity of the PP composites were investigated TCi thermal conductivity analyzer which is C-THERM Technologies trademark thermal conductivity measurement

system. All samples through plane thermal conductivity measured under the same condition that was at 25℃ and direct measurement method was used [130]. All measurements were repeated at 10 times and average value of through plane thermal conductivity was taken [131].

2.4.7 X-Ray Diffraction (XRD) Analysis

The crystallographic structures of the recycled carbon fiber, PP, and recycled carbon fiber reinforced PP composites were determined by X-ray diffractometer (Panalytical Empyrean) with a LynxEye detector. Specimens were scanned from 10 to 80°. The scan step size and time per step used in this study were 0.0248 and 0.2 s, respectively.

2.4.8 Scanning Electron Microscopy (SEM) Analysis

The surfaces of the composite samples and expanded vermiculite particles were investigated using a scanning electron microscope (SEM) (Carl Zeiss 300VP, Germany) operated at 3,0 kV. A thin layer of gold was coated on the fractured surface of the composites by using an automatic sputter coater (Emitech K550X) to reduce the extent of sample arcing during SEM observation.

2.4.9 Fourier Transformed Infrared Spectroscopy (FTIR) Analysis

FTIR-ATR analyses of the PP and quartz powder reinforced PP composites were carried out by using Bruker Alpha spectrometer. The analyses were performed in the range of 400-4000 cm^{-1}, with a resolution of 4 cm^{-1}.

2.4.10 X-Ray Photoelectron Spectroscopy (XPS) Analysis

XPS analysis was performed to obtain information about the surface chemistry of the powders. The basic mechanism of this technique is based on the use of photons of certain energy to activate atoms on the sample surface. The energies of electrons ejected from the sample surface are filtered and then the intensity of the energy defined is recorded by the detector. The energy spectra obtained in this way give the resonance peak characteristic of the electronic structure of the atoms on the sample surface. Moreover, since the number of electrons recorded is proportional to the number of atoms on the surface, it is possible to obtain information about the atomic composition of the surface.

3. RESULTS AND DISCUSSION

In this study, micronized quartz powders, which are widely used as fillers in industry, were subjected to surface modification with 4 different surface-active agents. PP matrix composite materials were produced to compare the effect of the surface modification process on the filler-matrix compatibility with the silanized quartz commercially available. The effects of surface modification process on micronized quartz powders and PP based composite materials are given in 2 separate sections.

3.1 Investigation of Quartz Powders

3.1.1 X-Ray Photoelectron Spectroscopy (XPS) Analysis

When looking at the density of the characteristic peak of O1s at 532.9 eV, it originates from the Si—O single bonds, which are referred to the —OH group on the silica surface. Si2p and Si2s peaks observed at 103.4 and 155.2 eV,respectively, originating from the Si—O—Si bond on the quartz surface [134]. Apart from the expected peaks, the weak C1s peak was seen at 285.2 eV in the micronized quartz sample. When the studies in the literature are examined, there are various comments that this peak is caused by the incomplete hydrolysis of alkoxide during the synthesis of quartz powders [135-137]. However, taking into account that the micronized quartz powders used in this study are produced from ore, there are findings in the literature that this weak peak may originate from the adhesive table used during XPS analysis [138].
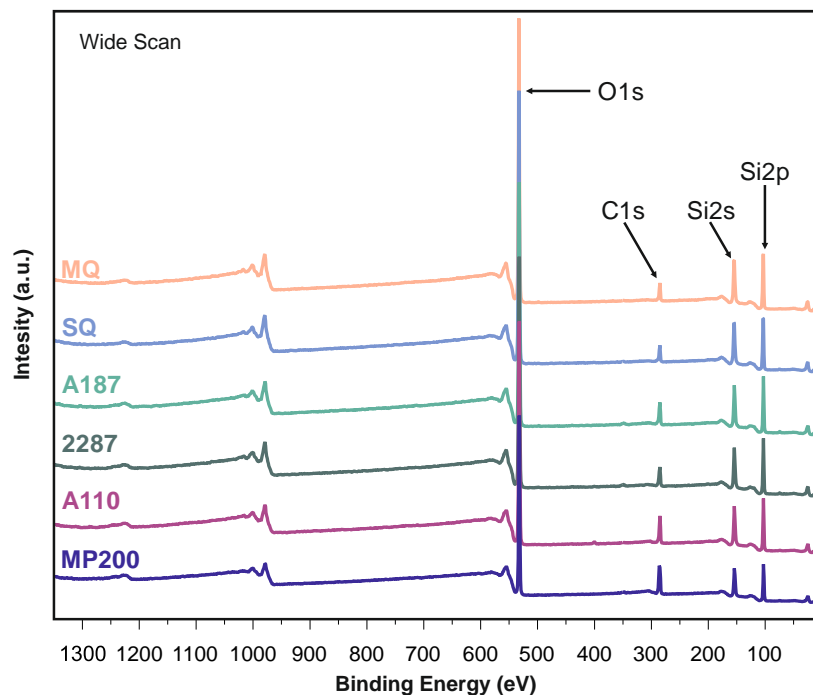
Figure 3.1 Wide scan XPS spectra of all powders samples.

The deconvolution of the C1s signal, given in Figure 3.2, exhibits three basic peaks, C—C or C—H, C—O or C—O—C, and O—C=O. C—C or C—H groups showed the greatest ratio among the all functional goups. The intensity of the C1s peak of the MQ sample appears to be lower than that of all surface-modified samples [139]. When the C1s signal peak of the P-MP200 sample is examined, the peak formation of the C—O—C bond at about 286.80 eV is noteworthy unlike all other examples. With the effect of this bond, the high C ratio seen in Table 3.1 was obtained compared to all powder samples [140].
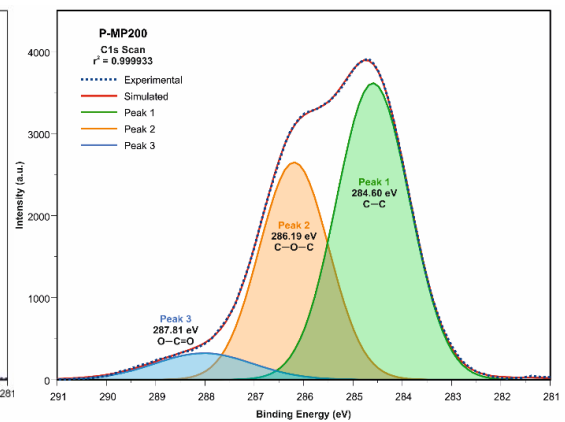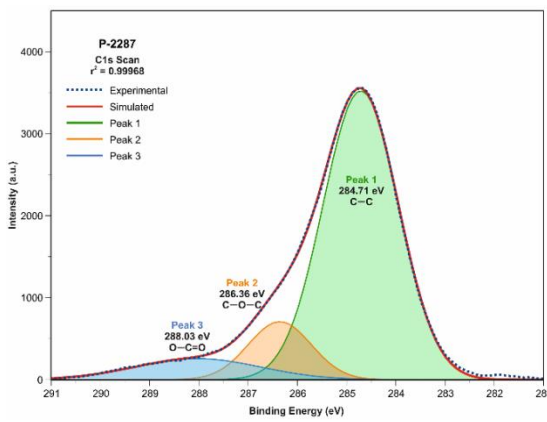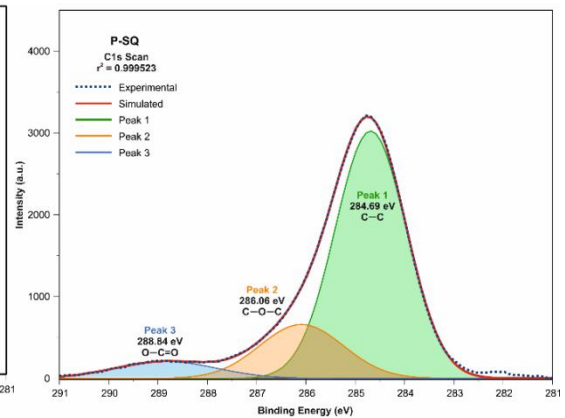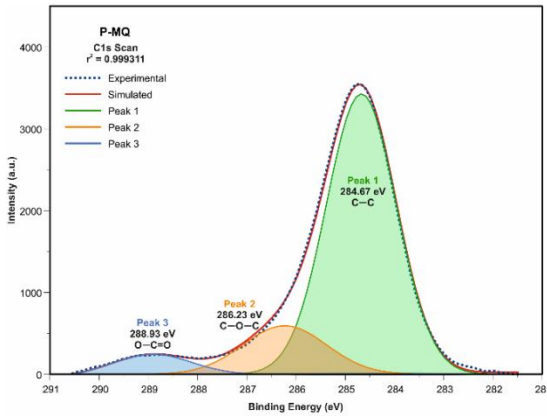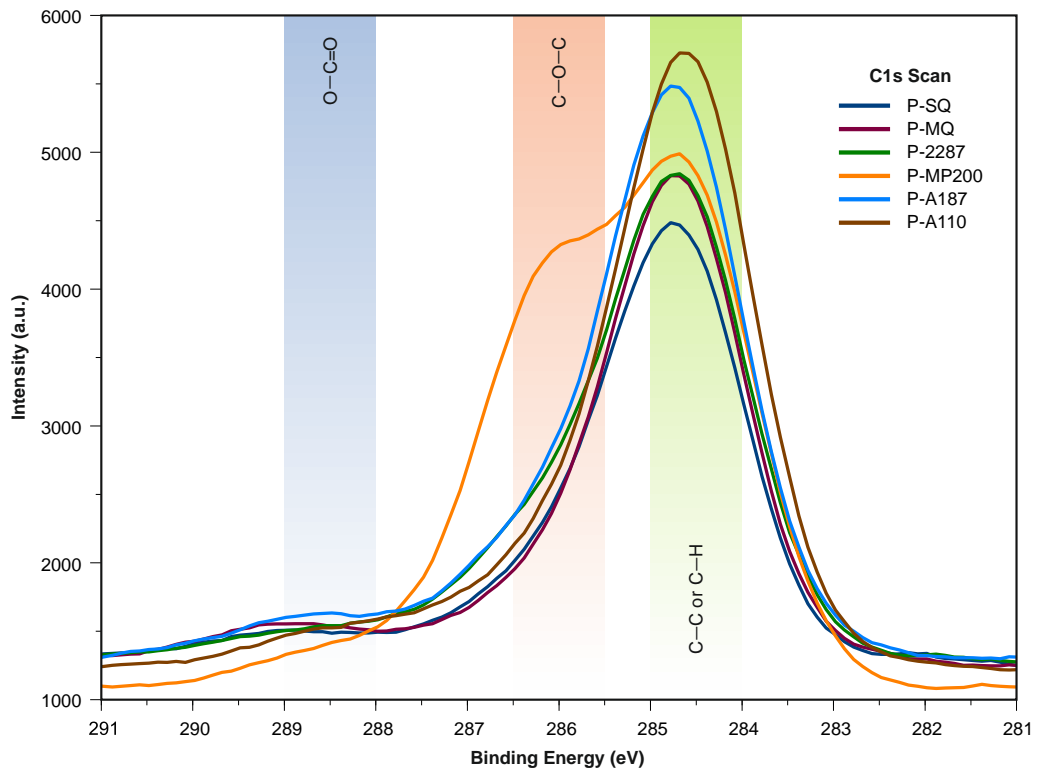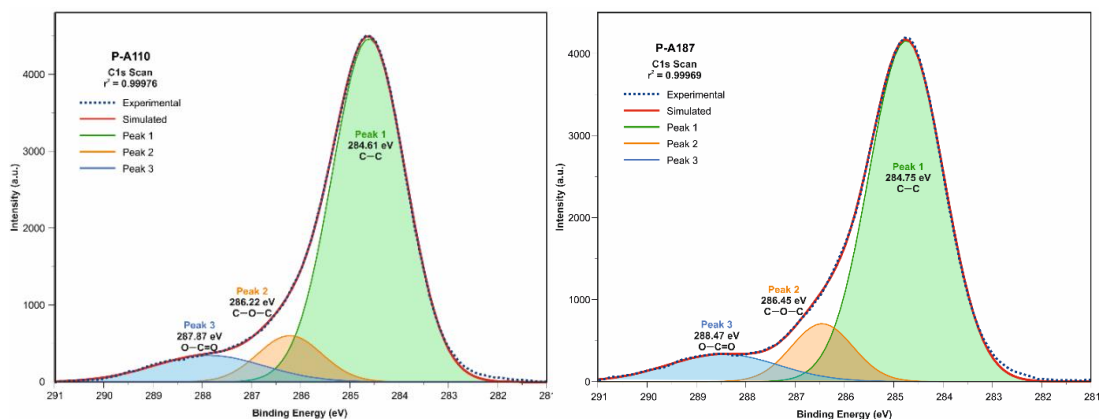
Figure 3.2 XPS peak deconvolution of C1s.

Peak intensities of O1s obtained from XPS analysis of quartz powders are given in Figure 3.3. When the peaks of the Si—O single bond are evaluated, it is seen that the peak intensities decrease with the effect of the modification. This situation is due to the decrease in the amount of oxygen and silicon on the surface of quartz powder with the effect of modification.

When O1s peaks of modified MQ filling materials were examined in detail, the most dramatic change was observed in the P-MP200 sample. In the P-MP200 sample, it is seen that the peak intensities of O1s have decreased considerably. This situation overlaps with the elemental analysis results given in table 3.2. While the oxygen content in the other three modified quartz samples was between 46-47%, this value was obtained to be 43.97% in the P-MP200 sample.

The sum of O and Si in the P-MQ sample was calculated approximately 93.88% by weight and 93.53% in the P-SQ sample (Table 3.1). In the modified quartz samples P-2287, P-MP200, P-A187 and P-A110, these values were obtained as 91.41%, 81.71%, 90.31% and 89.18%, respectively.
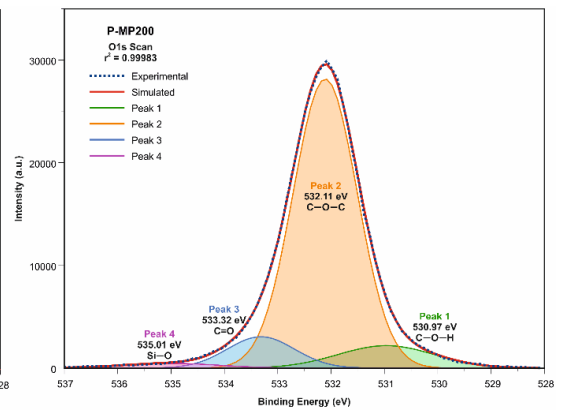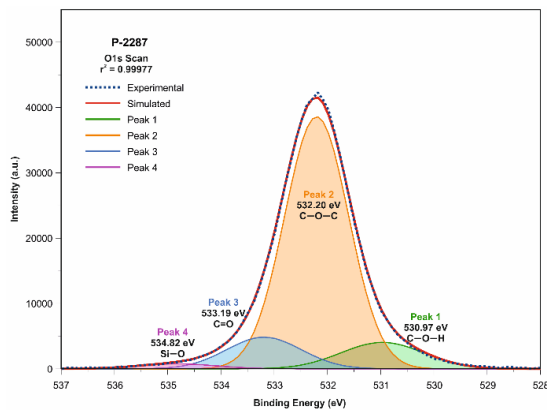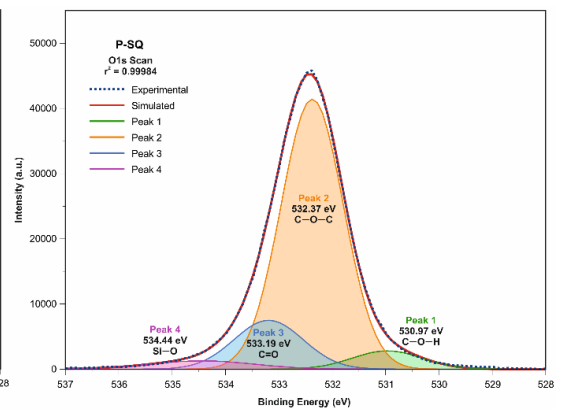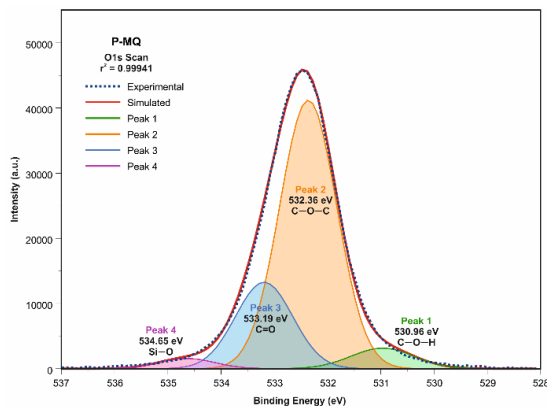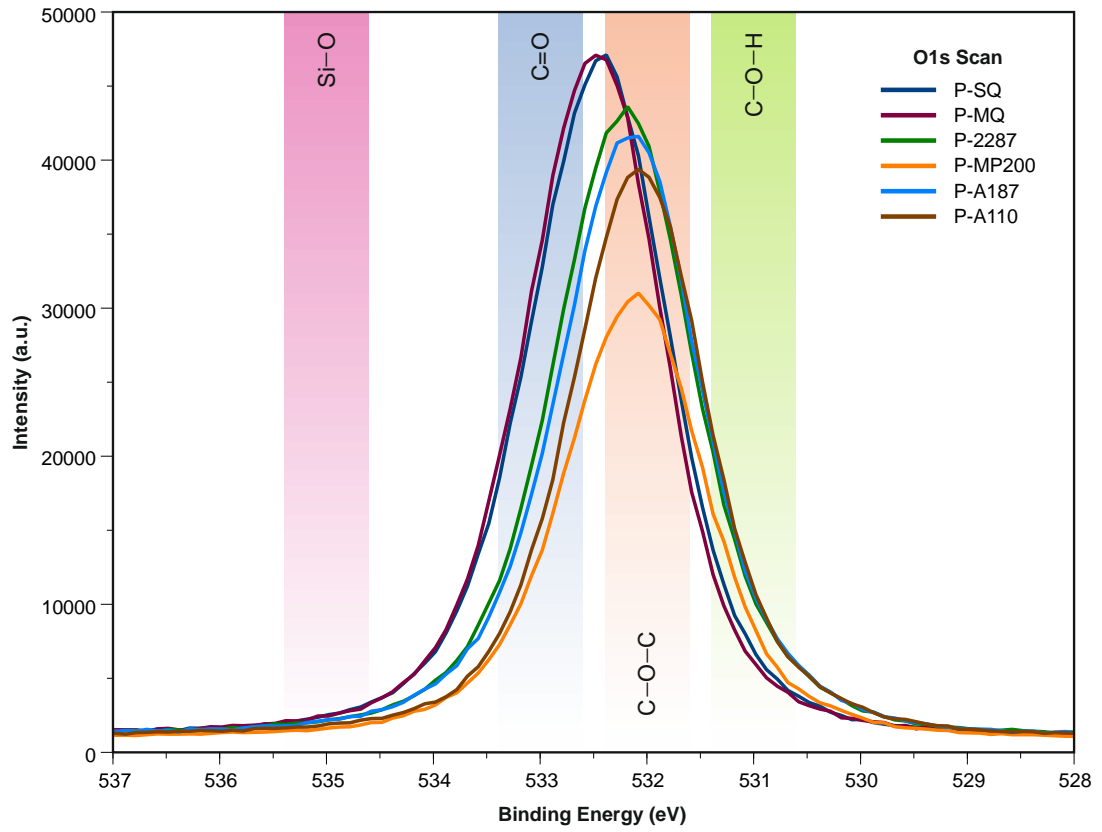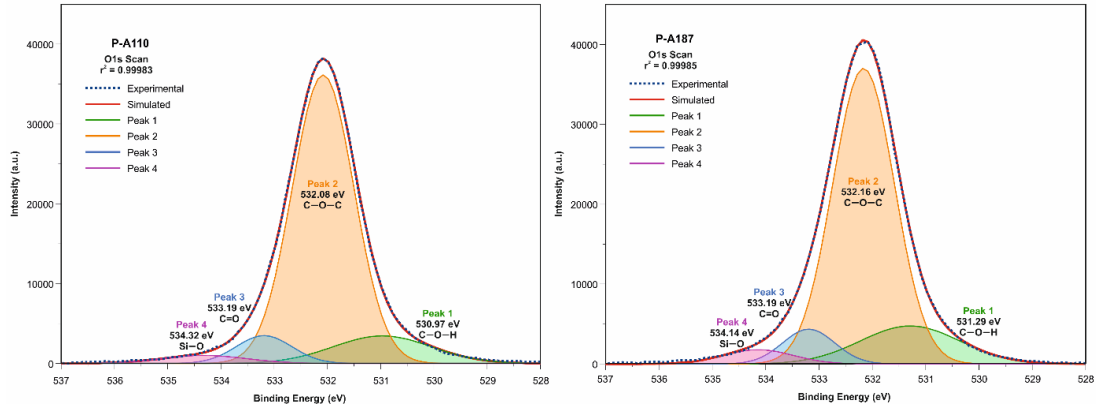
Figure 3.3 XPS peak deconvolution of O 1s.

Peak intensities Si2p obtained from XPS analysis of quartz powders are given in Figure 3.4. It is seen that the Si2p peak intensity decreases in MQ samples with the modification. In all modified samples, the intensity of the peaks at 103.53, 102.87 and 101.78 eV of Si—O, Si—OH and Si—O—Si bonds respectively decreased. Besides this decrease, the most important change was the peak intensities of the Si—O and Si—OH bond peaks under the Si2p peak. In the MQ sample, the intensity of the peaks of Si—O and Si—OH bonds were similar, while the peak intensity of the Si—O bond decreased dramatically with the modification.
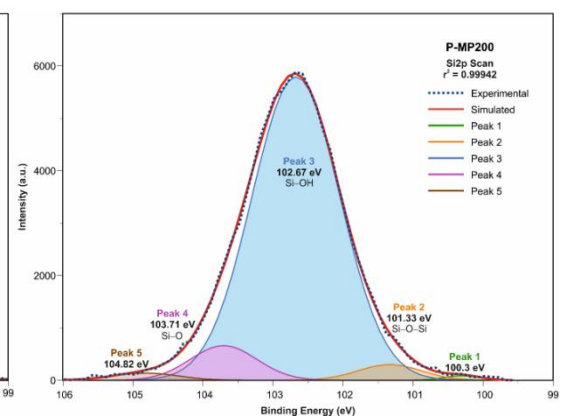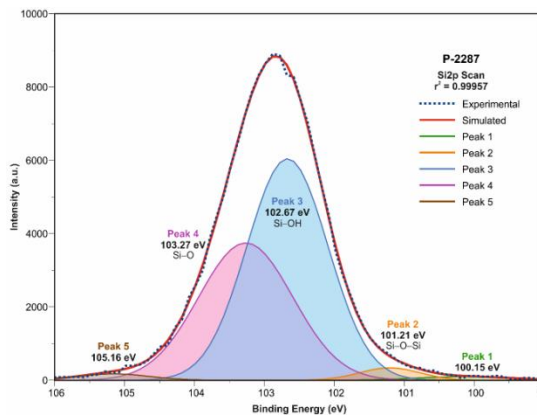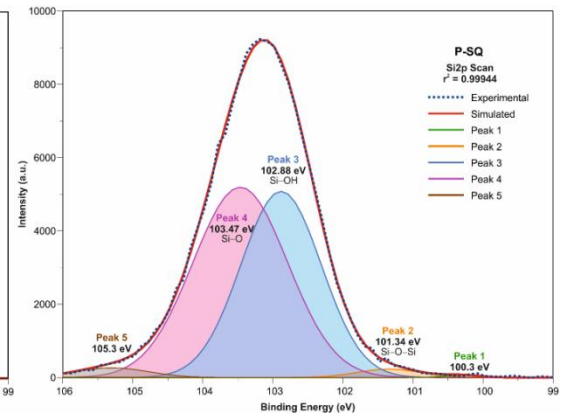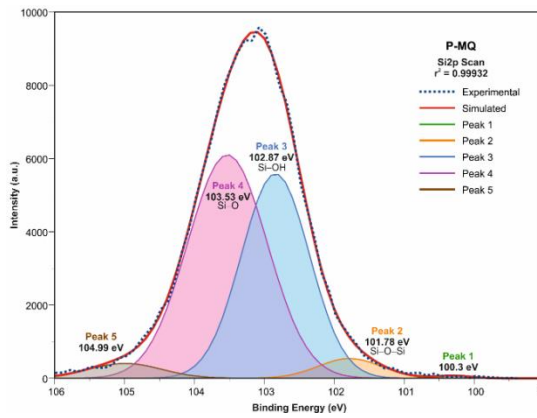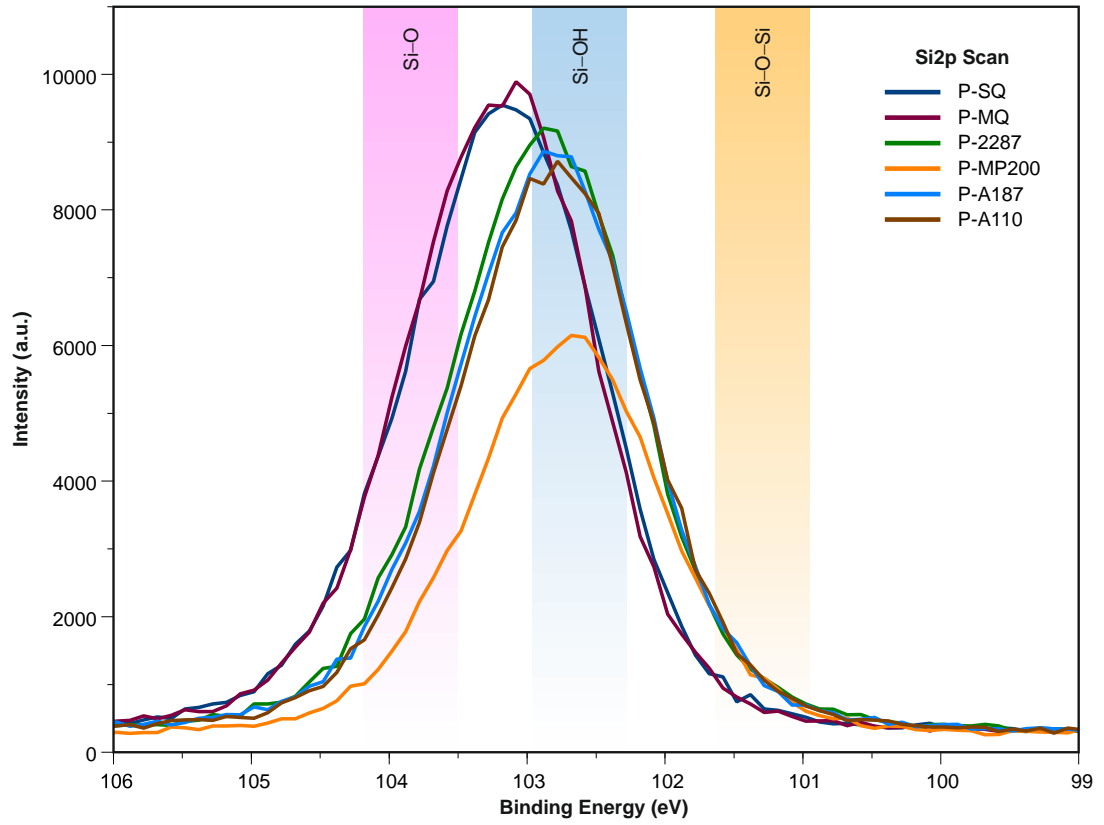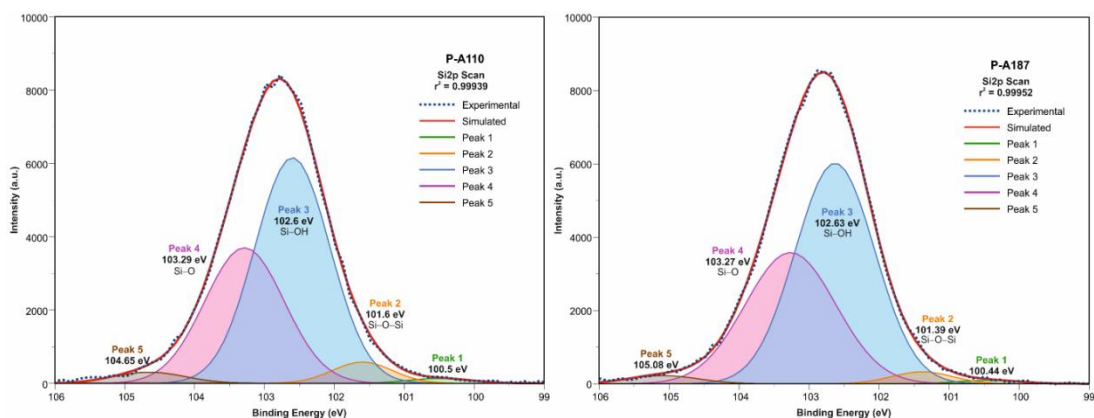
Figure 3.4 XPS peak deconvolution of Si1s.

Atomic element percentages and O/C ratio obtained from XPS analysis are listed in Table 3.1. The amount of C in the samples of P-MQ, P-SQ, P-2287, P-MP200, P-A187 and P-A110 were obtained as 6.12, 6.47, 8.59, 18.29, 9.69 and 10.82%, respectively. As can be seen from Table 3.1, P-MP200 exhibited the greatest C value among the samples, which indicates a better modification of quartz besides this sample has the lowest O/C value. In the modification process, it is observed that the amount of Si decreases while the amount of C increases with the effect of the functional groups of the coupling agent on the quartz surface. However, when looking at the C/Si ratios, it is 0.20 the lowest and 0.48 the highest in the modified quartz samples while 0.14 in the MQ sample. These XPS results confirmed that surface modification was successfully performed on the quartz surface [137].

Table 3.1 Summarizes the atomic weight concentrations, O/C and C/Sİ values of the samples.

Sample	O (%)	Si (%)	C (%)	O/C	C/Si
P-MQ	49.58	44.30	6.12	8.1	0.14
P-SQ	49.94	43.59	6.47	7.7	0.15
P-2287	47.79	43.62	8.59	5.7	0.20
P-MP200	43.97	37.74	18.29	2.4	0.48
P-A187	47.58	42.73	9.69	4.9	0.23
P-A110	46.13	43.05	10.82	4.3	0.25

3.1.2 Thermogravimetric Analysis (TGA)

The thermal degradation curve obtained from the TGA analysis made with micronized quartz, commercial silanized quartz and micronized quartz powders with surface modification is given in figure 3.5. When the degradation curve is examined,

it is seen that the degradation of the quartz samples with surface modification is higher than the unmodified samples on the surface.

When the degradation behavior is evaluated as two different regions, it is observed that the hydroxyl groups on the quartz surface decompose rapidly in the range of 40-200°C and the degradation continues especially in the samples with surface modification in the 200-600 °C range with increasing temperature [138,141,142]. This situation is thought to be a natural result of the decomposition of organic materials in the silane layer formed on the quartz surface with surface modification during increasing temperature. A similar situation has been observed with commercial silanized quartz powders. When the results are examined, it is confirmed from the thermal degradation curve that the silane layer is formed together with the surface modification on the micronized quartz surface.
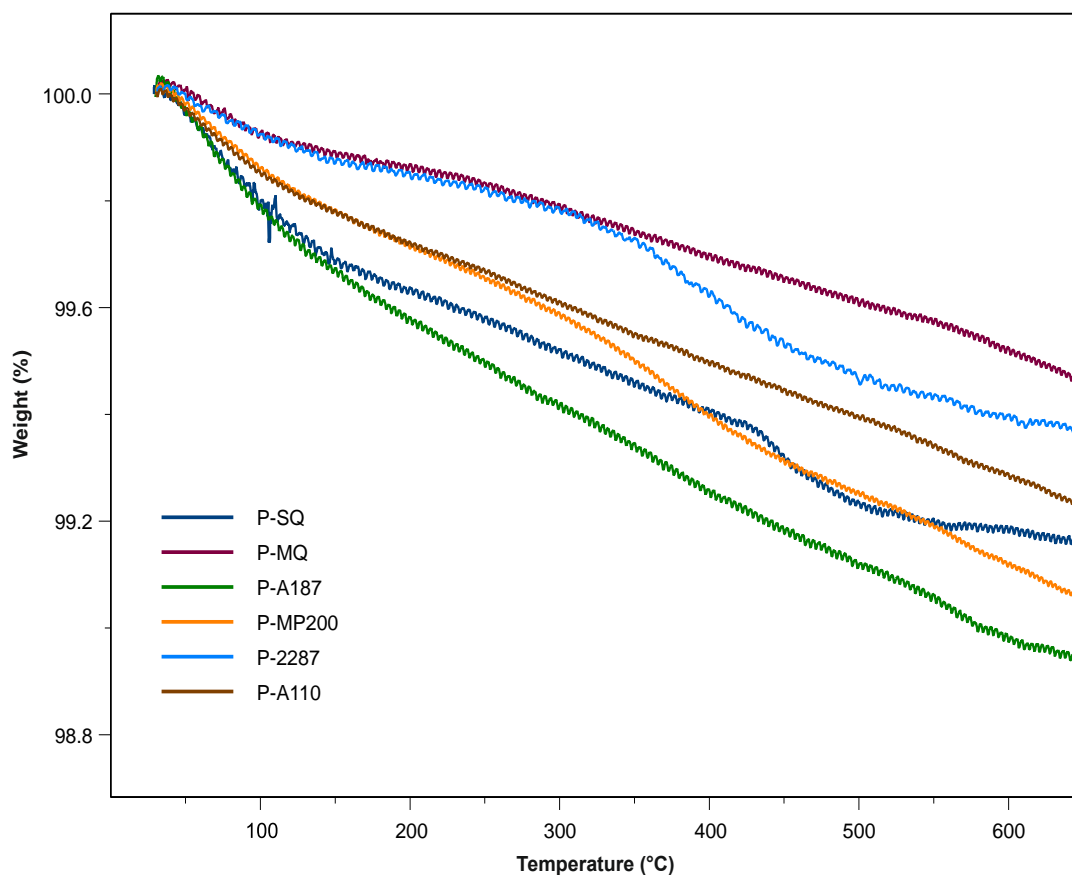
Figure 3.5 TGA thermograms of P-MQ, P-SQ and surface modified MQ powders.

3.1.3 X-Ray Diffraction (XRD) Analysis

XRD analysis of micronized quartz, commercial silanized quartz and surface modified quartz samples are given Figure 3.6. When the figure was examined, it is clear that the peaks at 21.83, 26.62, 36.49, 39.43, 40.23, 42.38, 45.72, 50.08, 55.30, 59.86, 63.98, 67.64, 67.83, 68.08, 73.43, 75.53, 77.51 and 79.78^o angles are present in all samples [143]. When surface modified quartz powders were examined, it was observed that no new peak occurred due to the modification process or content on surface modifying agents [97]. This can be attributed to the fact that the modification process applied to the MQ surface does not make any changes in the crystal structure of the MQ [104].
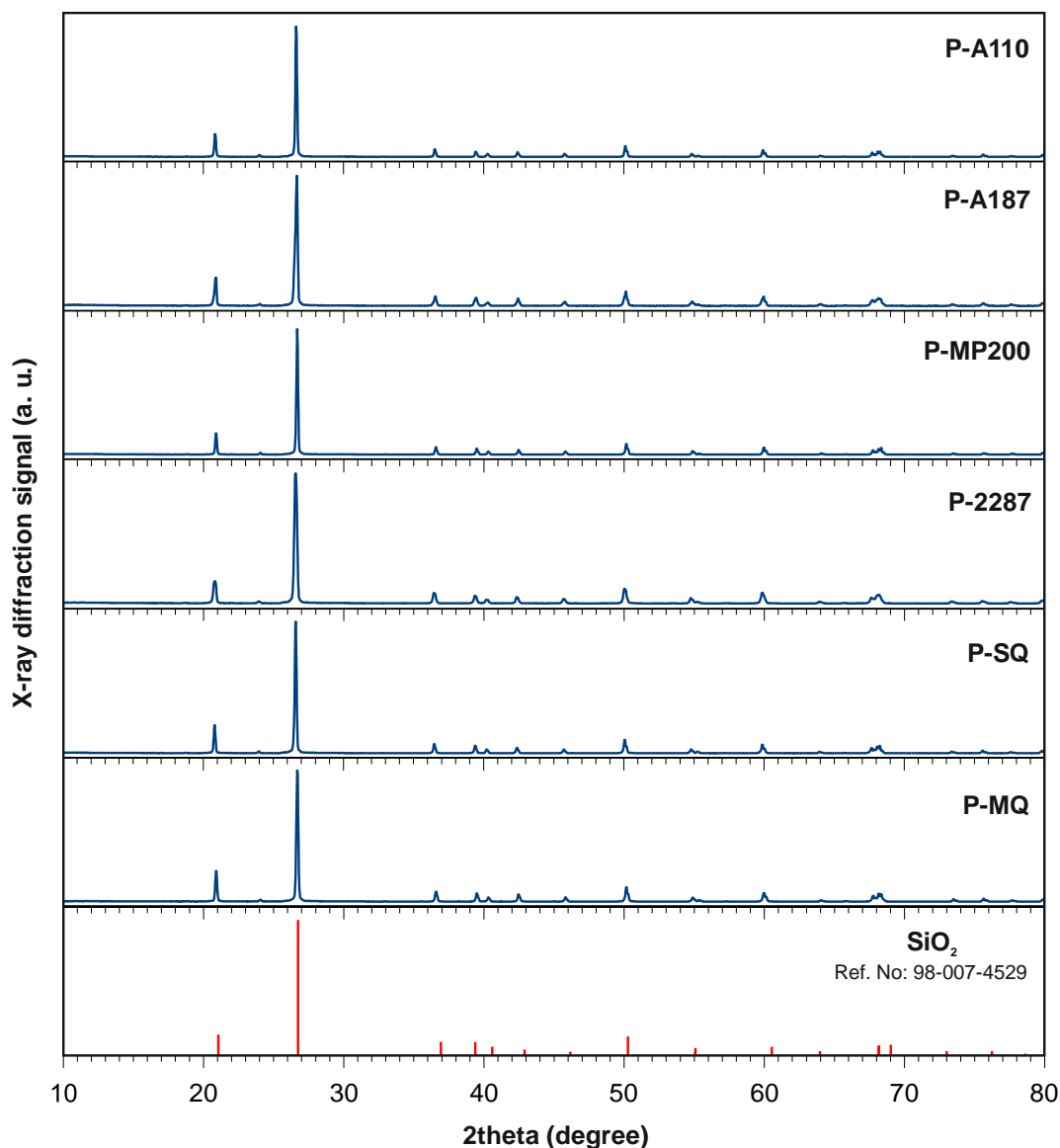
Figure 3.6 XRD patterns of SiO_2, P-MQ, P-SQ and surface modified MQ powders.

3.1.4 Scanning Electron Microscopy (SEM) Analysis

SEM images of P-MQ, P-SQ and modified quartz powder samples are shown Figure 3.7 and Figure 3.8. The effect of the modification process on the morphological properties of powders has not been fully visualized, as it is quite difficult to capture modified and unmodified samples of the same particles [97]. When comparing unmodified MQ and modified MQ powder samples, it is observed that agglomerations are reduced in modified MQ powder added composites due to the development of hydrophobic properties with the effect of the modification process.

This also reveals signally in commercial SQ and MQ examples. When the images are analyzed, especially in MQ and modified MQ samples, it is observed that there is a heterogeneous structure with very small particles and large particles together.
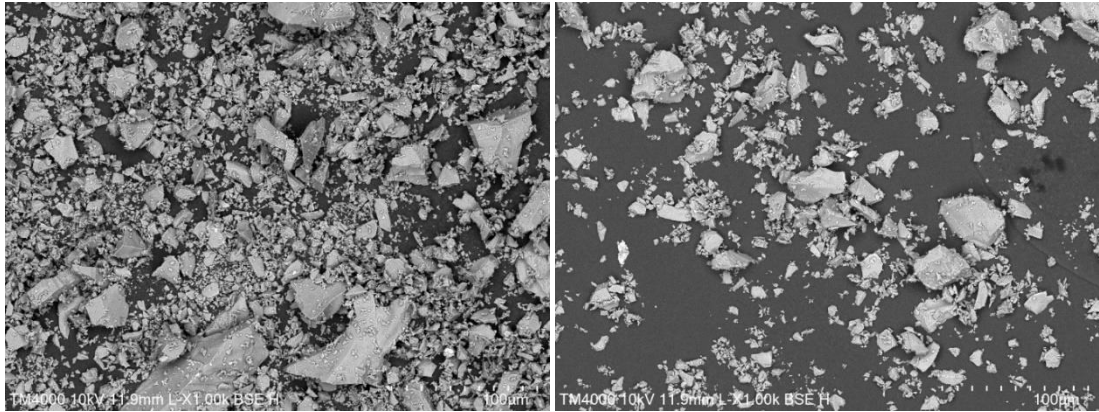
Figure 3.7 1kX magnification SEM image of a) P-MQ particles, b) P-SQ particles.
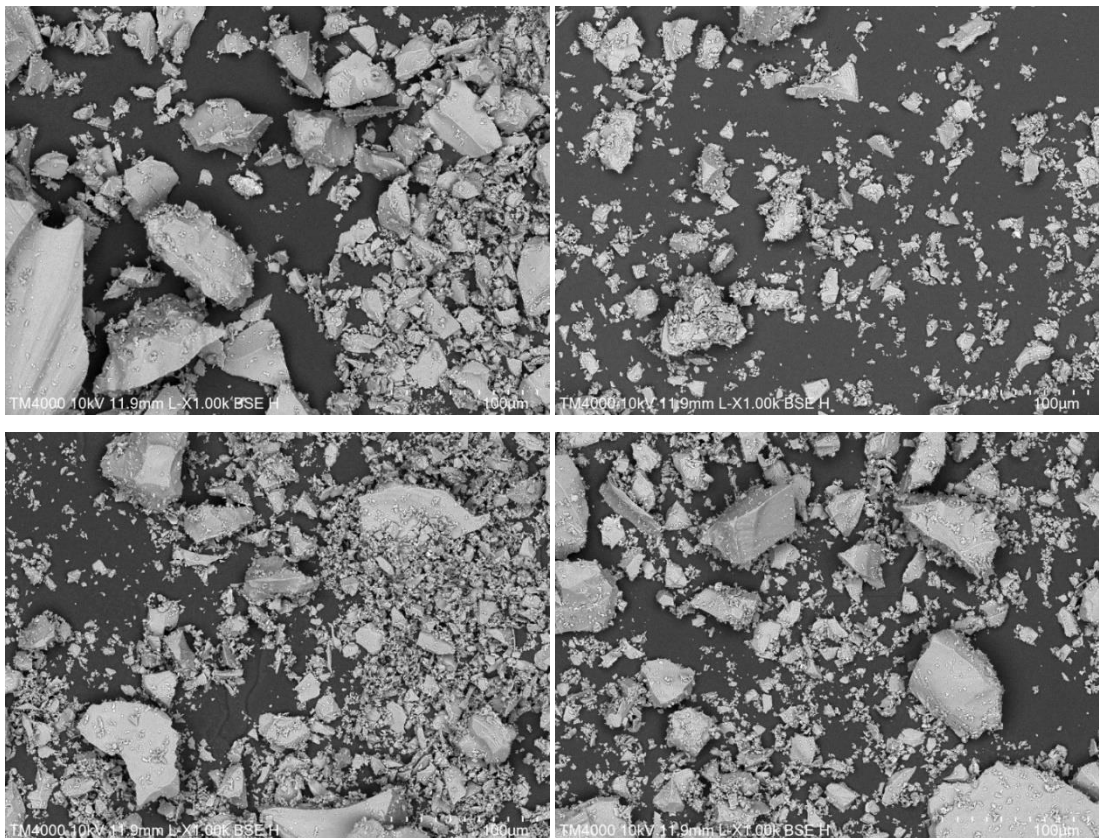
Figure 3.8 1kX magnification SEM image of a) P-2287 particles, b) P-MP200 particles, c) P-A187 particles, and d) P-A110 particles.

3.1.5 Fourier Transformed Infrared Spectroscopy (FTIR) Analysis

FTIR spectra of neat P-MQ, P-SQ and modified MQ powders fillers is given in Figure 3. 9. Absorption peaks of 1081, 1054, 795, 773 and 694 cm-1 wavelengths of Si — O bond were observed in all samples. The absorption peak of 2161 cm-1 wavelength is considered as CO absorption from the atmospheric environment by quartz powders [177]. When modified MQ powders and unmodified MQ powders were compared, the most significant change was observed in the absorption peak of O = C = O at 2363 cm-1 wavelength. With the modification, the intensity of the absorption peak of CO2 at this wavelength decreased and this peak was almost not observed in some modified MQ powders. This situation is evaluated to be caused by the breaking of various bonds on the surface of quartz powders in acidic solution during surface modification and the silane layer formed with the modification has the reducing effect of CO2 absorption.
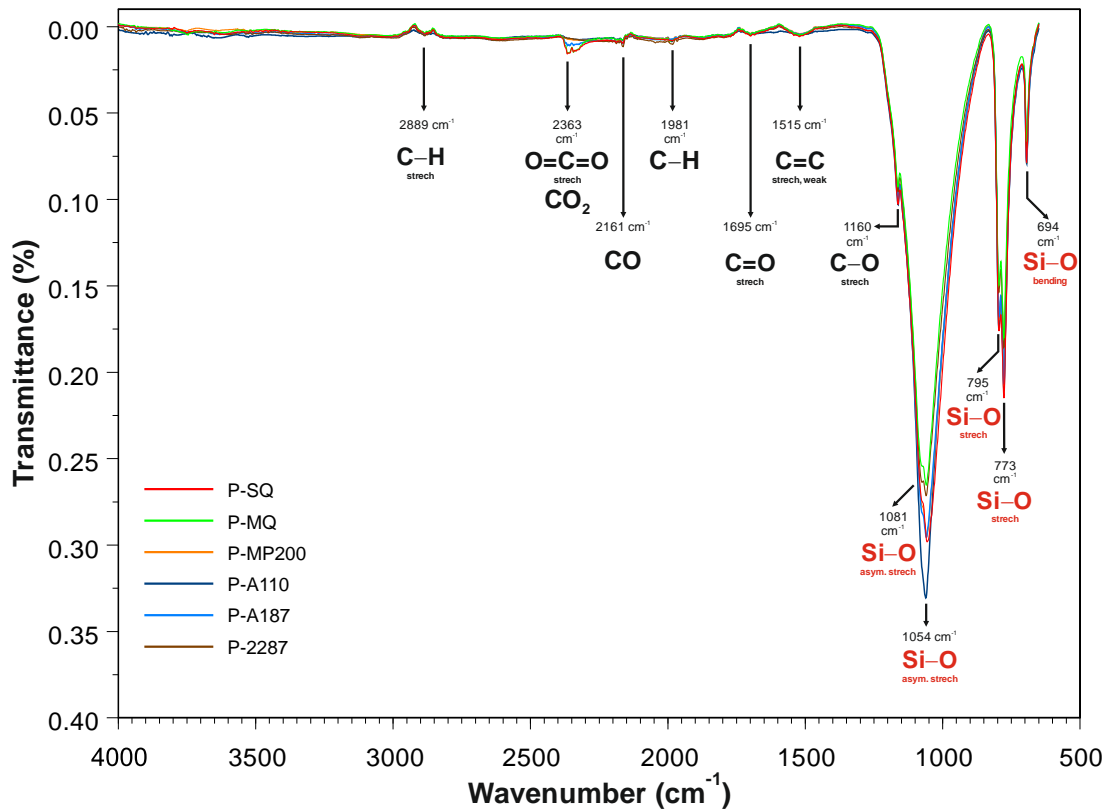
Figure 3.9 FTIR analysis of P-MQ, P-SQ and modified MQ powders

3.2 Quartz Added PP Based Composites

Tensile, Bending, viscoelastic (DMA), thermal (TGA, DSC, Thermal Conductivity), crystal structure (XRD), molecular properties (FTIR) and morphological (SEM) properties of PP based micronized quartz doped composite materials were investigated.

3.2.1 Mechanical Properties

Tensile tests and 3 point bending tests were performed to determine the mechanical properties of PP based quartz doped composite samples. The tensile strength of the composite materials, tensile modulus, % elongation, flexural strength and flexural modulus behavior were investigated.

3.2.1.1 Tensile Testing

Tensile strength and tensile modulus results of micronized quartz doped composite samples produced in high speed thermo-kinetic mixer is given in Figure 3.10. According to this figure, micronized quartz additive reduces the tensile strength of PP material. While tensile strength of PP was 34.20 MPa, 20% micronized quartz doped composite tensile strength is measured as 29.30 MPa, 30% micronized quartz doped composite is 26.28 MPa. As it is seen from the results, the tensile strength decreases as the micronized quartz amount increases in the composite [108]. The tensile strength of PP decreases approximately 14.33% in 10% by weight micronized quartz additive. The decrease in tensile strength compared to the pristine PP matrix material is due to the fact that the additive material cannot be wetted sufficiently by the matrix material, the powders are agglomerated, that is not dispersed, and there is poor adhesion between the matrix and the additive materials. In addition to the aggregation of quartz powders, increase of the filling rate in the composite, the tensile strength of the matrix has decreased gradually due to the increase of micro pores within the PP matrix [144, 145]. The SEM images obtained from the rupture zones after the tensile test support this result.

When Figure 3.10 is examined, it is seen that the quartz additive increases the tensile modulus of the composite material. The tensile modulus of PP is approximately 823 MPa. The tensile modulus of the composite material containing 30% by weight of

micronized quartz was increased approximately 62% compared to pristine PP and was measured as 1336 MPa. On the basis of tensile tests performed on 3 different composite materials, the tensile modulus of the 10% micronized quartz doped composite was measured as 1239 MPa, the tensile modulus of the 20% micronized quartz doped composite is 1169 MPa and the tensile modulus of the composite 30% micronized quartz doped composite was measured as 1336 MPa.
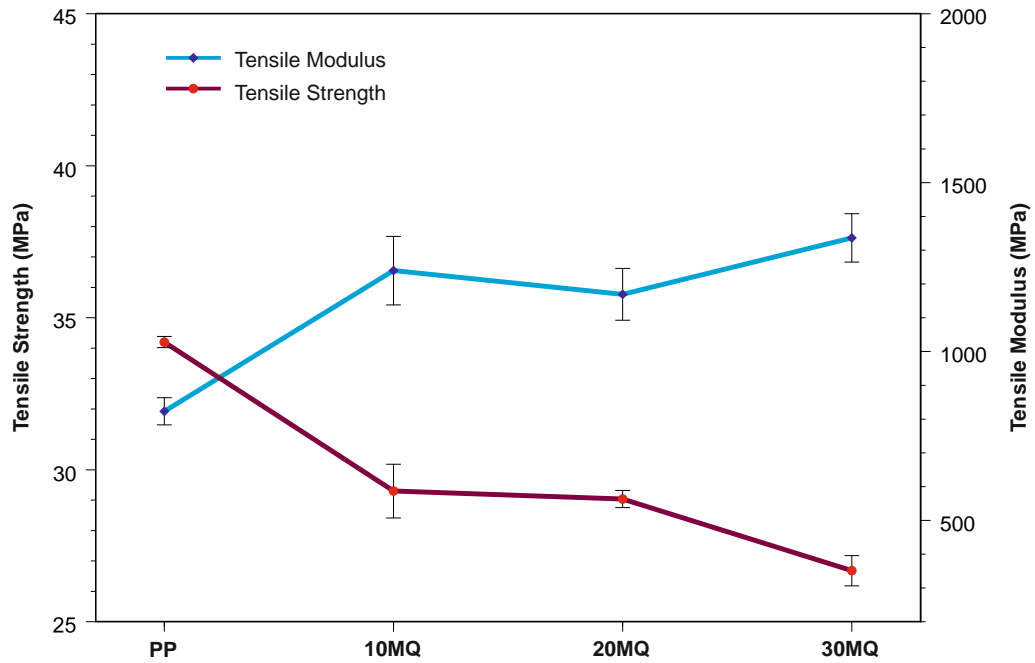
Figure 3.10 Tensile strength and tensile modulus of PP and MQ powder reinferced PP composites at various MQ weight fractions.

Tensile strength and tensile modulus results of silanized quartz doped composites are given in Figure 3.11. Silanized quartz additives reduce the tensile strength of PP material according to this figure. While the tensile strength of pristine PP was approximately 34.20 MPa, this parameter were measured by taking the mean of five measurements as 32.70, 30.07, 28.50, and 24.29 MPa for 10%, 20%, 30%, 40% silanized quartz added composites, respectively. When these results are examined, it is seen that the tensile strength decreases with the increase in the amount of silanized quartz filler material [144, 145]. The tensile strength of the 10SQ sample is approximately 10% higher and 32.70 MPa when it is compared to the 10MQ composite sample with a tensile strength of 29.30 MPa [108]. This is due to the fact that commercial silanized quartz powders provide better matrix-filling interfacial

alignment with PP matrix when compared to the commercial silanized quartz powders and micronized quartz powders. In particular, the decrease of tensile strength of the sample containing 40% by weight of silanized quartz was higher. A similar result was observed at the tensile module value. This situation is thought to be due to the fact that an ideal and homogenous mixture cannot be made and the amount of clumping is high due to the amount of filler material added to the PP [103].

The effect of silanized quartz additive on the tensile modulus of PP is given in Figure 3.11. When the figure is examined, it is seen that the silanized quartz additive increases the tensile modulus of PP. The tensile modulus of PP is 823 MPa. The tensile modulus of composite material containing 30% by weight of silanized quartz increased by 83% compared to PP and was measured as 1508 MPa. According to tensile tests performed on four different composite materials, tensile modulus values of the 10%, 20%, 30%, and 40% silanized quartz doped composites were measured as 1265, 1268, 1508, and 1397 MPa, respectively. When the tensile modulus value of 40SQ sample which contains 40% by weight of silanized quartz was examined, it was seen that the tensile modulus value was decreased compared to the 30SQ sample.
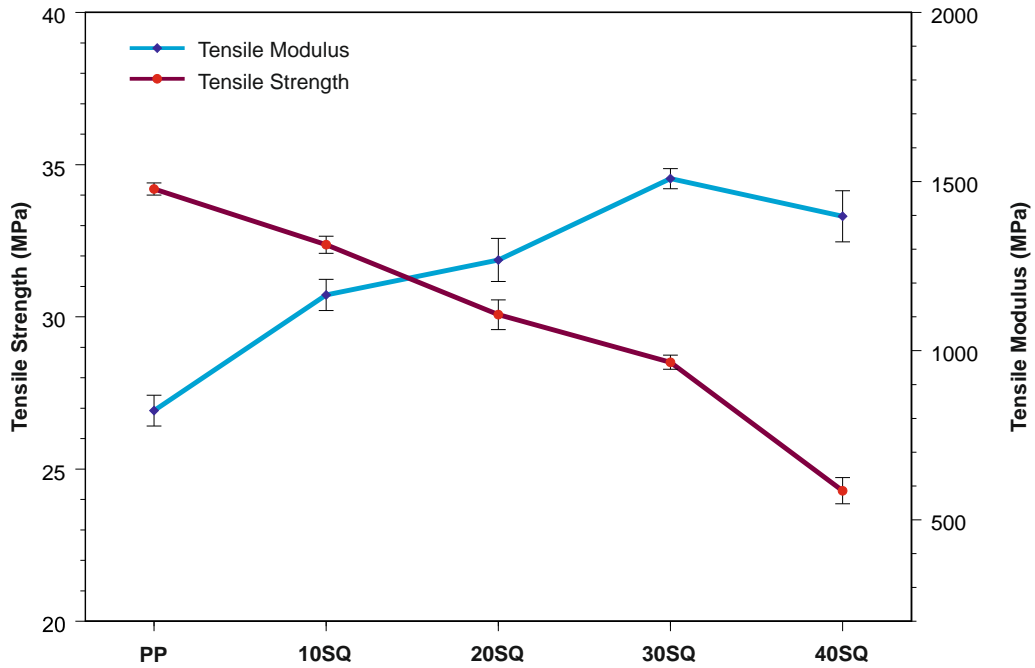
Figure 3.11 Tensile strength and tensile modulus of PP and SQ powder reinferced PP composites at various SQ weight fractions.

Tensile strength results of the surface modified quartz tempered composites are reported in Fig. 3.12. While the tensile strength of PP is 34.20 MPa, the tensile strengths of PP-2287, PP-MP200, PP-A187 and PP-A110 composites with the surface modification quartz powders containing four different surface modification agents is 32.44, 32.11, 31.81, and 32.4 MPa, respectively. When the results are examined, the tensile strength of 10% surface modified quartz added composites are similar to the tensile strength of 10% commercial silanized quartz added composites. The tensile strengths of the samples modified with four different surface modification agents are higher when compared with 10% micronized quartz added composite sample. This observation is accounted as the result of the surface modification process by increased filler material-matrix interface compatibility [103, 104].

Tensile modules of PP-2287, PP-MP200, PP-A187 and PP-A110 composite samples produced with surface modified quartz powders were obtained as 959, 986, 974 and 1064 MPa, respectively. Especially, the tensile strength and tensile modulus of the composite produced with the VEMAB A-110 modification agent were higher than the quartz added composite samples treated with other modification agents.

66
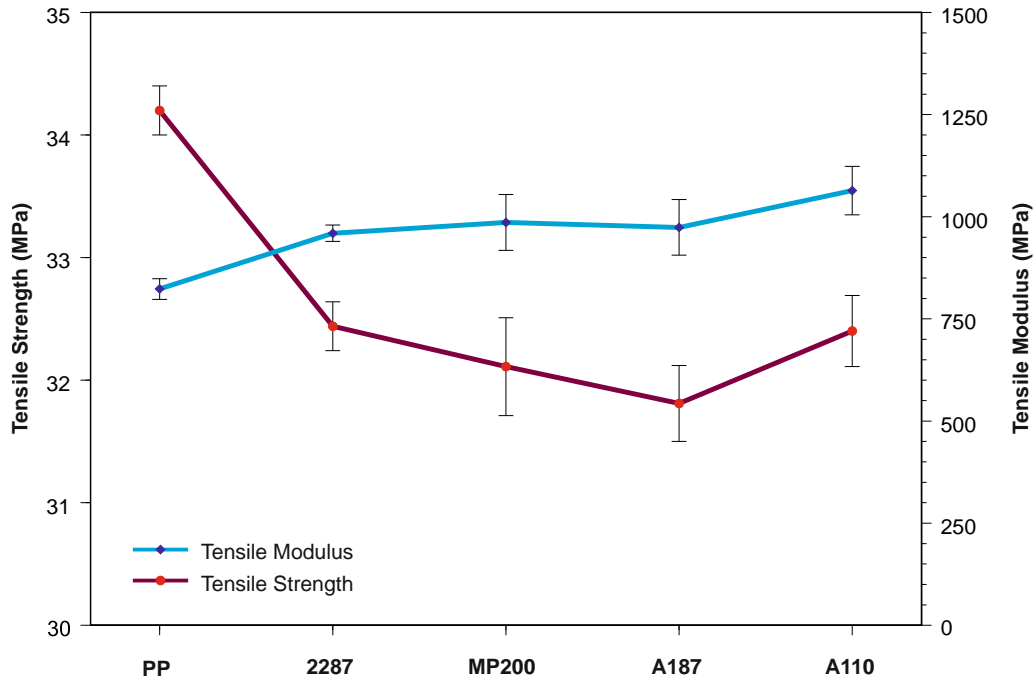
Figure 3.12 Tensile strength and Tensile modulus of PP and surface modified quartz powder reinforced PP composites at 10% weight fraction.

The percent elongation values of micronized quartz doped composites are given in Table 3.2 in comparison with the PP matrix as the mean of three measurements. The average of three measurements in PP material is calculated as approximately 15%. With the micronized quartz additive, the percentage elongation value of PP decreases. According to the tensile tests performed on composite samples, the mean percentage elongation values were measured as 6.17, 13.42, and 8.10 for 10MQ, 20MQ, and 30MQ samples, respectively. As the micronized quartz additive increases, the percentage elongation value decreases according to the matrix material as a result of increase in brittle behavior.

Table 3.2 Elongation % at PP and MQ powder reinforced PP composites at various MQ weight fractions.

Sample	Result 1	Result 2	Result 3	Standart Deviation	Avarage % Elongation
PP	16.88	13.88	14.33	1.62	15.03
10MQ	4.98	7.48	6.05	1.25	6.17
20MQ	12.74	14.62	12.90	1.04	13.42
30MQ	7.21	8.14	8.96	0.88	8.10

The percent elongation values of silanized quartz-doped composites are given in Table 3.3 as average of three measurements compared to PP matrix. The percentage elongation value of PP was found to be increased in silanized quartz additive in

contrast to micronized quartz powders. According to the tensile tests performed on four different composite materials, the mean percentage elongation values were measured as 24.45, 26.00, 20.53, and 14.93 for 10SQ, 20SQ, 30SQ, and 40SQ samples, respectively. When the amount of silanized quartz in the PP is 20%, the percentage elongation value is the highest and when the amount of additive is continued to increase, the percentage elongation value starts to decrease. Especially in 40SQ sample, this value fell below the PP matrix material. In this case, 40SQ sample, it is considered as this situation is due to the increase in clumps as a result of the increase in the amount of additive material in the PP and the decrease of the matrix-filling material stress transfer as a result of increase inhomogeneity.

Table 3.3 Elongation % at PP and SQ powder reinforced PP composites at various SQ weight fractions.

Sample	Result 1	Result 2	Result 3	Standart Deviation	Avarage % Elongation
PP	16.88	13.88	14.33	1.62	15.03
10SQ	26.40	19.83	27.12	4.02	24.45
20SQ	23.29	27.50	27.21	2.35	26.00
30SQ	22.59	18.00	21.00	2.33	20.53
40SQ	14.65	15.19	14.95	0.27	14.93

The percent elongation values of the surface modified quartz doped composites are given in Table 3.4 as three measurements average in comparison to the PP matrix. In contrast to micronized quartz powders, as in the case of commercial silanized quartz additives, it is seen that the percentage elongation value of PP increases with the modified quartz additive [97, 108]. According to the tensile tests performed on quartz added composite materials treated with four different modification agents, the average percentage elongation values were measured as 25.19, 21.32, 23.73, and 24.00 for 2287, MP200, A187, and A110 samples, respectively. There are slight differences in the percent elongation values of MQ powder composites treated with different modification agents [103].

Table 3.4 Elongation % at PP and surface modified quartz powder reinforced PP composites at 10% weight fraction.

Sample	Result 1	Result 2	Result 3	Standart Deviation	Avarage % Elongation

PP	16.88	13.88	14.33	1.62	15.03
2287	24.50	26.45	24.62	1.09	25.19
MP200	21.81	21.06	21.09	0.42	21.32
A187	20.29	25.26	25.64	2.99	23.73
A110	24.14	24.36	23.50	0.45	24.00

3.2.1.2 Three-Point Bending Test

The results of three-point bending tests to determine the flexural strength behavior of composite samples and PP are given between Figure 3.13 and Figure 3.15.

Flexural strength value obtained from mean of 4 measurements on PP plates produced from Petoplen MH 418 material is 48.32 MPa. The flexural strength of the 10% micronized quartz filled composite was measured as 53.45 MPa, 20% micronized quartz filled composites was 50.03% and 30% micronized quartz filled composites was measured as 43.78 MPa. The flexural strength of PP was increased in the samples with 10% and 20% by weight of the micronized quartz in the PP matrix but it was seen that this value decreased dramatically when the additive rate was 30%. This situation is thought to be caused by inhomogeneity within the composite material due to the high amount of aggregation when the production is made with high additive material in the Gelimat mixer. Similar effect is observed in tensile strength values of 30MQ samples. As the filling material increases, a more distinct matrix / filling material interface mismatch appears, and as a result of this situation, it is seen that the composite mechanical properties are weakened [146].

The effect of the micronized quartz amount in the micronized quartz doped composite material on the flexural modulus is given in Figure 3.13 in comparison with PP. The results show that the flexural modulus of the PP increases as the amount of micronized quartz in the composite increases. The flexural modulus of the 30MQ sample containing 30% by weight of micronized quartz was measured as 2172 MPa with an increase of about 54%. This is due to the fact that the micronized quartz powders involved in the composite play an active role in carrying the applied load. When the micronized quartz additive increases, the stiffness of PP increases.

69
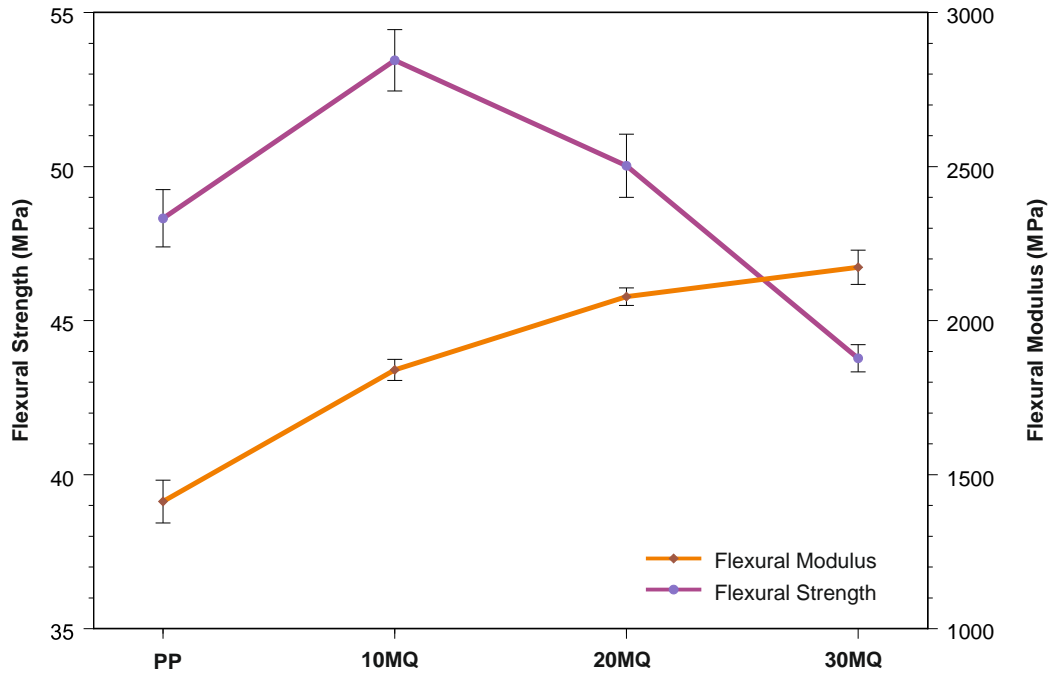
Figure 3.13 Flexural strength and Flexural modulus of PP and MQ powder reinferced PP composites at various MQ weight fractions.

Flexural strength results of silanized quartz doped composite samples obtained by three-point bending test are given in Figure 3.14 in comparison to PP. Flexural strengths of 10SQ, 20SQ, 30SQ and 40SQ samples were measured as 51.14, 47.61, 43.99 and 39.78 MPa, respectively. Flexural strength increased in the sample with 10% silanized quartz filled composite but the flexural strength decreases continuously as the amount of additive increases.

It is clearly seen in Figure 3.14 that the flexural modulus of silanized quartz-filled PP composites increases with the increase of additive amount. The highest flexural modulus value was obtained from 40SQ sample and it is 2469.67 MPa. The flexural modulus of the 40SQ composite sample is about 75% higher than PP. The reason for this behavior can be explained by mentioned before reasons like inhomogeneity and agglomerations.
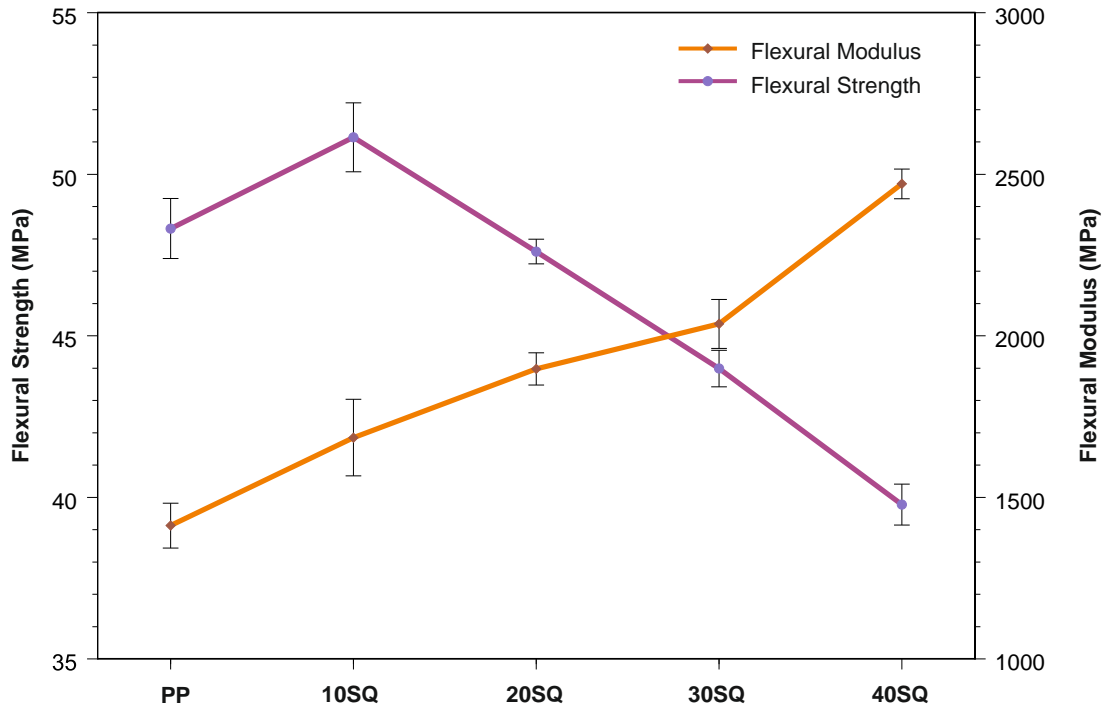
Figure 3.14 Flexural strength and flexural modulus of PP and SQ powder reinferced PP composites at various SQ weight fractions.

10% contribution of modified quartz powders produced by different surface modification agents into the PP matrix, is given in Figure 3.15 compared to the 10MQ and 10SQ composite samples. The flexural modulus of the composite samples PP, 10MQ, 10SQ, 2287, MP200, A187 and A110 was measured as 1412, 1840, 1684, 1574, 1796, 1815 and 1619 MPa, respectively. When these results were examined, it was seen that the flexural modulus values of the MP200 and A187 composite samples were especially higher than the other two modified quartz added composite samples.

It is resulted from the fact exhibiting different mechanical properties in the quartz doped samples with different surface agents, having different active groups that the used surface agents have and as a result of this, changes in the performance of matrix/filling interface compatibility [103]. It has been observed that silanized quartz doped sample has lower flexural modulus than micronized quartz doped composites and it is close to the composite samples of 2287 and A110. Surface modified quartz additive and commercial silanized quartz additive were found to increase less than micronized quartz added samples regarding to the flexural modulus in PP based composites.
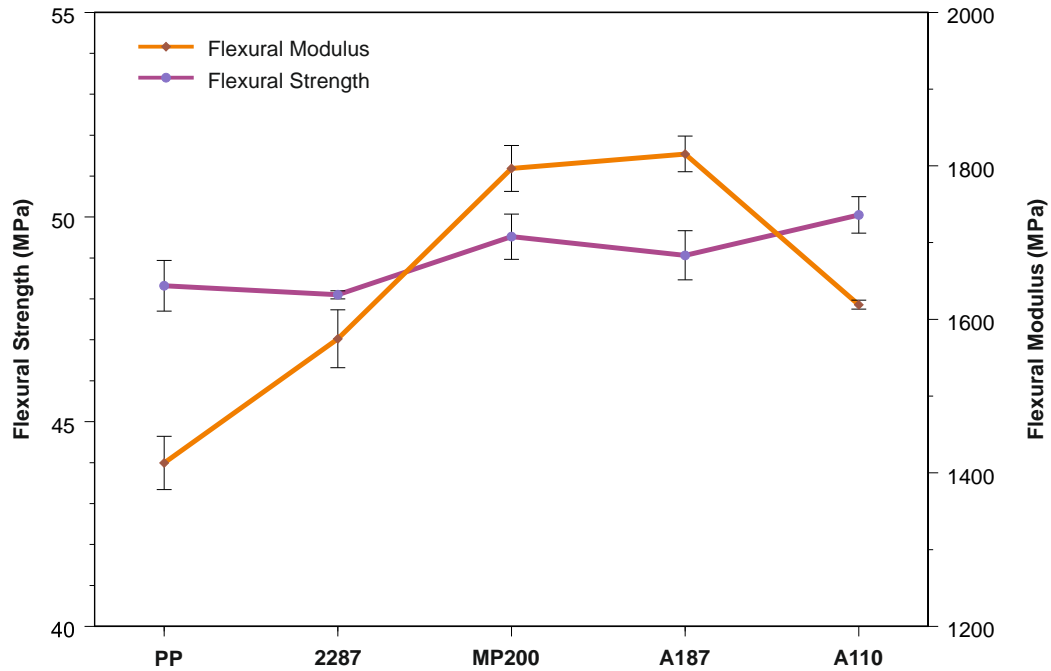
71

Figure 3.15 Flexural strength and flexural modulus of PP and surface modified quartz powder reinferced PP composites at 10% weight fraction.

3.2.2 Dynamic Mechanical Analysis (DMA)

Dynamic mechanical analyses were conducted to understand the viscoelastic behavior of neat PP and MQ-PP composites. The storage modulus (E′) and the loss modulus (E″) were determined from the analyses. E′ represents the stiffness of a viscoelastic material, which is proportional to the elastic energy stored elastically and is reversible [147]. Variations in storage modulus of PP and MQ-PP composites versus temperature as a function of MQ weight fractions is given in Figure 3.16.

The storage modulus values are reduced with increasing temperature due to an energy dissipation phenomenon including cooperative movements of the polymer chain [148, 149]. It was investigated that the storage modulus values of the composites were higher than that of PP and the stiffness of the MQ-PP composites enhanced with increasing weight fraction of MQ. The storage modulus of PP increases with adding the MQ filler, because the MQ is a stiffer material than the PP. The reason may be that the movement of the polymer chains are restricted by the MQ fillers with the increasing of temperature. The storage modulus values are also tabulated in Table 3.5. The results show that 10,20, and 30% loadings of MQ into PP lead to 5.2%, 13.6%, and 33.2% increases in storage modulus, respectively, when

compared to that of neat PP at 35 ℃. The increment in storage modulus was due to mechanical restrictions posed by increasing filler content embedded in the polymer matrix [129]. Comparing PP and MQ-PP composites with different MQ weight fractions at temperatures from 35 to 135℃, it is easy to find that the storage modulus of the composite containing 30 wt% MQ was higher than the other samples, although it was decreased by increasing temperature. On the otherhand, the low concentration of MQ in PP has least effect on variation of storage modulus versus temperature.

The retention ratio may be described as the ratio of the storage modulus at 135℃ to that at 35℃. The retention ratios of PP, 10MQ, 20MQ, and 30MQ were obtained to be 0.156, 0.158, 0.173, and 0.163, respectively. It can be seen from the retention ratios that the MQ-PP composites have improved mechanical properties compared to PP at high temperatures.

Table 3.5 Storage modulus values of MQ reinforced PP composites at various temperature.

Storage Modulus (MPa)						
Sample Name	**35℃**	**50℃**	**75℃**	**100℃**	**135℃**	**SM_{135}/SM_{35}**
PP	1782.20	1533.65	938.35	597.23	278.05	0.156
10MQ	1857.69	1627.38	1009.04	620.23	293.21	0.158
20MQ	2024.65	1813.45	1167.76	735.08	349.50	0.173
30MQ	2373.12	2084.33	1310.94	822.88	386.26	0.163

Figure 3.16 Variations in storrage modulus of PP and MQ-PP composites versus temperature as a function of MQ weight fractions.

Variations in storage modulus of PP and SQ-PP composites versus temperature as a function of SQ weight fractions are shown in Figure 3.17. The storage modulus values of the SQ-PP composites were obtained higher than that of PP and the stiffness of the SQ-PP composites also increased with SQ loadings. On the other hand, the storage modulus values of the SQ-PP are decreased with increasing temperature due to an energy dissipation phenomenon [149, 150]. The storage modulus of PP increases with adding the SQ filler. The presence of stiff quartz can produce a more rigid interface in the PP matrix. The mobility of the polymer chains can be also restricted by the SQ fillers with the increasing of temperature. However, it is interesting to note that the 10SQ and 20SQ composites have not a higher storage modulus than the untreated quartz filled PP composites. 30SQ composite has a higher storage modulus than the 30MQ composites.

Dı́ez-Gutie´rreza et al (1999) indicated that silane treated talc filled PP have a higher storage modulus than the untreated one because the silane treated talc generates a stiffer interface in the PP matrix [151]. The storage modulus values are also tabulated in Table 3.6. The DMA results represent that 10, 20, 30 and 40% filling of SQ into

PP lead to 0.2%, 11.8%, 40.0%, and 55.7% increases in storage modulus, respectively, when compared to that of neat PP at 35℃. The increase in storage modulus of PP is due to mechanical restrictions resulting from increasing content of the filler embedded in the polymer matrix [129]. By comparing PP and SQ-PP composites with different SQ weight fractions at temperatures between 35 and 135℃, it can be seen that the storage module containing 40% SQ is higher than the other samples. On the otherhand, the lowest concentration of SQ in PP shows the minimum effect on variation of storage modulus versus temperature.

Table 3.6 Storage modulus values of SQ reinforced PP composites at various temperature.

Storage Modulus (MPa)					
Samples	**35℃**	**50℃**	**75℃**	**100℃**	**135℃**	SM_{135}/SM_{35}
PP	1782.20	1533.65	938.35	597.23	278.05	0.156
10SQ	1794.85	1550.61	984.61	614.73	292.92	0.163
20SQ	1991.97	1770.26	1143.97	708.87	328.14	0.165
30SQ	2495.77	2202.15	1426.45	888.48	405.66	0.163
40SQ	2775.35	2443.45	1581.55	997.20	466.99	0.168

The retention ratios of PP, 10SQ, 20SQ, 30SQ and 40SQ were obtained to be 0.156, 0.163, 0.165, 0.163 and 0.168, respectively. It can be seen from the retention ratios that the SQ-PP composites have improved mechanical properties as compared to that of PP at high temperatures.
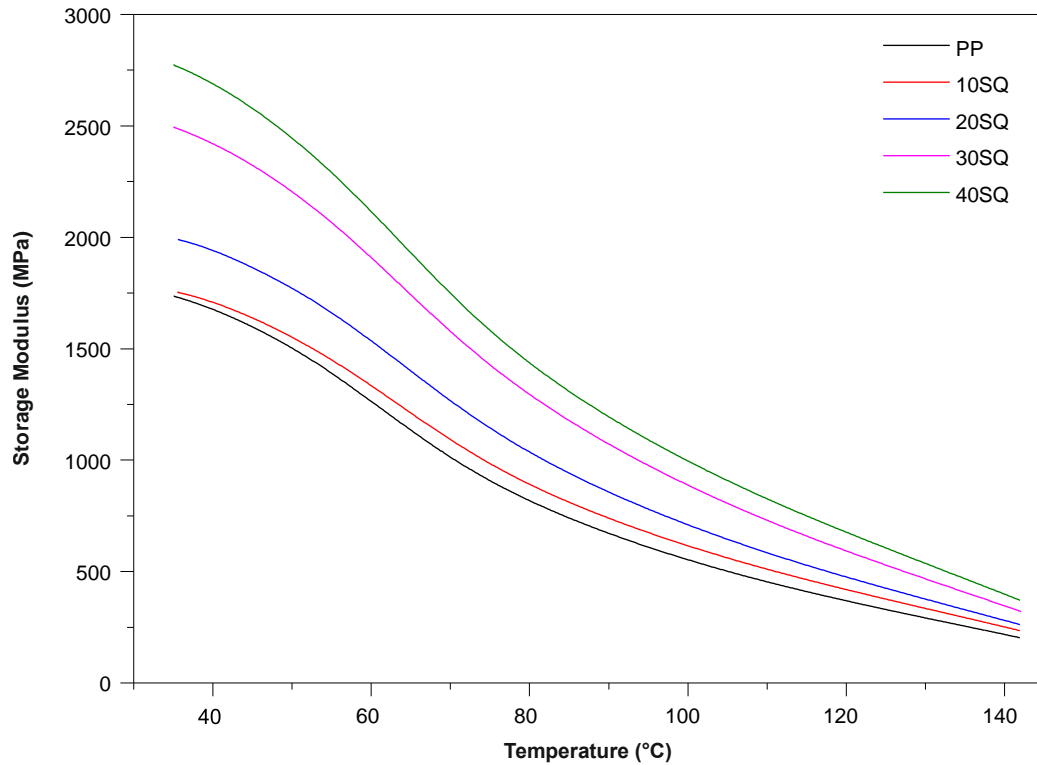
Figure 3.17 Variations in storage modulus of PP and SQ-PP composites versus temperature as a function of SQ weight fractions.

Variations in storage modulus of PP and the surface modified MQ loaded composites versus temperature were shown in Figure 3.18 and tabulated in Table 3.7. MP200 composite has the highest storage modulus value among all samples at 35℃. The storage modulus values of the all samples are decreased with increasing temperature because of an energy dissipation phenomenon [149, 150].

Table 3.7 Storage modulus values of modified MQ reinforced composites at various temperature.

	Storage Modulus (MPa)					
Samples	**35℃**	**50℃**	**75℃**	**100℃**	**135℃**	SM_{135}/SM_{35}
PP	1782.20	1533.65	938.35	597.23	278.05	0.156
A110	1925.82	1679.90	1045.84	642.72	300.71	0.156
A187	1823.85	1601.60	994.21	609.90	280.92	0.154
2287	1958.17	1710.89	1080.94	652.85	301.39	0.154
MP200	1987.92	1728.51	1067.30	656.59	306.84	0.154
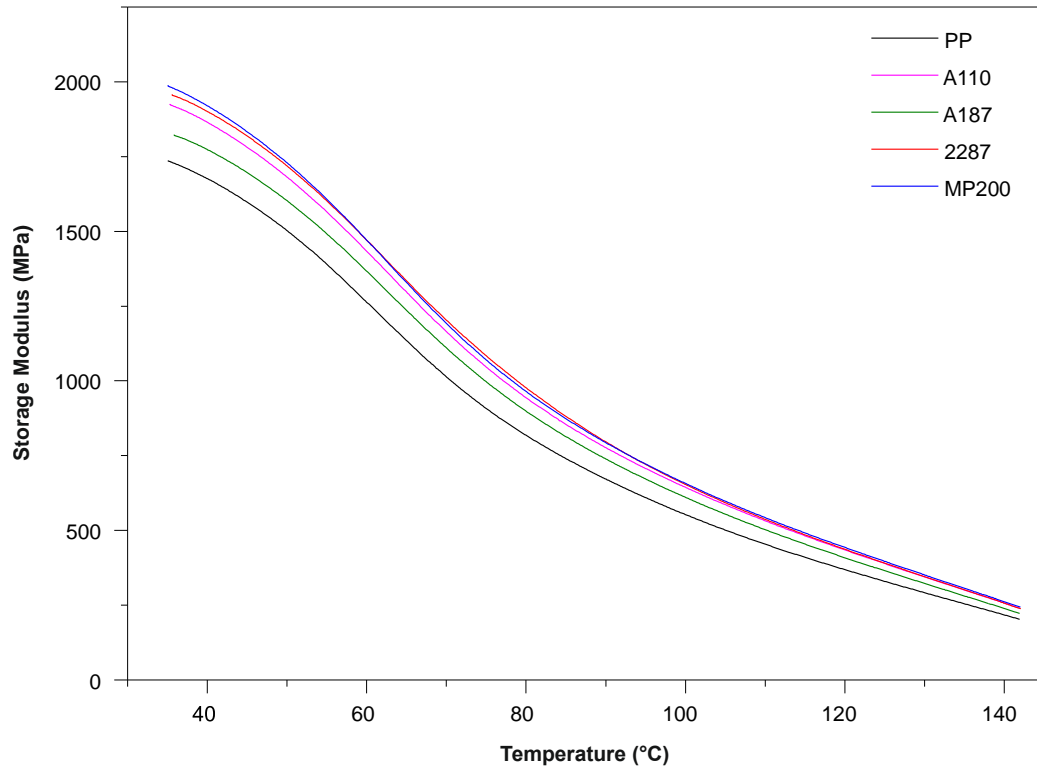
Figure 3.18 Variations in storage modulus of PP and Modified Quartz-PP composites versus temperature.

Figure 3.19 shows the loss modulus values of PP and MQ-PP composites. Loss modulus (E'') is a measure of viscous response of a material. It evaluates the energy dissipated as heat [150]. As was seen in Fig. 19, the E'' of all composites was higher than that of PP in the all temperature range. This may be related to decrease in the flexibility of polymer by decreasing the segmental mobility of polymer [152]. The loss modulus continued to increase as MQ weight fraction was increased. Samples (PP, 10MQ, 20MQ, and 30MQ) show α-relaxation peaks at about 66.3, 69.3, 67.5, and 68.0℃, respectively. The α-relaxation peak of PP increased after incorporation of MQ into PP. This may be attributed to higher viscous dissipation of the composites than that of polymer [152].
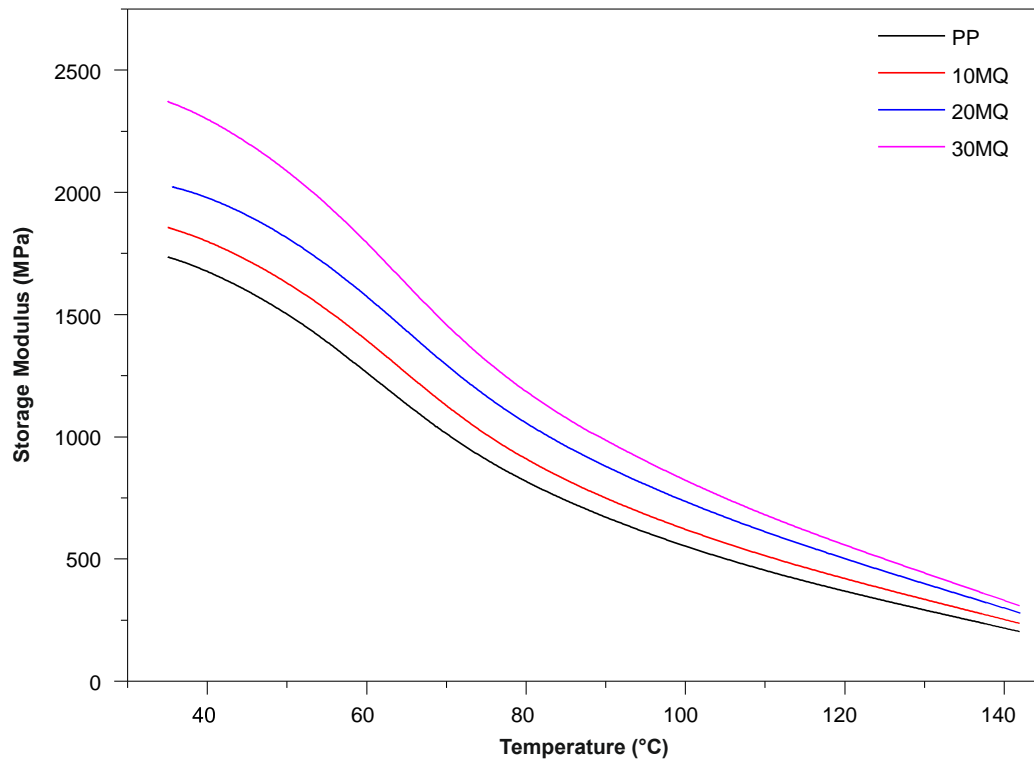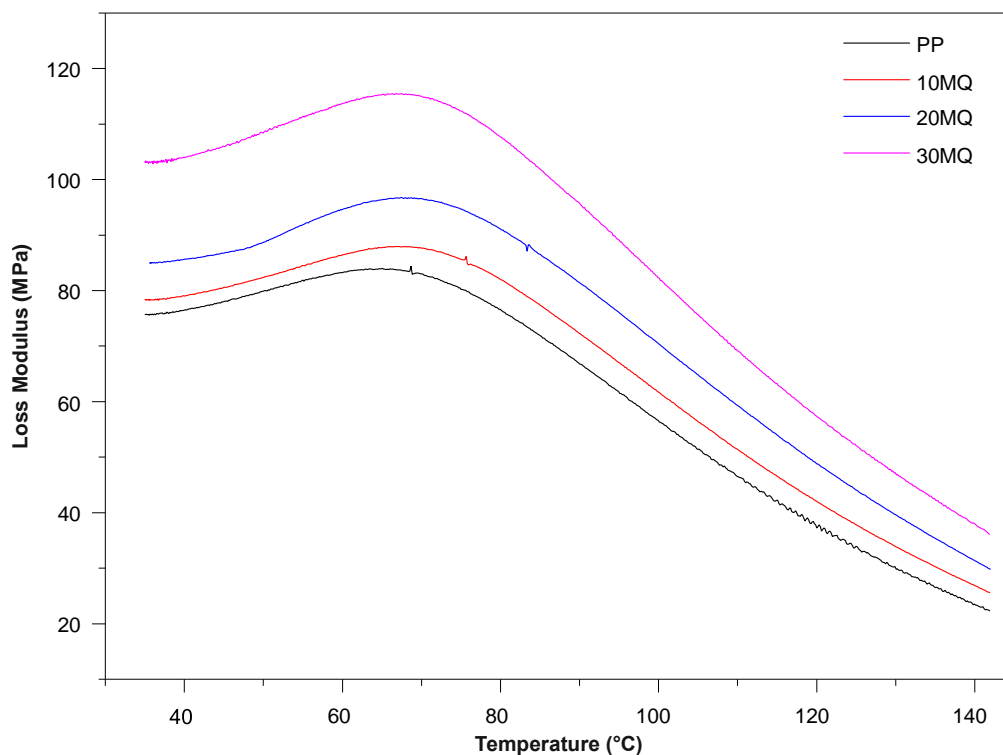
Figure 3.19 Variations in loss modulus of PP and MQ-PP composites versus temperature as a function of MQ weight fractions.

Figure 3.20 represents the variations in the loss modulus of PP and SQ-PP composites. As was seen in Fig. 3.20, the E″ of all composites was higher than that of PP in the entire temperature range. This may be related by decreasing the segmental mobility of polymer [152]. It can be seen that the loss modulus increases after loading of SQ fillers into PP. Samples (PP, 10SQ, 20SQ, 30SQ, and 40SQ) show α-relaxation peaks at about 66.3, 67.8, 68.4, 69.0 and 68.9℃, respectively. The α-relaxation peak of PP increased after incorporation of SQ into PP due to higher viscous dissipation of the composites than that of polymer [152].
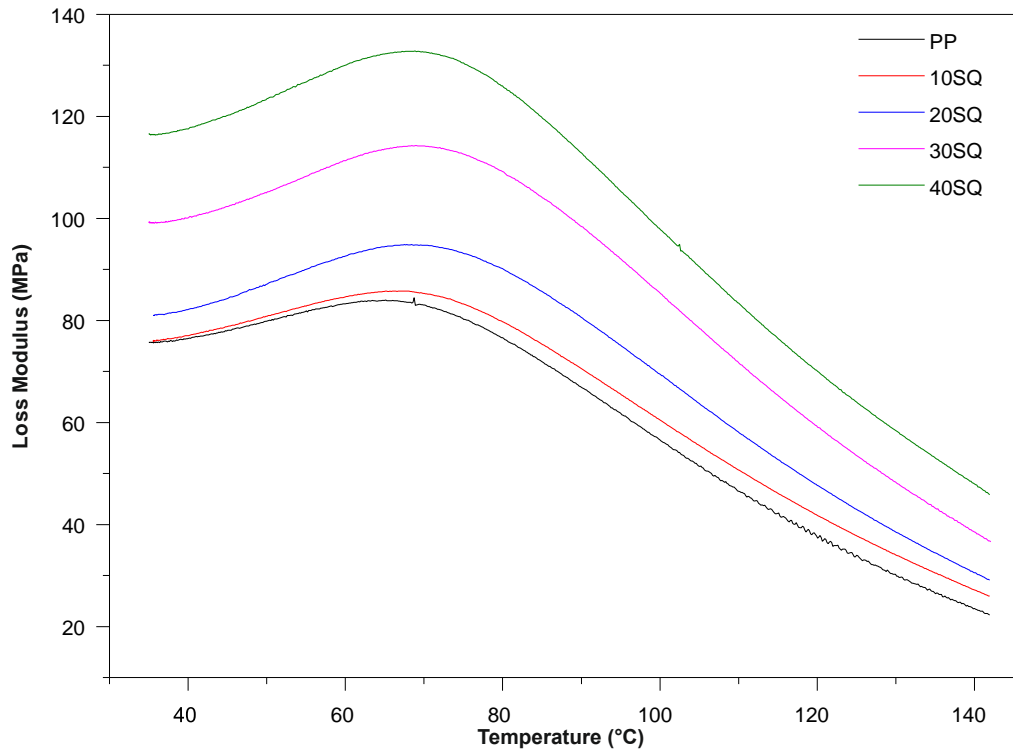
Figure 3.20 Variations in loss modulus of PP and SQ-PP composites versus temperature as a function of SQ weight fractions.

The variations in the loss modulus of PP and the surface modified filler loaded composites were shown in Figure 3.21. E″ of all composites was higher than that of PP in the all temperature range by decreasing the segmental mobility of polymer [152].
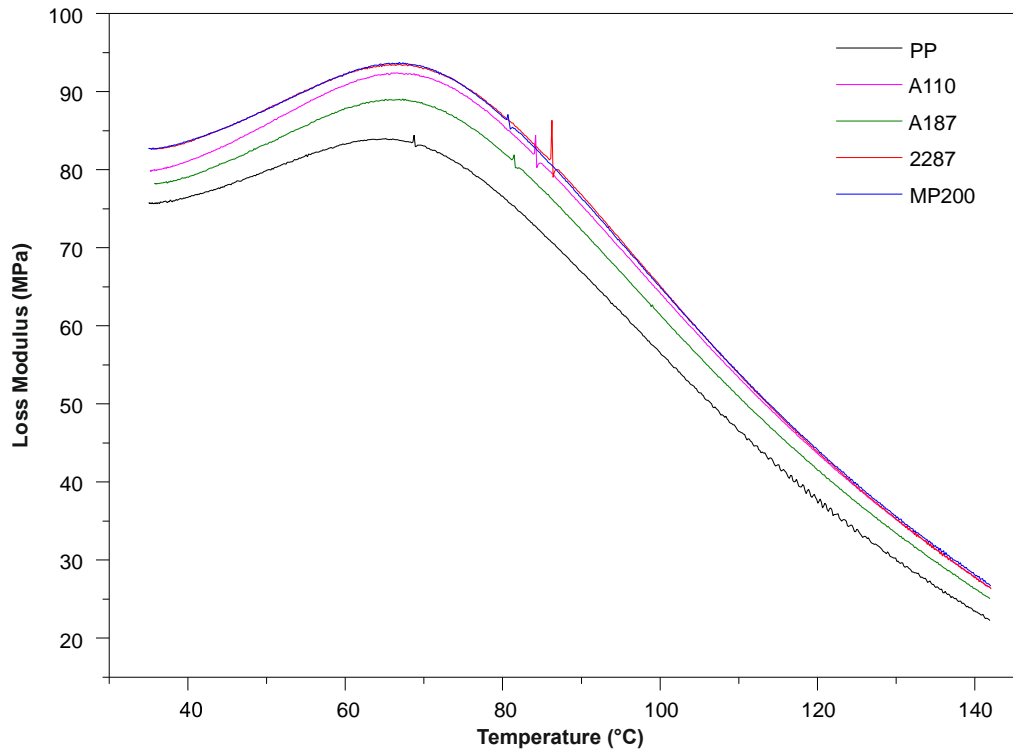
Figure 3.21 Variations in loss modulus of PP and Modified Quartz-PP composites versus temperature.

The effect of temperature on the tanδ of the composites at different fillier loadings are presented in Figure 3.22. Tanδ peak value reduces after all type quartz filler loading into PP. Incorporation of filler decreases the tanδ peak height by restricting the mobility of polymer molecules [146].
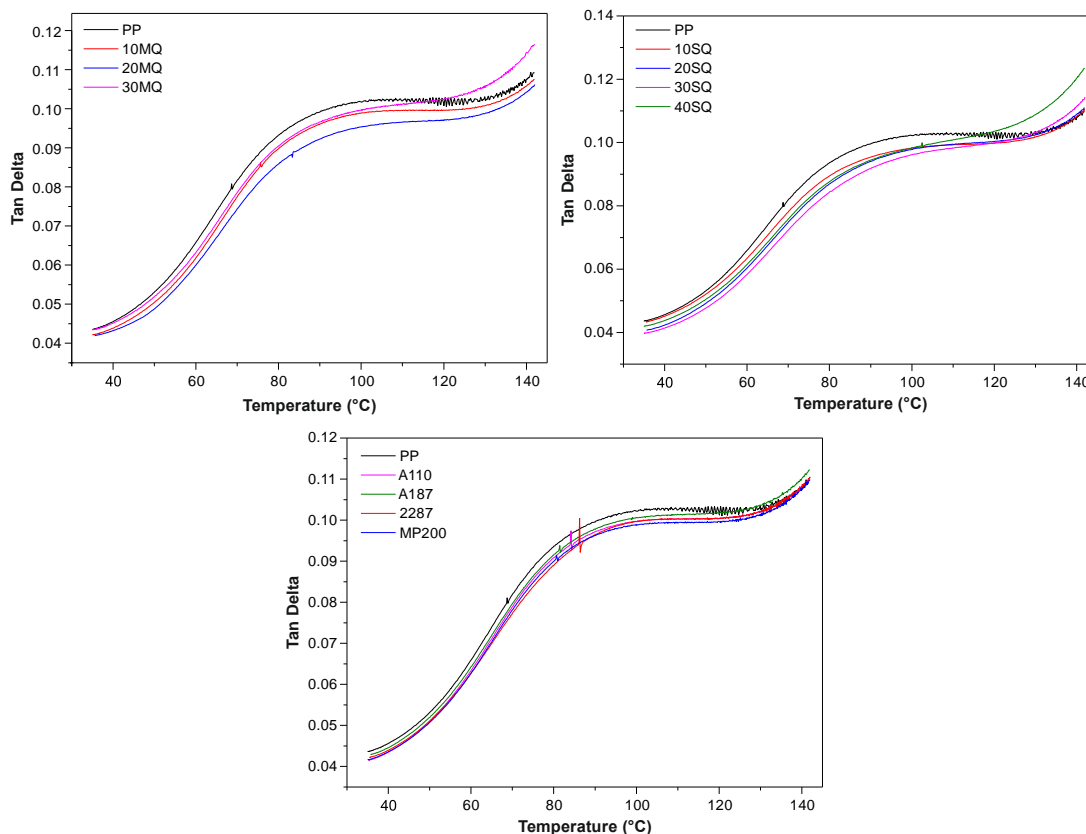
Figure 3.22 Variations in tanδ of a) MQ-PP composites, b) SQ-PP composites, and c) Modified Quartz-PP composites versus temperature.

3.2.3 Thermal Properties

Thermogravimetric analysis, differential scanning calorimetry analysis and thermal conductivity analysis were performed to determine the thermal properties of PP based quartz doped composite samples.

3.2.3.1 Thermogravimetric Analysis (TGA)

Thermogravimetric (TG) analyzes of PP based composite materials with MQ, SQ and modified quartz and neat PP sample were performed. In Figure 3.23, TGA curves of neat PP and composite samples with MQ are given. Onset temperature, maximum degradation temperature, and degraded weight values of all composite samples and neat PP material are given in Table 3.8. Neat PP and composites exhibited a one-stage degradation process. When TG analysis is examined, onset temperatures of PP, 10MQ, 20MQ and 30MQ samples were obtained as 435.86, 438.64, 439.08 and 444.27℃, respectively. As the amount of MQ added to PP increases, it was observed that the onset temperature of the composite material

81

increases. Maximum degradation temperatures of PP, 10MQ, 20MQ and 30MQ samples were measured as 460.26, 460.29, 463.30, and 467.12℃, respectively. When the results are examined, it is indicated that 10MQ sample does not have a significant effect on the maximum degradation temperature of the PP, but it is observed that the maximum degradation temperatures increase by increasing the amount of MQ in the PP.

Degraded weight values of PP, 10MQ, 20MQ and 30MQ samples were obtained as 99.75, 90.06, 80.48 and 70.55%, respectively. When the results are evaluated, the degraded weight value of PP decreases with increasing the amount of MQ quartz. Degraded weight values of 10MQ, 20MQ and 30MQ samples were consistent with the amount of %10, 20 and 30 MQ added to the composite. This result shows that the targeted matrix / filler amounts are almost reached during composite production and the desired ideal composite productions are done with Gelimat mixer.
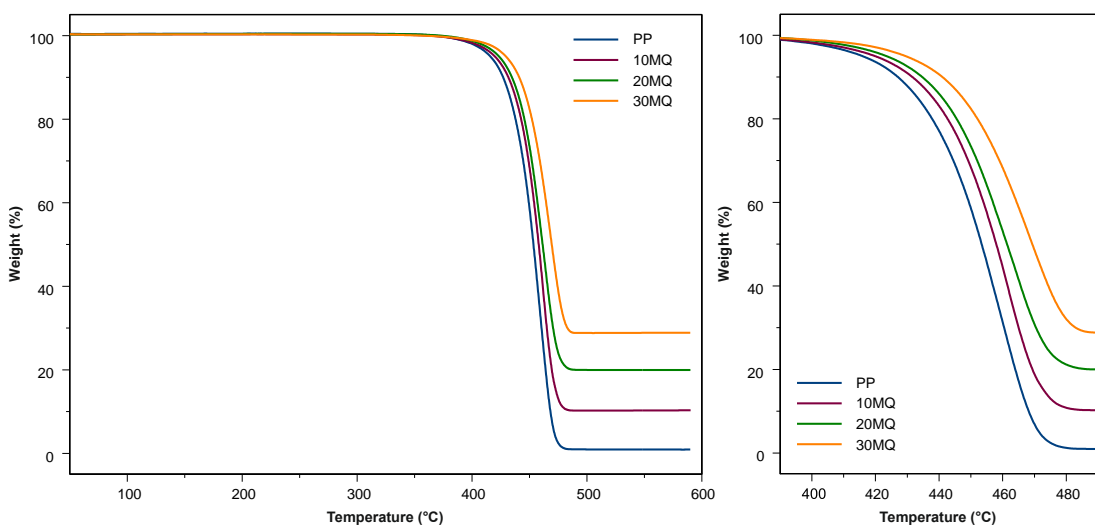
Figure 3.23 TGA thermograms of PP and MQ reinforced PP composites with various MQ powders weight fractions.

TGA curves of neat PP and SQ added composite samples are given in Figure 3.24. When the result of TG analysis is examined, the onset temperatures of PP, 10SQ, 20SQ, 30SQ and 40SQ samples were measured as 435.86, 438.32, 439.43, 444.93 and 447.28℃, respectively. As the amount of SQ added to PP increases, it is seen the onset temperature of the composite material increases.

Maximum degradation temperatures of PP, 10SQ, 20SQ, 30SQ and 40SQ samples were obtained as 460.26, 460.50, 463.15, 467.87 and 469.32℃, respectively. The effect of SQ added in PP on thermal properties shows similar performance when compared with MQ added samples. When the results are examined, it is concluded that 10SQ sample does not have a significant effect on the maximum degradation temperature of the PP, but the maximum degradation temperatures increase by increasing the amount of SQ in the PP. The reason for this increase may be due to the fact that the inorganic filler material exhibits a mass-carrying barrier behavior against volatile substances in the degraded polymer during degradation process [153].

Degraded weight values of PP, 10SQ, 20SQ, 30SQ and 40SQ samples were measured as 99.75, 90.18, 82.17, 71.44 and 62.56%, respectively. The degraded weight value of PP decreases with the increase of SQ quartz [146]. Degraded weight values of 10SQ, 20SQ, 30SQ and 40SQ samples were consistent with the amount of %10, 20, 30 and 40 SQ added to the composite.
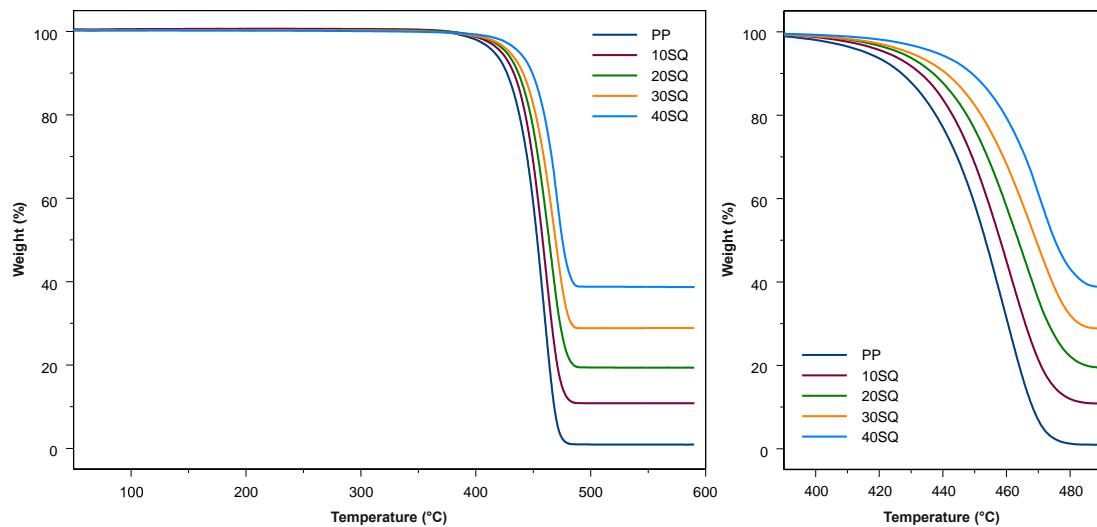
Figure 3.24 TGA thermograms of PP and SQ reinforced PP composites with various SQ powders weight fractions.

TGA curves of neat PP and modified quartz added composite samples are given in Figure 3.25. When TG analysis is examined, onset temperatures of PP, 2287, MP200, A187 and A110 samples were obtained as 435.86, 438.34, 438.45, 438.41 and 438.37℃, respectively. It is observed that the onset temperatures of PP based composite materials containing 10% modified quartz by weight have increased a fair

amount. It was seen that this increase is similar compared to 10MQ and 10SQ composite samples containing the same amount of quartz.

Maximum degradation temperatures of PP, 2287, MP200, A187 and A110 samples were obtained as 460.26, 460.88, 460.78, 460.69 and 460.47℃, respectively. When the results are examined, it is demonstrated that the modified quartz additive does not significantly affect the maximum degradation temperature of PP. Degraded weight values of PP, 2287, MP200, A187 and A110 samples were measured as 99.75, 90.08, 90.10, 88.69 and 88.76%, respectively. Looking at the degraded weight values of A187 and A110 samples, it is found that they are lower than the other two samples. This situation is thought to be due to the fact that the amount of modified quartz has caused a deviation in the calculated ratio of 90/10 matrix / filling material as a result of the modified quartz aggregation during the composite production and hence homogeneous dispersion. It has been observed that the modification process in MQ and modified MQ added composites changed the onset temperature and maximum degradation temperature of the quartz doped PP based composite material and the modification does not cause a significant change.
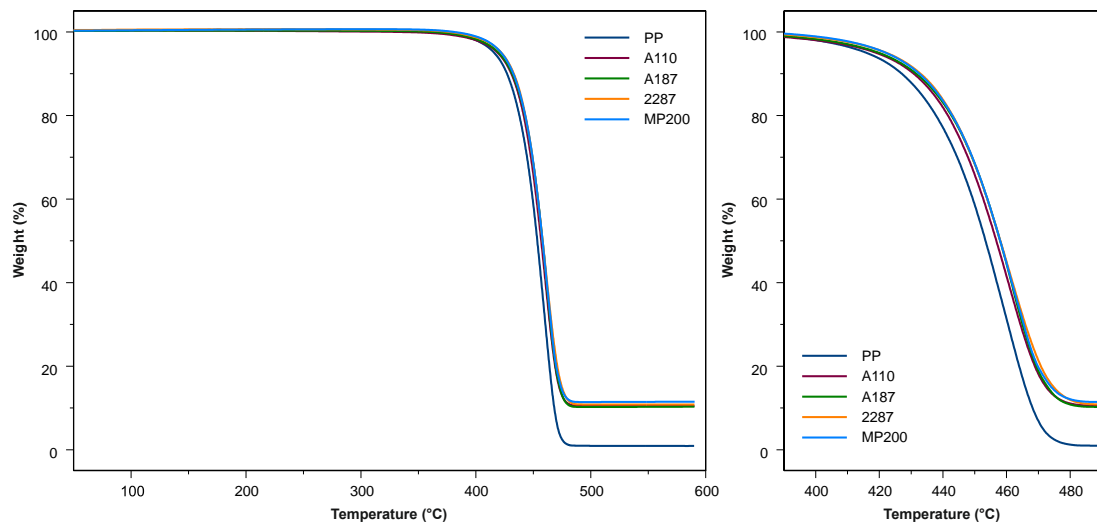
Figure 3.25 TGA thermograms of PP and modified MQ reinforced PP composites with various MQ powders weight fractions.

84

Table 3.8 TGA data of neat PP, MQ-PP, SQ-PP and modified MQ-PP composites samples.

Materials	T_{onset} (℃)	Max Degredation Temperature (℃)	Degraded Weight (%)
PP	435.86	460.26	99.75
MQ-PP Composites			
10MQ	438.64	460.29	90.06
20MQ	439.08	463.30	80.48
30MQ	444.27	467.12	70.55
SQ-PP Composites			
10SQ	438.32	460.50	90.18
20SQ	439.43	463.15	82.17
30SQ	444.93	467.87	71.44
40SQ	447.28	469.32	62.56
Modified MQ-PP Composites			
2287	438.34	460.88	90.08
MP200	438.45	460.78	90.10
A187	438.41	460.69	88.69
A110	438.37	460.47	88.76

3.2.3.2 Differential Scanning Calorimetry (DSC) Analysis

DSC analysis results of neat PP and all composite samples with quartz are given in Table 3.9. Many critical parameter values were analyzed with DSC analysis such as melting temperature (T_m), crystallization temperature (T_C), crystallization enthalpy (ΔH_C), melting enthalpy (ΔH_m), and crystallinity (X_C).

The T_C value of all quartz doped PP based composite materials is higher than PP matrix material. While the T_C value of PP is 118.34℃, it can be seen from the Table 3.9 that this value is 123.58℃ in the 40 SQ sample. T_C value of 10MQ, 10SQ, 2287, MP200, A187 and A110 samples with 10% quartz additive by weight were measured as 121.99, 121.45, 122.68, 123.12, 122.53 and 122.44℃, respectively. It is concluded that the surface modified quartz composites increase the T_C value of the composite material more compared to the non-modified MQ additive samples. It is shown in the table that the quartz composite added to PP decreases T_m value. It can be seen from

85

the table that this decrease is higher in unmodified micronized quartz doped composites and less in surface modified quartz doped composites.

When the values given in Table 3.9 are analyzed, it is observed that the values of ΔHC and ΔH_m change significantly with the quartz additive. When the ΔH_C values of MQ doped samples are compared with the PP matrix material, the ΔH_C values for samples of 10MQ, 20MQ and 30MQ are calculated as 102.9 J/g, 88.06 J/g and 79.39 J/g, respectively, while the value of PP is 82.79 J/g. When the results are examined, it is investigated that if 10% by weight of MQ is added to the PP, the ΔH_C value increases by 24% approximately. However, this ΔH_C value decreases as while the amount of MQ in the composite increases. In the 30MQ sample, the ΔH_C value was lower than the PP matrix material. A similar situation was observed in composite materials with SQ additives. When the amount of SQ in the composite was 10% by weight, the highest ΔH_C value was observed. As the amount of SQ in the composite was increased, the values of ΔH_C approached the neat PP value, and in the 30SQ and 40SQ sample, values lower than neat PP were obtained. Similar results were evaluated at ΔH_m values. The change in melting enthalpy is an indicator of the change in the degree of crystallization. The X_C values of neat PP and quartz doped composites were calculated in the following correlation using ΔH_m values.

$$X_C(\%) = \frac{\frac{\Delta Hm}{\emptyset_{PP}}}{\Delta H_0} X100$$

(1)

$\emptyset_{pp}$ given in the correlation is the amount of PP in the composite by weight and ΔH_0 is the melting enthalpy of 100% crystalline PP. This value is taken from the literature as 209 J.g-1 [154]. Looking at the results given in Table 3.9, the X_C value of PP which was 37.90% has increased with the quartz additive. When looking at the samples with 10% quartz additive, it has increased approximately 33%. This increase may be associated with the nucleation effect of quartz powders added into PP and the increase in nucleation and mobility ratio of PP chains [146, 155]. When the amount of quartz added to the composite is increased, it is observed that the X_C value has not a significant change.

Table 3.9 DSC characterizastion results of neat PP, MQ-PP, SQ-PP and modified MQ-PP composites samples.

Samples	T_m (℃)	T_C (℃)	ΔH_C (J/g)	ΔH_m (J/g)	X_C (%)
PP	167.72	118.34	82.70	79.23	37.90
MQ-PP Composites					
10MQ	164.48	121.99	102.9	98.08	52.14
20MQ	164.64	122.19	88.06	84.12	50.31
30MQ	165.57	122.20	79.39	73.31	50.11
SQ-PP Composites					
10SQ	165.34	121.45	99.57	93.37	49,64
20SQ	165.45	122.03	91.23	85.23	50.98
30SQ	164.84	122.81	79.27	74.81	51.14
40SQ	165.28	123.58	67.22	62.01	49.45
Modified MQ-PP Composites					
2287	165.06	122.68	100.00	93.20	49.55
MP200	165.31	123.12	101.60	95.26	50.64
A187	165.71	122.53	100.70	92.97	49.43
A110	165.14	122.44	102.20	94.03	49.99

3.2.3.3 Thermal Conductivty Analysis

The thermal conductivity results of micronized quartz reinforced PP based composites in comparison with PP matrix are given in Figure 3.26. The thermal conductivity of PP varies between 0.1-0.30 W/mK [156, 157]. The thermal conductivity of quartz is between 7.7-8.4 W/mK [158]. In the study, while the thermal conductivity of the PP matrix material was measured as 0.15 W/mK, it was measured as 0.267, 0.307 and 0.327 W/mK for 10MQ, 20MQ and 30MQ samples, respectively.

It is observed that the thermal conductivity of the composite increases as the amount of micronized quartz added to PP increases. This can be explained by the fact that the crystalline materials conduct heat better than amorphous materials. As the crystal quartz powders incorporated into the amorphous PP material convey the heat better [159], the thermal conductivity of the composite has increased with the quartz addition.

Another parameter affecting the thermal conductivity in composite materials is nonhomogeneous distribution of fillers. As the amount of quartz added to the PP increases, the agglomeration increases further and the filling material distribution

within the composite becomes nonhomogeneous. This causes a decrease of increasing thermal conductivity [160].
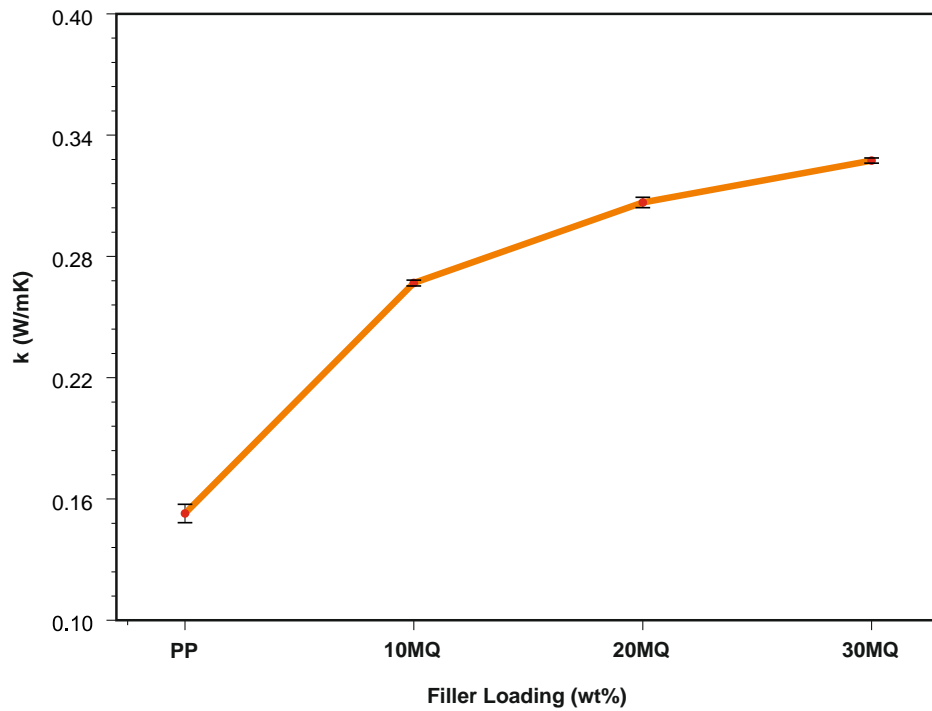
Figure 3.26 Thermal conductivity values of PP and MQ reinforced PP composites with various MQ powders weight fractions.

The thermal conductivity results of siliconized quartz doped PP based composites is given in Figure 3.27. Thermal conductivity values of 10SQ, 20SQ, 30SQ and 40SQ samples with silanized quartz were measured as 0.264, 0.285, 0.333 and 0.392 W/mK, respectively. It is seen that the thermal conductivity of composite increases as silanized quartz amount increases.
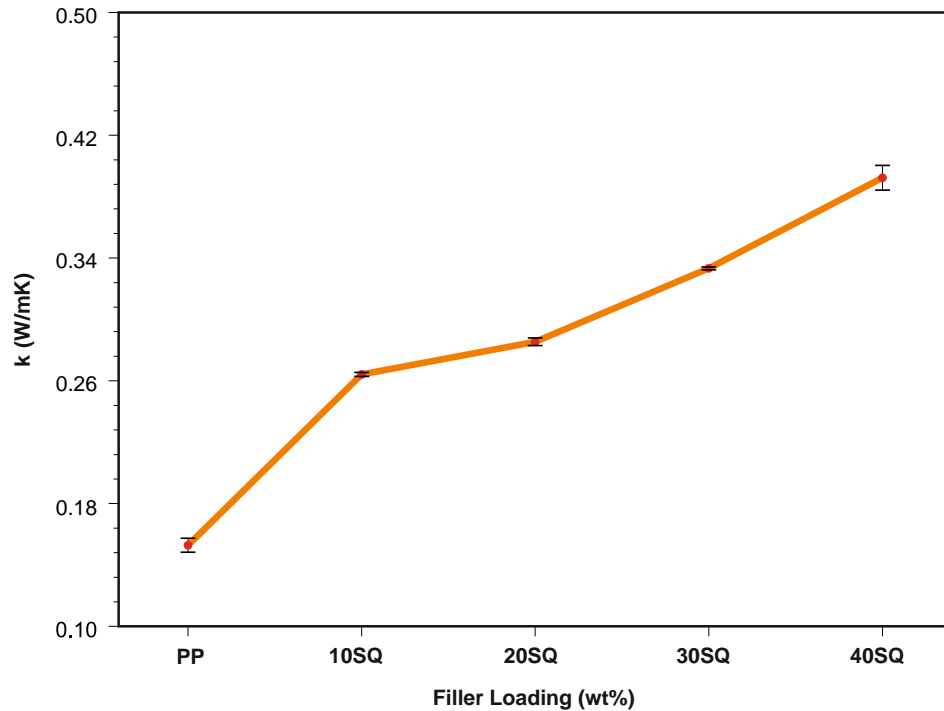
Figure 3.27 Thermal conductivity values of PP and SQ reinforced PP composites with various SQ powders weight fractions.

The thermal conductivity results of the surface modified quartz doped PP based composites is given in Figure 3.28 in comparison with PP matrix. While the thermal conductivity of the matrix material was measured as 0.15 W/mK, for the samples 2287, MP200, A187 and A110, it was measured as 0.267, 0.329, 0.360 and 0.317 W/mK, respectively.

Thermal conductivity values of samples containing 10% by weight of modified quartz were higher compared to 10% micronized quartz and silanized quartz doped samples. Especially in the samples of MP200, A187 and A110, the thermal conductivity value was higher than the 30% micronized and silanized quartz samples. This may be due to the small amount of pores in the composite and less flocculation [159]. In addition, it has been found in the literature that the thermal conductivity value of the pressed composite samples is increased according to the castings depending on the production technique. During hot pressing, the more homogeneous heat distribution may have reduced the amount of pores. The other important parameter that affects the thermal conductivity value of composite materials is matrix-filling material interface compatibility [159, 160]. As a result of the surface modification process which increas the matrix-filler interface

compatibility, the thermal conductivity values has been increased compared to the non-modified samples.
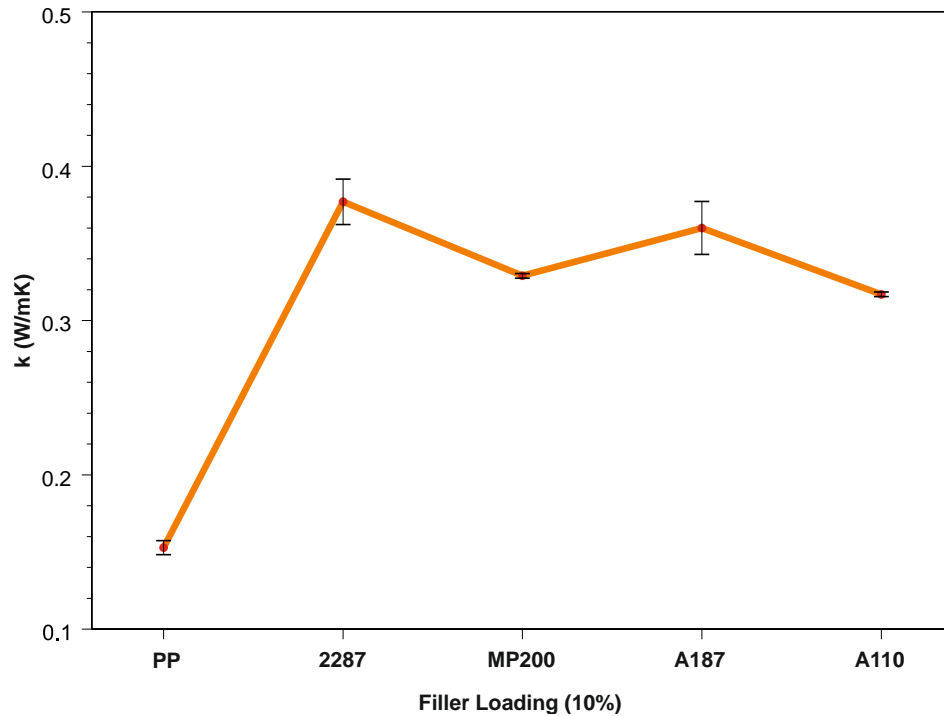
Figure 3.28 Thermal conductivity values of PP and modified MQ reinforced PP composites.

3.2.4 X-Ray Diffraction (XRD) Analysis

XRD measurements were performed in order to examine the effect of quartz additive on the crystal structure of PP. In Figure 3.29, XRD patterns of PP and PP based quartz added composites are given. When the XRD patterns given in the figure are evaluated, it is attributed that the peaks at 2θ = 14.2, 17.1, 19.0, 21.2 and 21.8º are characteristic peaks of the α-phase of PP. These peaks belong to the crystal planes of PP (110), (040), (130), (111) and (131), respectively [161]. There are also 2θ = 16.1 and 21.8º peaks reflected from the (300) and (301) crystal planes belongs to β-phase of the PP. When the pattern of PP is examined, it is observed that the diffraction peaks belongs to the typical monoclinic α form are intense. It is known that the α-phase is the dominant crystalline structure [162, 163]. The β-phase usually occurs by adding special nucleation agents or by applying special processes.

It is found that as the amount of quartz in the composite increases, the intensity of some peaks of PP decreases. Especially in the 40SQ sample containing 40% SQ by

90

weight, the peaks at 26 and 29° of PP were not seen. When XRD patterns of modified quartz doped samples are examined, it is observed that they show a similar distribution with MQ and SQ added composite samples. This is because the modification process does not cause a change in the crystal structure of quartz and the chemical composition of the powders. [97, 104]. From the XRD measurements performed, the presence of quartz in PP-based composite materials has been confirmed.
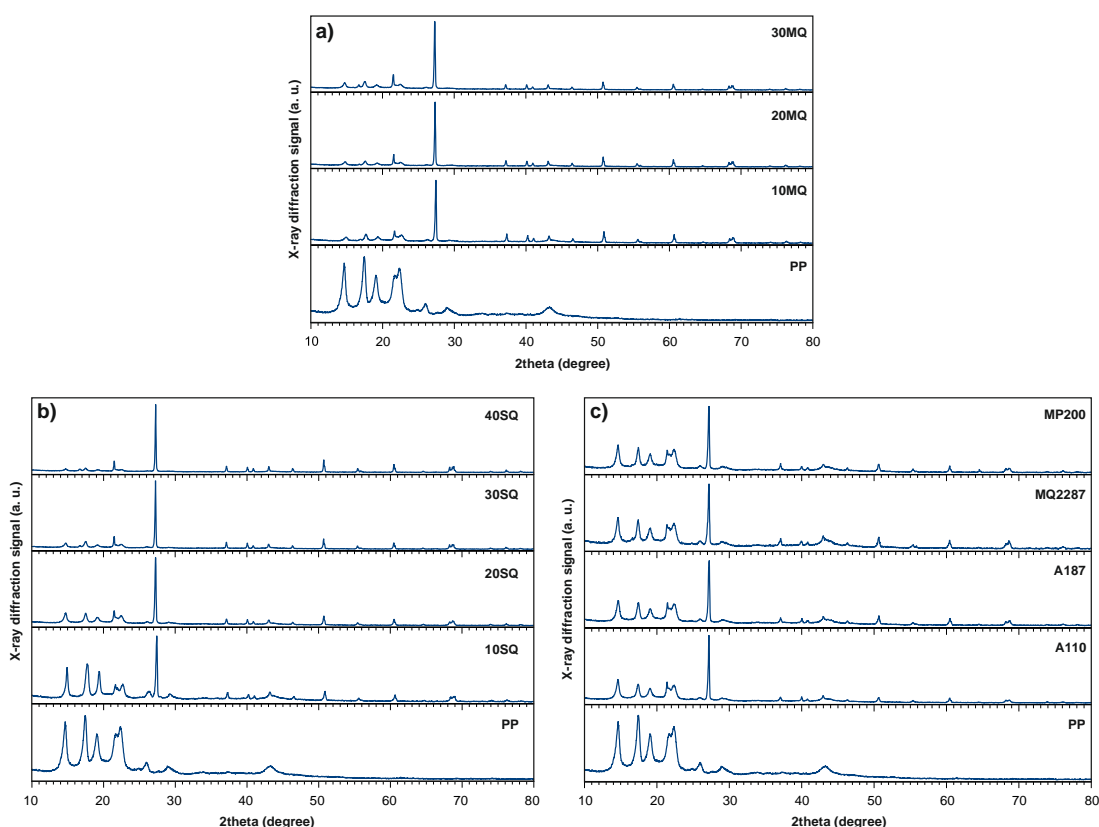
Figure 3.29 XRD patterns of a) MQ-PP composites, b) SQ-PP composites, and c) Modified Quartz-PP composites.

3.2.5 Fourier Transformed Infrared Spectroscopy (FTIR) Analysis

FTIR spectra of neat PP, MQ-PP, SQ-PP and modified MQ added composite materials are given in Figure 3.30, 3.31 and 3.32. According to the information obtained from the related literature, the vibrational models of the FTIR peaks are summarized in Table 3.10. The peaks at 1375 and 1452 cm^{-1} can be referred to the symmetrical bending vibration of CH_3— and CH_2— groups in PP. In addition to this, 2915 and 2948 cm^{-1} peaks are caused by the asymmetrical stretching vibration of the CH_2— and CH_3— groups in PP [147, 164-166]. When the results are analyzed, it is

evaluated that new peaks are formed at wavelengths of 462, 694, 795 and 1081 cm^{-1} when quartz is added to the PP. They originate from the bending stretching and asymmetrical stretching vibration models belong to the Si—O and Si—O—Si group of the SiO$_2$ quartz molecule [120, 167, 168]. As the amount of quartz in PP increases, the permeability percentage of these peaks increases. In 30MQ sample containing 30% quartz by weight, it is indicated that the peaks at 1081 and 462 cm^{-1} wavelengths become more clear.
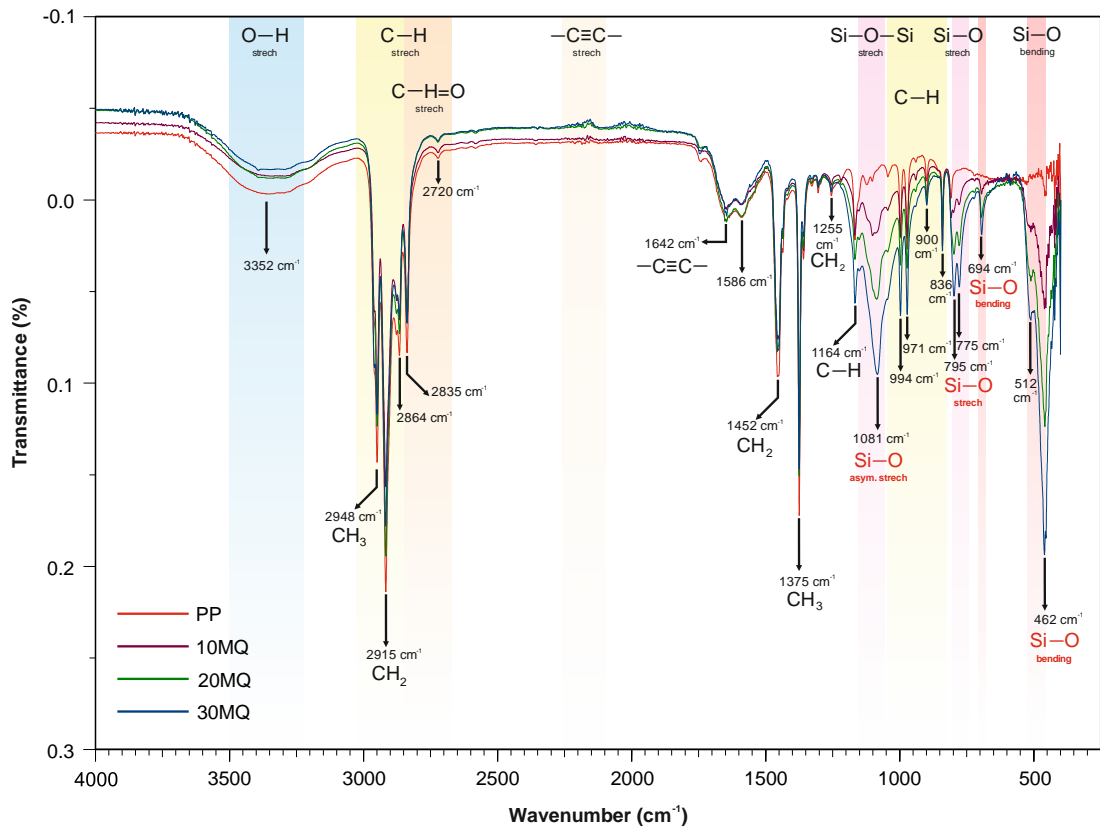
Figure 3.30 FTIR spectra of PP and MQ reinforced PP composites with various MQ powders weight fractions.

FTIR analysis results of SQ added PP based composite materials are given in Figure 3.31. It is seen that quartz peaks are formed with SQ, which is doped in PP. In addition, it is observed that as the amount of SQ in PP increases, the intensity of quartz peaks increases. In 40SQ sample containing 40% SQ by weight, the intensity of the peaks at 1081 and 462 cm^{-1} wavelengths are increased. Compared to MQ composite materials, it is revealed that there is no new peak formation in SQ added PP based composite materials. Considering the SQ ratio in the composite and the

thickness of the silanized layer on the SQ surface, it is difficult to observe the effect of silanization on the FTIR spectrum of the composite produced.
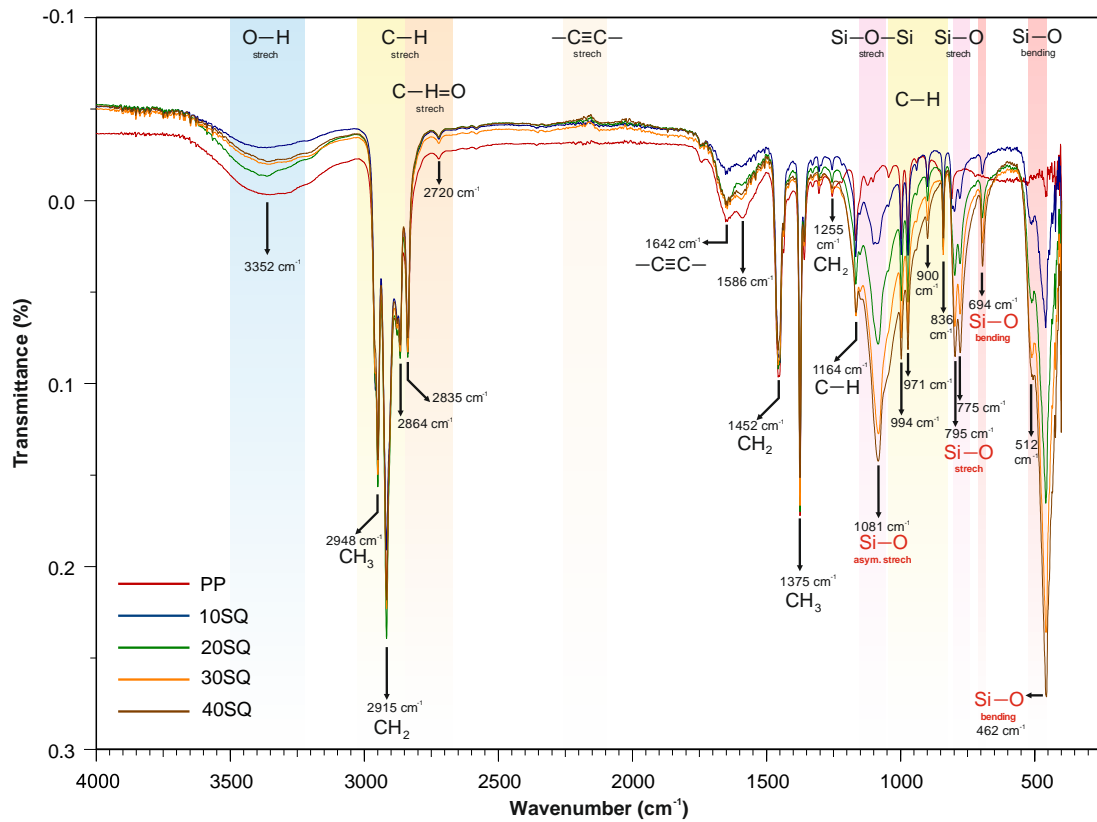
Figure 3.31 FTIR spectra of PP and SQ reinforced PP composites with various SQ powders weight fractions.

FTIR analysis results of PP based composite materials with modified quartz additive are given in Figure 3.32. In PP based composite materials containing 10% modified quartz by weight, it is found that new peaks are formed at wavelengths of 462, 694, 795 and 1081 cm^{-1} with the effect of added quartz. The FTIR spectrum shows a similar result compared to 10MQ sample with 10% unmodified MQ additive by weight.
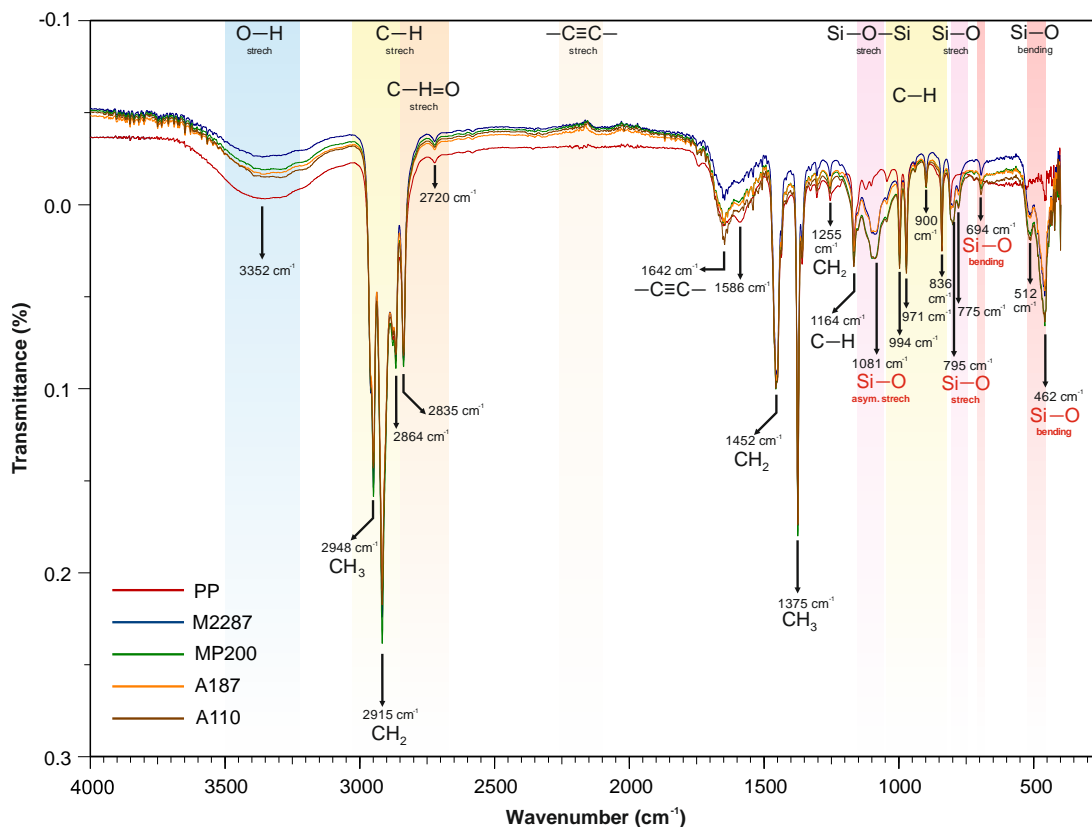
Figure 3.32 FTIR spectra of PP and modified MQ reinforced PP composites.

Table 3.10 FTIR spectra summary of all composite samples.

Wave number (cm⁻¹)	Vibration model	Assignment
462	Bending	Si—O
694	Bending	Si—O
795	Streching	Si—O
836	Rocking	C—H
971	Rocking	CH₃—
	Streching	C—C
994	Rocking	CH₃—
	Streching	C—C
1081	Asymmetrical streching	Si—O—Si
1164	Wagging	C—H
	Rocking	CH₃—
1375	Symmetrical bending	CH₃—
1452	Symmetrical bending	CH₂—
1642	Asymmetrical bending	C≡C
2864	Streching	C—H
2915	Asymmetrical streching	CH₂—
2948	Asymmetrical streching	CH₃—
3352	Streching	O—H

3.2.6 Scanning Electron Microscopy (SEM) Analysis

The morphology of the fracture surfaces of quartz-doped PP-based composites were investigated by SEM analysis. Between Figure 3.33-3.35, the images of all samples of composite at 1kX zoom from SEM analysis are given.

When the fracture surfaces obtained after the tensile test of MQ doped PP based composite materials given in Figure 3.33 are examined, MQ powders are observed in the matrix. The distribution of MQ powders in the matrix has a homogeneous structure. However, there are many small pores around the filling material, which can be seen from the figure, and it seems that the matrix/filling material interface compatibility is weak. When the rate of additives' amount increases, the homogeneous dispersion decreases. As the amount of filling material in the matrix increases, compatibility of the matrix/filling material interface weakens. As seen in Figure 3.33 (c), the formation of larger sizes of MQ particles on the fracture surface was observed with the addition of high amount of MQ into the PP matrix. As a result, the tensile strength of the composite decreased dramatically at high addition rates. At the same time, it is evaluated that the fracture surface of unmodified MQ additive composites has a more fragile compared to SQ and modified MQ additive samples, and PP breaks without exhibiting long elongation behavior. This is in agreement with the low percentage breaking elongation values taken during the tensile test.
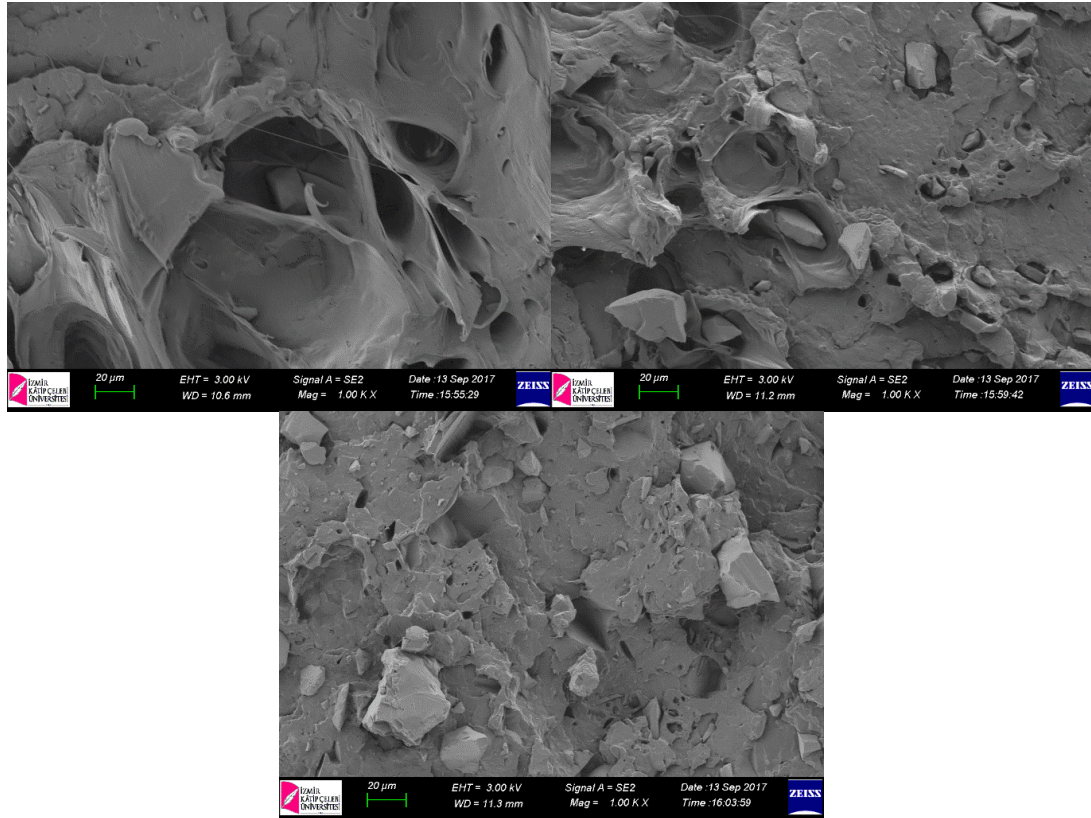
Figure 3.33 1kX SEM images of MQ-PP composites a) 10MQ, b) 20MQ, and c) 30MQ composites.

In Figure 3.34, SEM images obtained from the fracture surfaces of PP based composites with SQ additive are given. Composites with SQ additive are homogeneously distributed in the PP matrix. Although the interaction of the matrix/filling material is low, the interface interaction is better compared to the composites with MQ additive and as a result of this; it gave better results in the tensile strength test. Matrix/filling material interaction decreased as the amount of filling material in the composite increased. As a result of the weakening of the matrix / filling material interface compatibility, the transfer of the applied load from the matrix material to the filling material has decreased and this weakened the mechanical properties of the composite. When the fracture surfaces of composites are examined, a ductile fracture mechanism has been formed compared to MQ added composites. This confirms the percentage grab elongation values obtained in the tensile test.
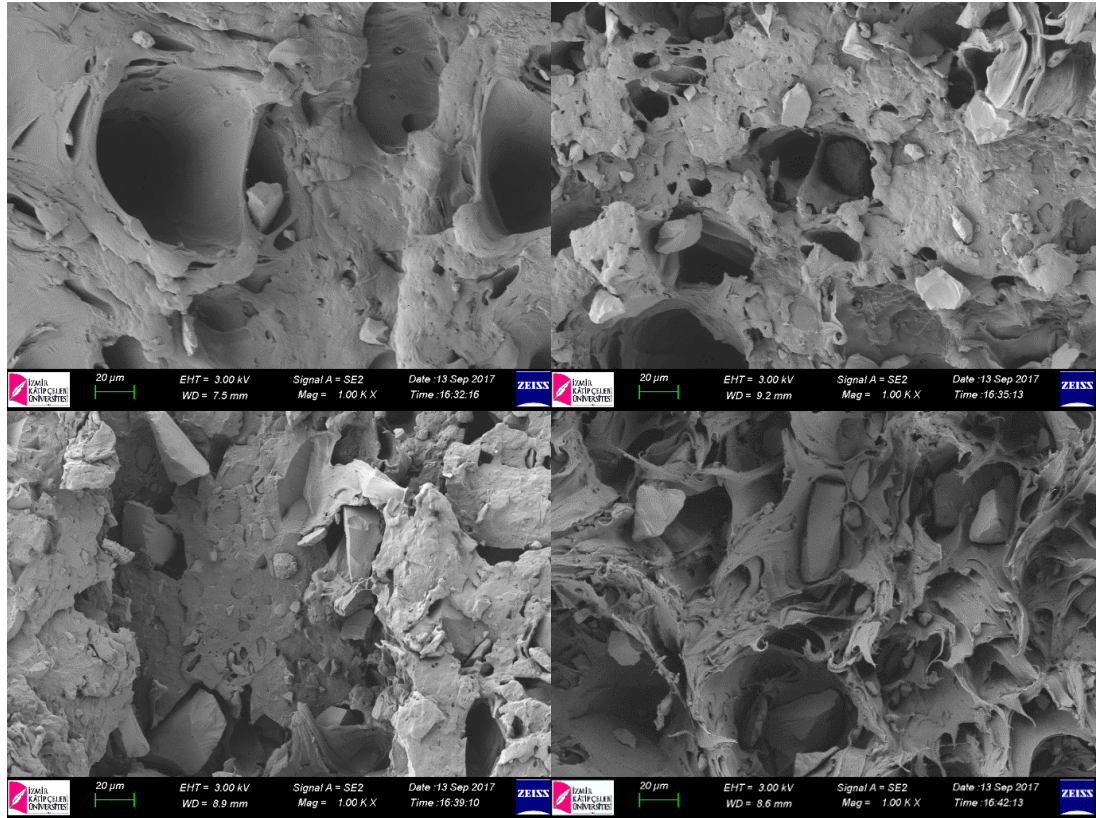
Figure 3.34 1kX SEM images of SQ-PP composites a) 10SQ, b) 20SQ, C) 30SQ, and D) 40SQ composites.

SEM images of MQ composites modified with four different surface modification agents are given in Figure 3.35. It is observed that MQ composites treated with different modification agents show different interface interactions. Especially in A110 sample, gap formation was significantly higher than the other three samples. Since the modification agents used have different functional groups, it is an expected situation that the PP/MQ composite system will exhibit different interface interactions. However, different interface interactions have been effective in generating different thermal conductivity results. The higher thermal conductivity values of the 2287 and A187 samples can be explained by the fact that there are different functional groups and as a result, the interfacial interaction occurs differently compared to the composite samples with MQ additive treated with two other modification agents. Compared to unmodified MQ additive samples, it is concluded that the interface interaction is higher. As a result, tensile strength and percentage elongation values of composites were higher than composites with MQ additives.
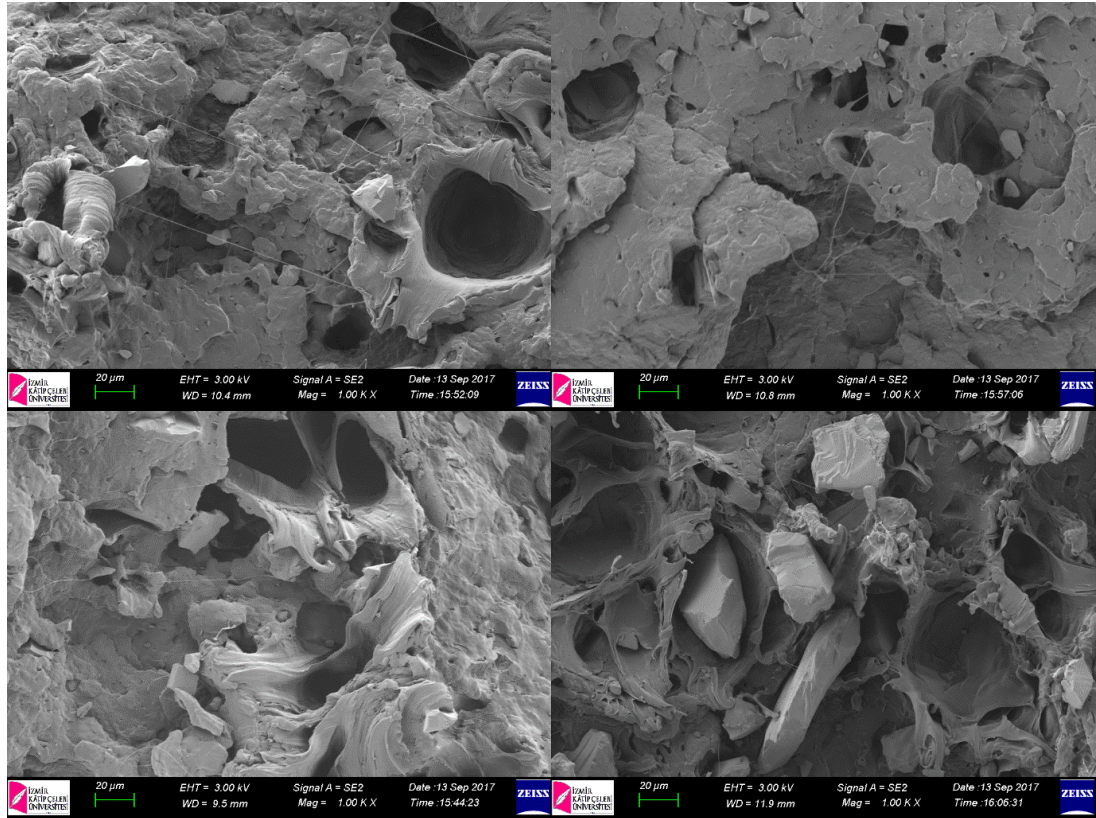
Figure 3.35 1kX SEM images of modified MQ-PP composites a) 2287, b) A187, c) MP200, and d) A110 composites.

4. CONCLUSION

In this thesis, the effect of quartz amount and surface modified quartz additive in the production of PP matrix composite material with micronized quartz powder was investigated. Changing mechanical, viscoelastic, physical and thermal properties in the composites produced were examined depending on both quartz amount and surface modification. The results obtained in the thesis study are discussed in three separate sections.

Effect of Surface Modification on Micronized Quartz Powders with Four Different Surface Coupling Agents

Micronized quartz powders have been modified with four different surface coupling agents under the same conditions. In the XPS analysis performed after the

modification, it was seen that the C1s peak intensity increased with the effect of the modification, and the intensity of the O1s and Si2p peaks decreased. Considering the results of the chemical analysis obtained from XPS analysis of unmodified MQ and modified MQ powders, it was observed that the amount of C increased with the modification effect. As a result, the O/C ratio was decreasing while the C/Si ratio was increasing. These values gave different results in different modification agents. The lowest O/C ratio and the highest C/Si ratio were obtained especially in MQ samples modified with MP200 modifying agent. It is confirmed from these results that different modification agents with different functional groups show different performance characteristics in MQ modification. With the XPS analysis, it is revealed that the modification process on the MQ surface has been successfully completed.

TGA results confirm the effect of surface modification on MQ powders as the amount of degradation. The degradation amount of the modified samples due to the temperature was higher than the samples without the modification. This is an expected result for the modifying agents that disintegrates with increasing temperature. Organic functional groups present in the modification agents were decomposed with increasing temperature and more mass loss was observed in these samples. The modification process did not cause a significant change in the degradation/temperature curve of the MQ powders.

It was seen from the XRD analysis in order to obtain information about the crystal structures of unmodified MQ and modified MQ samples that the modification did not affect the crystal structure of MQ. The XRD spectra of all powder samples appeared similar.

Changing morphological properties of MQ powders after modification were examined from the SEM analysis and the agglomeration decreased as a result of the development of the hydrophobic properties of MQ powders with the modification process.

According to the results obtained from the FTIR analysis, the interaction of MQ powders with the atmospheric environment has decreased and the amount of CO_2

absorption in MQ powders has decreased as a result of the changing surface properties with the modification.

The Effect of Quartz Amount on the Properties of Composite Material in PP Based Composite Materials

According to the analyzes made to determine the mechanical properties of PP based composite materials containing different proportions of MQ and commercial SQ, the tensile strength of the composite decreases with the increase in the amount of filling material. However, with the increase of filling material, the tensile modulus of the composite increases significantly.

When the mechanical properties of composites with MQ and SQ additives are compared, the most important difference is the difference of breaking elongation during the tensile test of composites. While the MQ added in PP decreases the breaking elongation of the composite, the SQ added in the PP increases the breaking elongation of the composite. In the silanized quartz doped composites, the increase in tensile elongation is caused by the effect of not only the physical interactions as in MQ doped samples but also other bonds formed between the matrix and the silane layer on the quartz surface. According to the bending test results, the bending strength of PP slightly increases after the addition of MQ and SQ. As the amount of filling material in the composite gets higher and higher, this increase decreases and the bending strength shows a decrease compared to the matrix under a particular matrix/filler material. The bending module increases with the increase the amount of the filling material in the matrix in both MQ and SQ doped samples.

According to the DMA results, the MQ and SQ that are added in the PP was increased the composite's storage module and loss module. This increase continues as the amount of additives in the composite increases. As a result of inhibition the movement of polymeric chains at increased temperatures by quartz filling materials, the high temperature storage module increases with an increase in the amount of filling material compared to PP matrix. As the temperature increases, the storage module values in all samples decrease due to better energy distribution. With MQ and SQ added to PP, the α-relaxation peak intensity increases because the composites exhibit more viscous dispersion properties than the polymer matrix. The same

amount of MQ and SQ added in PP caused the observation of similar effects on viscoelastic properties. Along with MQ and SQ additive, the tanδ value of the composites decreased. MQ and SQ added to PP have improved the viscoelastic properties of PP.

The degradation temperature and onset temperature of composites with MQ and SQ additives increase with the increase in the amount of additives. The reason for this increase may be due to the fact that the filling material exhibits a mass-carrying barrier behavior during the decomposition of PP with increasing temperature. The percentage of degraded weight is compatible with the matrix/filler ratios intended to be produced. When TGA results of composites with MQ and SQ additives are compared, they exhibit similar thermal stability properties.

According to the results of DSC analysis, MQ and SQ added to PP increased the crystallization temperature, crystallization enthalpy, melting enthalpy and crystallinity values, and decreased the melting temperature value. As the amount of MQ and SQ in PP increases, ΔH_C and ΔH_m values decrease. These values were lower than the values of matrix material in additives of 30% quartz and above. The X_C value rises rapidly with the amount of quartz added to the PP. This rise cannot be increased with the increase in quartz amount but remains stable. The increase in X_C is thought to be resulted from the change in the nucleation and mobility ratio of PP chains during the nucleation process.

With the MQ and SQ added to the PP, the thermal conductivity of the PP increases. Due to the high thermal conductivity of quartz with crystal structure, this increase continued as the amount of quartz added into PP increased. Although MQ and SQ added samples exhibit similar thermal conductivity results, in SQ added composites, thermal conductivity values increased a little more as a result of increased compatibility of matrix and filling material interfaces.

As a result of FTIR analysis, it was examined that the peaks arising from the vibrational movements of the Si—O bond corresponding to certain wavelengths with the effect of MQ and SQ powders added to the PP. As the amount of MQ and SQ in PP increases, the intensity of these peaks increases. FTIR spectra of MQ and SQ samples exhibit similar characteristics.

SEM results showed that MQ and SQ powders are homogeneously distributed in PP matrix. When the interface interaction between the matrix and filler materials is low, it results in poor matrix/filler interface compatibility. The surface chemical bonding structure of MQ powders does not have similar properties in order to achieve good interface compatibility with the PP matrix material. With the effect of the functional groups on the silanized quartz surface, SQ added samples exhibit improved matrix / filling material interface behavior than MQ added samples.

The Effect of Surface Modification of MQ Powders on Properties of PP Based Composite Material

The mechanical properties of PP-based composite materials with 10% by weight modified MQ additives are more advanced compared to unmodified MQ additive composite materials. Different performance occur between composite materials with the effect of different functional groups among the quartz added samples modified with different surface modification agents. Quartz samples modified with 3-glycidoxypropylmethyldiethoxysilane and 3-aminopropyltriethoxysilane showed better tensile strength properties. Tensile rupture elongation of composites with modified MQ additives was obtained higher than PP matrix material. Compared to unmodified MQ added samples, tensile rupture elongation of surface modified quartz added composites increases. Flexural strength and flexural modulus gave the best results in 3-glycidyl-oxypropyl-trimethoxy-silane modified MQ added composites.

Modified MQ added composites give better results on viscoelastic properties compared to unmodified MQ added composites. E′ and E″ values vary depending on the modification agent used in modified quartz doped samples. MQ composites modified with 3-glycidyl-oxypropyl-trimethoxy-silane (MP200) and 3-glycidoxypropylmethyldiethoxysilane (Coatosil 2287) were the best viscoelastic examples. Due to the interfacial compatibility of the matrix/filling material, the varying viscoelastic properties of the composite change significantly with the surface modification process.

Since the modification process does not cause a change in the crystal structure of quartz, the XRD spectrum should give similar results with unmodified MQ added composites. As a result of FTIR analysis, no new peak formation was observed in

modified MQ added composites. There is no significant change in FTIR analysis due to the modification agents, except for the peaks created by the vibrational movements of the various C—O and C—H bonds in the matrix material and the vibrational movements of the Si—O bond from the quartz additive.

TGA and DSC analyses showed that the thermal analysis of MQ and unmodified MQ added composites with the same amount of surface modification gave similar results. The modification process did not significantly affect the degradation behavior of PP-based composite materials against temperature. Thermal conductivity values differ significantly depending on the modification agent used. The transfer of the applied heat from the matrix to the filling material is faster as a result of the matrix/filling material interface compatibility developed with the modification proses. As a result, the thermal conductivity of composites has been improved significantly compared to unmodified MQ composites. MQ samples modified with 3-glycidoxypropylmethyldiethoxysilane and 3-aminopropyltriethoxysilane showed the highest thermal conductivity performance.

When the SEM analysis of MQ and MQ added composites is analyzed, the matrix/filling material interface interaction is low, but the improved filling material interface interaction behavior is displayed in composites with modified MQ additive.

With this study, the applicability of the surface coupling agent technique has been demonstrated in order to improve the mechanical, thermal and viscoelastic properties of the composite in quartz-added polymer based materials. At the same time, the feasibility of the practical and low cost composite material production technique, such as high speed thermo-kinetic mixer, which is an alternative to complex and costly composite production techniques, to make experimental studies on polymer based composite materials with hard particle additive has been validated.

REFERENCES

1. Raghavendra G, Kumar KA, Kumar MH, Kumar BR, Ojha S. Moisture absorption behavior and its effect on the mechanical properties of jute-reinforced epoxy composite. Polymer composites. 2017;38(3):516-522.
2. Agarwal G, Patnaik A, Sharma RK, Agarwal J. Effect of stacking sequence on physical, mechanical and tribological properties of glass–carbon hybrid composites. Friction. 2014;2(4):354-364
3. Jawaid M, Khalil HPSA, Bakar AA, Khanam P N. Chemical resistance, void content and tensile properties of oil palm/jute fibre reinforced polymer hybrid composites. Materials and Design. 2011;32:1014-1019.
4. Ornaghi HL, Bolner AS, Fiorio R, Zattera AJ, Amico SC. Mechanical and dynamic mechanical analysis of hybrid composites molded by resin transfer molding. Journal of applied polymer science. 2010;118(2): 887-896.
5. Chung DDL. Composite Materials: Science and Applications. Second Edition. New York: Springer;2010.
6. Yi XS, Du S, Zhang L. Composite Materials Engineering, Volume 1: Fundamentals of Composite Materials. China Mainland: Chemical Industry Press;2006.
7. Deniz ME. Kompozit malzemelerim üretim yöntemleri ve ısıl işlemle presleme tekniğini kullanarak kompozit malzeme üretecek bir düzeneğin tasarım ve imalatı: Harran Üniversitesi;2005.
8. Chung DDL. Composite Materials: Science and Applications. Functional Materials for Modern Technologies. Springer;2003
9. Mazumdar SK. Composites Manufacturing: Materials, Product and Process Engineering. New York: CRC Press LLC;2002.
10. Strong AB. Composites Manufacturing Fundamentals of Materials, Methods, and Applications. Second Edition. Michigan: Society of Manufacturing Engineers;2008.
11. Fidan S. Polimer matrisli kompozitlerin darbe davranışlarının İncelenmesi ve oluşan hasarların mikro tomografi yöntemiyle incelenmesi: Kocaeli Üniversitesi;2011.
12. Türkmen İ. Cam Elyaf Takviyeli Kompozit Malzemelerde Elyaf Tabaka Sayısına Bağlı Mekanik Özelliklerin ve Darbe Dayanımının İncelenmesi: Celal Bayar Üniversitesi;2012.
13. Hull D, Clyne T.W. An Introduction to Composite Materials. Second Edition.Cambridge Solid State Science Series;1996
14. Ekici E. Alüminyum matrisli B_4C takviyeli ve grafit katkılı kompozitlerin üretilmesi, mekanik özellikleri ve frezede işlenebilirliğinin incelenmesi: Gazi Üniversitesi;2012.

15. Peters ST. Handbook of Composites. Second edition. California: Thomson Science is a division of International Thomson Publishing;1998.
16. Baş. A. Plastik katkı maddelerinin, izotaktik polipropilen ahşap kompozitlerin yapı ve Özelliklerine Etkisi: Yalova Üniversitesi;2015.
17. Harris B. Engineering Composite Materials. London: The Institute of Materials;1999.
18. Chawla N, Chawla KK. Metal Matrix Composites. Springer;2006
19. Clyne TW and Hull D. An Introduction to Composite Materials. Third edition. New York: Cambridge University Press; 2016.
20. Low IM. Advances in Ceramic Matrix Composites. Woodhead Puplishing;2014
21. Department of Defense. Composite materials handbook: Volume 5. Ceramic matrix composites
22. Deborah DL. Chung. Composite Metarials. Second edition. NewYork: Springer;2010.
23. Deniz ME. Kompozit malzemelerin üretim yöntemler ve ısıl işlemle presleme tekniğini kullanarak kompozit malzeme üretecek bir düzeneğin tasarım ve imalatı: Harran Üniversitesi;2005.
24. Basutkar AG, Kolekar A. A review on properties and applications of ceramic matrix composites. International Journal of Research and Scientific Innovation (IJRSI). 2015;2(7):28-30.
25. Barut C. Aramid esaslı kompozit malzemelerin balistik performanslarının ve mekanik davranışlarının incelenmesi: Afyon Kocatepe Üniversitesi; 2015.
26. Pandya KS, Veerraju C, Naik NK. Hybrid composites made of carbon and glass woven fabrics under quasi-static loading. Materials and Design.2011;32: 4094-4099.
27. Das R. Polymeric Materials for Clean Water. Springer Series on Polymer and Composite Materials. Springer;2019
28. Ramdani N. Polymer and Ceramic Composite Materials. Emergent Properties and Applications. Taylor & Francis Group;2019
29. Friedrich K, Fakirov S, Zhang Z. Polymer Composites from Nano- to Macro-Scale. New York: Springer; 2005.
30. Sheikh-Ahmad JY. Machining of polymer composites. New York: Springer; 2009.
31. Karslı M. Hafif silahlar için polimer kompozit malzeme seçimi: Karadeniz Teknik Üniversitesi; 2016.
32. Hollaway L. Handbook of Polymer Composites for Engineers. First Published. Cambridge: Woodhead Publishing Ltd; 1994.
33. Biron M. Thermoplastics and Thermoplastic Composites: Technical Information for Plastics Users. Elsevier Science:2007.
34. Mallick PK. Materials, Design and Manufacturing for Lightweight Vehicles. First Published. Cambridge: Woodhead Publishing Limited;2010.
35. Matthews FL. Rawlings RD. Composite Materials: Engineering and Science. Cambridge: Woodhead Publishing Limited;1999.
36. Karian HG. Handbook of Polypropy1ene and Polypropylene Composıtes. Second Edition. New York: Marcel Dekker, Inc;2003.
37. Stewarta R, Goodship V, Guild F, Green M, Farrow J. Investigation and demonstration of the durability of air plasma pre-treatment on polypropylene

automotive bumpers. International Journal of Adhesion & Adhesives.2005;25: 93-99.

38. Hufenbach W, Böhm R, Thieme M, Winkler A, Mäder E, Rausch J, Schade M. Polypropylene/glass fibre 3D-textile reinforced composites for automotive applications. Materials and Design. 2011;32: 1468–1476.

39. Tos P, Artiaco S, Coppolino S, Conforti LG, Battiston B. A simple sterile polypropylene fingernail substitute. Chirurgie de la Main.2009; 28: 143–145.

40. Thomassin JM, Huynen I, Jerome R, Detrembleur C. Functionalized polypropylenes as efficient dispersing agents for carbon nanotubes in a polypropylene matrix; application to electromagnetic interference (EMI) absorber materials. Polymer.2010; 51: 115-121.

41. Mark HF. Encyclopedia of Polymer Science and Technology. Third Edition. Wiley. 2003

42. Tripathi D. Practical Guide to Polypropylene. First published. Shropshire: Rapra Technology Limited; 2002.

43. Svoboda P, Zeng C, Wang H, Lee LJ, Tomasko DL. Morphology and mechanical properties of polypropylene/ organoclay nanocomposites. Journal of Applied Polymer Science.2002;85: 1562-1570.

44. Yetgin SH. Otomotiv sektörü için polimer köpük malzeme üretimi ve karakterizasyonu: Sakarya Üniversitesi;2012.

45. Garcıa-Lopez D, Picazo O, Merino JC, Pastor JM. Polypropylene–clay nanocomposites: effect of compatibilizing agents on clay dispersion. European Polymer Journal.2003;39: 945-950.

46. Yaşar H. Plastikler Dünyası.2. Baskı. Ankara;2001.

47. Kauffman GB. Reinforced Plastics: Properties & Applications. California;1991.

48. Standard A. ASTM D1566-19 Standart Terminology Relating Rubber. ASTM International. West Conshohocken PA. 2019.

49. Kwei TK. Interfaces in polymer, ceramic, and metal matrix composites. Journal of polymer science: Part C: Polymer letters.1989;27:141-147.

50. Hull D. An Introduction to Composite Materials.First editon. Cambrige: Cambrige University Press;1981.

51. Wypych G. Handbook of Fıllers. 2nd Edition. New York: Plastics Design Library;2000.

52. Li Y, Fang QF, Yi ZG, Zheng K. A study of internal friction in polypropylene (PP)filled with nanometer-scale CaCO3 particles. Materials Science and Engineering.2004:A 370; 268-272.

53. Shah DU. Developing plant fibre composites for structural applications by optimising composite parameters: a critical review. Journal of Materials Science. 2013; 48: 6083-6107.

54. Wang RM, Zheng SR, Zheng YP. Polymer Matrix Composites And Technology. First published Cambridge:Woodhead Publishing Limited;2011.

55. Drzal LT, Rich MJ, Lloyd PF. Adhesion of graphite fibers to epoxy matrices: I. The role of fiber surface treatment. The Journal of Adhesion.1983;16(1): 1-30.

56. Bhushan B. The Mechanics and Materials Science. Ohio: CRC Press; 2000.

57. Patel VA, Bhuva BD, Parsania PH. Performance evaluation of treated–untreated jute–carbon and glass–carbon hybrid composites of bisphenol-c based mixed epoxy–phenolic resins. Journal of Reınforced Plastıcs and Composıtes.2009;28(20): 2549-2555.

58. Peterson AM, Jensen RE, Palmese GR. Thermoreversible and remendable glass–polymer interface for fiber-reinforced composites. Composites Science and Technology.2011;71: 586-592.
59. Kabir MM, Wang H, Lau KT, Cardona F. Chemical treatments on plant-based natural fibre reinforced polymer composites: An overview. Composites. 2012;Part B 43; 2883-2892.
60. Bledzki AK, Gassan J. Composites reinforced with cellulose based fibres. Prog. Polym. Sci. 1999; 24: 221-274.
61. Li X, Tabil LG, Panigrahi S. Chemical treatments of natural fiber for use in natural fiber-reinforced composites: A review. J Polym Environ.2007; 15: 25-33.
62. Mallick PK. Compsites Engineering Handbook. Michigan: Marcel Dekker, Inc;1997.
63. Baiardo M, Frisoni G, Scandola M,1 Licciardello A. Surface chemical modification of natural cellulose fibers. Journal of Applied Polymer Science.2002;83:38-45.
64. Kalia S, Kaith BS, Kaur I. Pretreatments of natural fibers and their application as reinforcing material in polymer composites—A review. Polymer Engineering And Science.2009;49(7):1253-1272.
65. Leonard Y, Mwaikambo, Ansell MP. Chemical modification of hemp, sisal, jute, and kapok fibers by alkalization. Journal of Applied Polymer Science.2002; 84: 2222-2234.
66. Suna RC, Tomkinsona J, Ma PL, Liang SF. Comparative study of hemicelluloses from rice straw by alkali and hydrogen peroxide treatments. Carbohydrate Polymers.2000;42 :111-122.
67. Tan MY, Kuan HTN, Meng Chuen Lee. Characterization of alkaline treatment and fiber content on the physical, thermal, and mechanical properties of ground coffee waste/oxobiodegradable hdpe biocomposites. International journal of polymer. Science. 2017; 3; 1-12.
68. Vilay V, Mariatti M, Taib RM, Todo M. Effect of fiber surface treatment and fiber loading on the properties of bagasse fiber–reinforced unsaturated polyester composites. Composites Science and Technology.2008;68;631-638.
69. Husa MS, Drzal LT, Mohanty AK, Misra M. Effect of chemical modifications of the pineapple leaf fiber surfaces on the interfacial and mechanical properties of laminated biocomposites. Composite Interfaces.2008; 15; 169-191.
70. Goda K, Sreekala MS, Gomes A, Kaji T, Ohgi J. Improvement of plant based natural fibers for toughening green composites—Effect of load application during mercerization of ramie fibers. Composites: Part A.2006; 37; 2213–2220
71. Liu W, Mohanty AK, Askeland P, Drzal LT, Misra M. Influence of fiber surface treatment on properties of Indian grass fiber reinforced soy protein based biocomposites. Polymer.2004; 45: 7589-7596.
72. Ray D, Sarkar BK, Rana AK, Bose NR. The mechanical properties of vinylester resin matrix composites reinforced with alkali-treated jute fibres. Composites: Part A.2001;119-127.
73. Holmberg KV, Abdolhosseini M, Li Y, Chen X, Gorr S U. Conrado aparicio bio-inspired stable antimicrobial peptide coatings for dental applications. Acta Biomaterialia.2013;9: 8224-8231.

74. Bonhomme C, Monredon SD, Ribot F, Babonneau F. Covalent grafting of organoalkoxysilanes on silica surfaces in water-rich medium as evidenced by ^{29}Si NMR. J Sol-Gel Sci Technol.2009;50:152-157.
75. Capobianco JA, Shih WY, Shih WH. 3-mercaptopropyltrimethoxysilane as insulating coating and surface for protein immobilization for piezoelectric microcantilever sensors. Review of Scientific Instruments. 2007;78: 46106.
76. Revzin A, Russell RJ, Yadavalli VK, Koh WG, Deister C, Hile DD, Mellott MB, Pishko MV. Fabrication of poly (ethylene glycol) hydrogel microstructures using photolithography. Langmuir. 2001;17: 5440-5447.
77. Li H, Wang R, Hu H, Liu W. Surface modification of self-healing poly(urea-formaldehyde) microcapsules using silane-coupling agent. Applied Surface Science .2008;255:1894-1900.
78. Mittal KL. Silanes and Other Coupling Agents.Volume 5. Boston:CRC Press; 2009.
79. Plueddemann EP. Silane Coup-ling Agents. Second edition. New York: Springer;1991.
80. Hermanson GT. Bıoconjugate Technıques.Third edition. London: Elsevier;2013.
81. Ahmed W. Jackson MJ. Emerging Nanotechnologies for Manufacturing. Second Edition. Oxford: Elsevier;2009.
82. Chen GX, Kim HS, Kim ES, Yoon JS. Compatibilization-like effect of reactive organoclay on the poly(L-lactide)/poly(butylene succinate) blends. Polymer.2005;46:11829-11836.
83. Kole S, Santra R, Bhowmick AK. Studies of in-situ compatibilized blend of silicone and EPDM rubbers. Rubber Chemistry and Technology.1994; 67 (1); 119–128.
84. Zhang W, Yan W, Pan R, Guo W, Wu G. Synthesis of silane-grafted ethylene vinyl acetate copolymer and ıts application to compatibilize the blend of ethylene- propylene-diene copolymer and silicone rubber. Polymer Engineering And Science.2018;58(5):719-728.
85. Demir T, Tinçer T. Preparation and characterization of poly(ethylene terephthalate) powder-filled high-density polyethylene in the presence of silane coupling agents. Journal of Applied Polymer Science.2001;79:827-835.
86. Oyman ZO, Tinçer T. Melt blending of poly(ethylene terephthalate) with polypropylene in the presence of silane coupling agent. Journal of Applied Polymer Science. 2003; 89; 1039-1048.
87. Shieh YT, Chuang HC. DSC and DMA studies on silane-grafted and water-crosslinked LDPE/LLDPE blends. Journal of Applied Polymer Science.2001; 81: 1808-1816.
88. Gan Q, Qi R; Zhang J, Yu J, Huang S. Preparation of high-performance polyethylene via a novel processing method of combining dynamic vulcanization with a silane-grafted water-crosslinking technique. Journal of Applied Polymer Science.2011;119:2539-2548.
89. Nachtigall SMB, Felix AHO, Mauler RS. Blend compatibilizers based on silane- and maleic anhydride–modified polyolefins. Journal of Applied Polymer Science.2003;88:2492-2498.
90. Zhang A, Wang Y, Zhuang C. Discussion the effect on ımproving granite bituminous mixture performance by adding coupling agent. Applied Mechanics and Materials.2012;204-208: 4115-4118.

91. Min Y, Fang Y, Huang X, Zhu Y, Li W, Yuan J, Tan L, Wang S, Wu Z. Surface modification of basalt with silane coupling agent on asphaltmixture moisture damage. Applied Surface Science.2015;346:497-502.

92. Xie J, Wu S, Pang L, Lin J, Zhu Z. Influence of surface treated fly ash with coupling agent on asphalt mixture moisture damage. Construction and Building Materials.2012;30:340-346.

93. Matinlinna JP, Lassila L, Vallittu PK. The effect of three silane coupling agents and their blends with a cross-linker silane on bonding a bis-GMA resin to silicatized titanium (A novel silane system). Journal of Dentistry.2006; 34 (10): 740-746.

94. Liu XM, Thomason JL, Jones FR. The Concentration of Hydroxyl Groups on Glas Surfaces and their Effect on the Structure of Silane Deposits. University of Sheffield.2009.

95. Shui M. Polymer surface modification and characterization of particulate calcium carbonate fillers. Applied Surface Science.2003; 220: 359-366.

96. Grate JW, Warner MG, Pittman JW, Dehoff KJ, Wietsma TW, Zhang C, Oostrom M. Silane modification of glass and silica surfaces to obtain equally oil-wet surfaces in glass-covered silicon micromodel applications. Water Resources Research.2013;49:4724–4729.

97. Nath DCD, Bandyopadhyay S, Gupta S, Yua A, Blackburn D, White C. Surface-coated fly ash used as filler in biodegradable poly(vinyl alcohol) composite films: Part 1—The modification process. Applied Surface Science. 2010;256:2759-2763.

98. Demir H, Balköse D, Ülkü S. Influence of surface modification of fillers and polymer on flammability and tensile behaviour of polypropylene-composites. Polymer Degradation and Stability.2006;91:1079-1085.

99. Sang J, Aisawa S, Miura K, Hirahara H, Jan O, Jozef P, Pavol M. Adhesion of carbon steel and natural rubber by functionalized silane coupling agents. International Journal of Adhesion & Adhesives.2017;72:70-74.

100. Yan H, Yuanhao W, Hongxingc Y. TEOS/silane-coupling agent composed double layers structure: a novel super-hydrophilic surface. Energy Procedia.2015;75:349-354.

101. Chuang W, Geng-sheng J, Lei P, Bao-lin Z, Ke-zhi L, Jun-long W. Influences of surface modification of nano-silica by silane coupling agents on the thermal and frictional properties of cyanate ester resin. Results in Physics.2018;9:886-896.

102. Jiang J, Cao J, Wang W, Xue J. How silanization influences aggregation and moisture sorption behaviours of silanized silica: analysis of porosity and multilayer moisture adsorption. Royal Society Open Science.2018;5(6):1-11.

103. Bravaya NM, Saratovskikh SL, Panin AN, Faingold EE, Zharkov IV, Babkina ON, Vasil'ev SG, Bubnova ML, Volkov VI, Lobanov MV. Influence of silane coupling agent on the synthesis and properties of nanocomposites obtained via in situ catalytic copolymerization of ethylene and propylene in the presence of modified Nafen™ Al2O3 nanofibers. Polymer.2019;174:114-122.

104. Qi Y, Luo Q, Shen J, Zheng L, Zhou J. Chen W. Surface modification of BMN particles with silane coupling agent for composites with PTFE. Applied Surface Science. 2017;414:147-152.

105.   Komagata Y, Ikeda H, Fujio Y, Nagamatsu Y, Shimizu H. Surface modification of feldspar porcelain by corona discharge and its effect on bonding to resin cement with silane coupling agent. Journal of The Mechanical Behavior of Biomedical Materials. 2020;105:1-9.

106.   Zheng N, He J, Zhao D, Huang Y, Gao J, Mai YW. Improvement of atomic oxygen erosion resistance of carbon fiber and carbon fiber/epoxy composite interface with a silane coupling agent. Materials & Design.2016;109:171-178.

107.   Min Y, Fang Y, Huang X, Zhu Y, Li W, Yuan J, Tan L, Wang S, Wu Z. Surface modification of basalt with silane coupling agent on asphaltmixture moisture damage. Applied Surface Science.2015;346:497-502.

108.   Xu S, Zhang M, Li, SY, Zeng HY, Du JZ, Chen CR, Pan Y. Surface modification of phosphorus-containing hydrotalcite using rare-earth coupling agent and its application in polypropylene. Powder Technology.2019;342:555-561.

109.   Qiao B, Wang TJ, Gao H, Jin Y. High density silanization of nano-silica particles using γ-aminopropyltriethoxysilane (APTES). Applied Surface Science.2015; 351:646-654.

110.   Surya I, Ismail H, Azura AR. The comparison of alkanolamide and silane coupling agent on the properties of silica-filled natural rubber (SMR-L) compounds. Polymer Testing.2014;40: 24-32.

111.   Ifuku S, Yano H. Effect of a silane coupling agent on the mechanical properties of a microfibrillated cellulose composite. International Journal of Biological Macromolecules.2015;74: 428-432.

112.   Cheng G, Tong B, Tang Z, Yu X, Wang H, Ding G. Surface functionalization of coal powder with different couplingagents for potential applications in organic materials. Applied Surface Science.2014;313:954-960.

113.   Zhu BL, Zheng H, Wang J, Ma J, Wu J, Wu R. Tailoring of thermal and dielectric properties of LDPE-matrix composites by the volume fraction, density, and surface modification of hollow glass microsphere filler. Composites Part B.2014; 58:91-102.

114.   Lamastra FR, Mori S, Cherubini V, Scarselli M, Nanni F. A new green methodology for surface modification of diatomite filler in elastomers. Materials Chemistry and Physics.2017;194:253-260.

115.   Iyer KA, Torkelson JM. Importance of superior dispersion versus filler surface modification in producing robust polymer nanocomposites: The example of polypropylene/nanosilica hybrids. Polymer.2015; 68: 147-157.

116.   Liu Y, Guo L, Wang W, Sun Y, Wang H. Modifying wood veneer with silane coupling agent for decorating wood fiber/high-density polyethylene composite. Construction and Building Materials.2019;224:691-699.

117.   Fang L, ChangL, Guo W, Chen Y, Wang Z. Influence of silane surface modification of veneer on interfacialadhesion of wood–plastic plywood. Applied Surface Science.2014;288:682-689.

118.   Nishiyama N, Horie K. Hydrolysis and Condensation Mechanisms of a Silane Coupling Agent Studied by ^{13}C and ^{29}Si NMR. Journal of Applied Polymer Science.1987;34: 1619-1630.

119.   Wen Z, Xu C, Qian X, Zhang Y, Wang X, Song S, Dai M, Zhang C. A two-step carbon fiber surface treatment and its effect on the interfacial properties of

CF/EP composites: The electrochemical oxidation followed by grafting of silane coupling agent. Applied Surface Science. 2019;486:546-554.

120. Su X, Shi B. Effect of silane coupling agents with different non-hydrolytic groups on tensile modulus of composite PDMS crosslinked membranes. Reactive and Functional Polymers.2016;98:1-8.

121. Carrillo LQ, Boronat T, Montanes N, Balart R, Torres-Giner S. Injection-molded parts of fully bio-based polyamide 1010 strengthened with waste derived slate fibers pretreated with glycidyl- and amino-silane coupling agents. Polymer Testing.2019;77:1-10.

122. Karnati SR, Oldham D, Fini EH, Zhang L. Application of surface-modified silica nanoparticles with dual silane coupling agents in bitumen for performance enhancement. Construction and Building Materials.2020;244:1-9.

123. Gopakumar T, Pagé D. Compounding of nanocomposites by thermokinetic mixing. Journal of Applied Polymer Science. 2005; 96(5); 1557-1563.

124. Seki Y, Avci B, Uzun S, Kaya N, Atagur M, Sever K, Sarikanat M. The using of graphene nano-platelets for a better through-plane thermal conductivity for polypropylene. Polymer composites. 2019; 40 (52); 1320-1328.

125. Altay L, Atagur M, Akyuz O, Seki Y, Sen I, Sarikanat M, Sever K. Manufacturing of recycled carbon fiber reinforced polypropylene composites by high speed thermo- kinetic mixing for lightweight applications. Polymer composites. 2018; 39 (10); 3656-3665.

126. Standard A. ASTM D638-10 Standard test methods for tensile properties of plastics. ASTM International. West Conshohocken PA. 2010.

127. Standard A. ASTM D790-10 Standard Test Methods: Flexural properties of unreinforced and reinforced plastics and electrical insulating materials. ASTM International. West Conshohocken PA. 2010.

128. Kaya N. Manufacturing and characterization of thermal conductive polymeric composite materials. Izmır Katip Celebi Unıversity; 2018.

129. Kaya N, Atagur M, Akyuz O, Seki Y, Sarikanat M, Sutcu M, Sever K. Fabrication and characterization of olive pomace filled PP composites. Composites Part B: Engineering. 2018; 150; 277-283.

130. Standard Test Method for Thermal Endurance of Coating Powders Used for Integral Bus Bar Insulation Systems.

131. Pak SY, Kim HM, Kim SY, Youn JR. Synergistic improvement of thermal conductivity of thermoplastic composites with mixed boron nitride and multi-walled carbon nanotube fillers. Carbon.2012; 50(13); 4830-4838.

132. Shchukarev A, Rosenqvist J, Sjöberg S. XPS study of the silica–water interface. Journal of Electron Spectroscopy and Related Phenomena.2004; 137; 171–176.

133. Yang G, Ma H, Yu L, Zhang P. Preparation and characterization of layer-by-layer self-assembled polyelectrolyte multilayer films doped with surface-capped SiO2 nanoparticles. Journal of Colloid and Interface Science.2009; 333; 776–781.

134. Idrisa A, Mana Z, Mauluda AS, Bustamb MA, Mannan HF, Ahmed I. Investigation on particle properties and extent of functionalization of silica nanoparticles. Applied Surface Science.2020; 506; 144978.

135. Kumar GG, Karunagaran B, Nahm KS, Elizabeth RM. Nanometer sized silver particles embedded silica particles-spray method. Nanoscale Res Lett.2009; 4; 452–458.

136. Liu P, Liu W, Xue Q. In situ chemical oxidative graft polymerization of aniline from silica nanoparticles. Materials Chemistry and Physics.2004; 87; 109–113.

137. Kim S, Kim E, Kim S, Kim W. Surface modification of silica nanoparticles by UV-induced graft polymerization of methyl methacrylate. Journal of Colloid and Interface Science.2005; 292; 93–98.

138. Xiao Y, Zou H, Zhang L, Ye X, Han D. Surface modification of silica nanoparticles by a polyoxyethylene sorbitan and silane coupling agent to prepare high-performance rubber composites. Polymer Testing.2020; 81; 106195.

139. Yang G, Ma H, Yu L, Zhang P. Preparation and characterization of layer-by-layer self-assembled polyelectrolyte multilayer films doped with surface-capped SiO2 nanoparticles. Journal of Colloid and Interface Science. 2009; 333; 776–781.

140. Perruchot C, Khan MA, Kamitsi A, Armes SP, Watts JF, von Werne T, Patten TE. XPS characterisation of core–shell silica–polymer composite particles synthesised by atom transfer radical polymerisation in aqueous media. European Polymer Journal. 2004; 40; 2129–2141.

141. Khajehzadeh M, Moghadam M, Rahmaniasl S. Structural, spectroscopic characterization (UV–vis, FT–IR and NMR) and TGA, TEM, FE–SEM, NBO and FMO analysis for $(Pd^{II}–PNHC)_n@nSiO^2$. Journal of Molecular Structure.2020; 15; 127526.

142. Tabrizy VA, Denoyel R, Hamouda AA. Characterization of wettability alteration of calcite, quartz and kaolinite: Surface energy analysis. Colloids and Surfaces A: Physicochem. Eng. Aspects.2011; 384; 98– 108.

143. Karunadasa KSP, Manoratne CH, Pitawala HMTGA, Rajapakse RMG. The composition, unit cell parameters and microstructure of quartz during phase transformation from α to β as examined by in-situ high-temperature X-ray powder diffraction. Journal of Physics and Chemistry of Solids.2018; 117; 131–138.

144. Siriwardena S, Ismail H, Ishiaku US. A comparison of the mechanical properties and water absorption behavior of white rice husk ash and silica filled polypropylene composites. Journal of Reinforced Plastics and Composites.2003; 22 (18); 1645-1666.

145. Leong YW, Abu Bakar MB, Ishak ZAM, Ariffin A, Pukanszky B. Comparison of the mechanical properties and ınterfacial ınteractions between talc, kaolin, and calcium carbonate filled polypropylene composites. Journal of Applied Polymer Science. 2004; 91; 3315–3326.

146. Sever K, Metehan Atagür M, Melike Tunçalp M, Altay L, Seki Y, Sarıkanat M. The effect of pumice powder on mechanical and thermal properties of polypropylene. Journal of Thermoplastic Composite Materials. 2019; 32 (8); 1092-1106

147. Atagur M, Seki Y, Pasaoglu Y, Sever K, Seki Y, Sarikanat M, Altay M. Mechanical and thermal Properties of Carpinas betulus fiber filled polypropylene composites. Polymer Composites. 2020.

148. Sui G, Zhong WH, Fuqua MA, Ulven CA. Crystalline Structure and Properties of Carbon Nanofiber Composites Prepared by Melt Extrusion. Macromolecular Chenistry and Physics. 2007; 208 (17); 1928-1936.

149.   Q. Yuan a, Misra RDK. Impact fracture behavior of clay–reinforced polypropylene nanocomposites. Polymer. 2006; 47; 4421–4433.

150.   Thomas S, Joseph K, Malhotra SK, Goda K, Sreekala MS. Polymer Composites, Macro- and Microcomposites. Polymer Composites. 2012.

151.   Díezb -Gutiérrez S, Rodríguez- Pérez MA, De Saja JA, Velasco JI. Dynamic mechanical analysis of injection -moulded discs of polypropylene and untreated and silane -treated talc -filled polypropylene composites. Polymer.1999; 40; 5345-5353.

152.   Atagur M, Sarikanat M, Uysalman T, Polat O, Elbeyli IF, Seki Y, Sever K. Mechanical, thermal, and viscoelastic investigations on expanded perlite–filled high-density polyethylene composite. Journal of Elastomers & Plastics. 2018; 50 (8); 747-761

153.   Torres-Giner S, Montanes N, Boronat T, Quiles-Carrillo L, Balart R. Melt grafting of sepiolite nanoclay onto poly(3-hydroxybutyrate-co-4-hydroxybutyrate) by reactive extrusion with multi-functional epoxy-based styrene-acrylic oligomer. European Polymer Journal.2016; 84; 693-707.

154.   Selvakumar V, Manoharan N. Thermal properties of polypropylene/ montmorillonite nanocomposites. Indian Journal of Science and Technology.2014; 7 (7); 136–139.

155.   Ghanbari A, Heuzey MC, Carreau PF, Ton-ThaT MT. A novel approach to control thermal degradation of PET/organoclay nanocomposites and improve clay exfoliation. Polymer.2013; 54; 1361-1369.

156.   Uwa CA Sadiku ER, Jamiru T, Huan Z, Mpofu K, Hamam Y, Ibrahim ID, Ramatsetse B. Sustainable polypropylene nanocomposite for lightweight and low thermal conductivity application. Procedia Manufacturing. 2020;43:567–575

157.   Liu H, Gu S, Cao H, Li X, Li Y. A dense packing structure constructed by flake and spherical graphite: Simultaneously enhanced in-plane and through-plane thermal conductivity of polypropylene/graphite composites. Composites Communications. 2020;19:25–29

158.   Zhang N, Yu X, Pradhan A, Puppala AJ. Thermal conductivity of quartz sands by thermo-time domain reflectometry probe and model prediction. Journal of Materials in Civil Engineering. 2015;27(12):

159.   Burger N, Laachachi A, Ferriol M, Lutz M, Toniazzo V, Ruch D. Review of thermal conductivity in composites: Mechanisms, parameters and theory. Progress in Polymer Science. 2016;61:1-28

160.   Zhai S, Zhang P, Xian Y, Zeng J, Shi B. Effective thermal conductivity of polymer composites: Theoreticalmodels and simulation models. International Journal of Heat and Mass Transfer. 2018;117:358–374

161.   Nishino T, Matsumoto T, Nakamae K. Surface structure of isotactic polypropylene by X-ray diffraction. Polymer Engineering And Science. 2000;40(2):336-343

162.   Varga J. β-Modification of isotactic polypropylene: preparation, structure, processing, properties, and application. Journal of Macromolecular Science. Part B-Physics. 2002;41:1121-1171

163.   Favaro MM, Branciforti MC, Bretas RES. A X-ray study of β-phase and molecular orientation in nucleated and non-nucleated injection molded polypropylene resins. Materials Research. 2009;12(4):455-464

164. Hedrick SA, Chuang SSC. Temperature programmed decomposition of polypropylene: in situ FTIR coupled with mass spectroscopy study. Thermochimica Acta. 1998;315:159-168

165. Fang J, Zhang L, Sutton D, Wang X, Li T. Needleless melt-electrospinning of polypropylene nanofibres. Journal of Nanomaterials. 2012;2(3):1-9

166. Pang AL, Ismail H. Tensile Properties, Water Uptake, and Thermal Properties of Polypropylene/Waste Pulverized Tire/Kenaf (PP/WPT/KNF) Composites. BioResources. 2013;8(1):806-817

167. Vahur S, Teearu A, Peets P, Joosu L, Leito I. ATR-FT-IR spectral collection of conservation materials in the extended region of 4000-80 cm^{-1}. Anal Bioanal Chem. 2016;408:3373–3379

168. Farias TMB, Gennari RF, Chubaci JFD, Watanabe S. FTIR spectra and TL properties of quartz annealed at high temperatures. Physics Procedia. 2009;2:493–496

169. Dana JD. Manual of mineralogy. 21st Ed: John Wiley & Sons: USA;1993

170. Khan HM, Ehlermann DAE. Analysis of fading cgaracteristics of quartz sand as a dosimeter and in irradiation identification applications. Radiation Physics and Chemistry.1995;46: 1185-1187

171. Cadogan, PH. The Moon: Our Sister Planet: Cambridge University Press: New York; 1981

172. Cordani, UG. Sıgolo JB. Marte: Novas descobertas, Institute Astronomico e Geofisico – IAG/SP: Sao Paulo; 1997

173. [Evans RC. An introduction to Crystal Chemistry: Cambridge University Pres: Cambridge;1966

174. Paradysz RE, Smith WL. Crystal Controlled Oscillators for Radiation Environments. Radiation Effects. 1975: 26; 213-218

175. Lell E, Kriedl NJ, Hensler JR. Radiation effects in quartz , silica and glasses. Progress in Ceramic Science:1968;4: 3-40

176. Griscom DL. Defects and impurities in μ-quartz and fused silica. Pergammon: New York;1978: 232-252

177. Idriss H, Llorca J. Low Temperature Infrared Study of Carbon Monoxide Adsorption on Rh/CeO$_2$. Catalysts.2019;9(7):598

CURRICULUM VITAE

ORHAN AKYÜZ

Girne Street No:102 Apt:5 Karşıyaka / Izmir
GSM: (532) 732 35 72
orhanakyuz@yahoo.com

EDUCATION

PhD   Materials Science and Engineering, İzmir Katip Çelebi University
      2020
MS   Department of Physics, Celal Bayar University
      2012
BS   Physics , Celal Bayar University
      2010
High School Vali Erol Çakır High School
      2004

WORK EXPERIENCE

Er-Bakır Elektrolitik Bakır Mamulleri A.Ş.   05/2018   -
Present
R&D Strategy, Project Monitoring and Coordination Chief
Completing the R&D Center installation process, Creating the organizational
structure, Creating the distribution of personnel duties and instructions, Creating
R&D projects and distributing them to the Project Teams, Coordinating the projects,
Creating suggestions for enriching the technical content of the projects, Managing
the publication and patent processes, Providing training to R&D personnel on Project
writing and execution, Coordinating the application processes to national and
internationl incentive funds.

Batel Elektromekanik A.Ş. 01/2015 - 05/2018
Deputy Production Manager
Carrying out the management and management of production personnel, Coordinating continuous improvement activities, eliminating bottlenecks in production, Providing personnel training, Coordinating modernization digitalization studies, Preparing periodical technical and financial reports, Conducting 5S studies, Creating projects to support R&D department.

Dokuz Eylül University 01/2013 - 08/2013
Academician (contract employee)
Teaching of alternative current circuit analysis in Electronic Technology Program to formal and secondary education classes.

Thesis Study

PhD Thesis: Surface Modification of Micronized Quartz Powders and Investigation of Additives as Filling Material in Polymer Matrix Composite Materials, İzmir Katip Çelebi University.
Master's Thesis: Borading of 2365 and 2344 Steels by Plasma Electrolysis Technique and Investigation of Their Surface Properties, Celal Bayar University.

PUBLICATIONS

Articles Published in International Refereed Journal (SCI & SSCI)
1. **O. Akyuz,** N. Kaya, M. Can, S. Demic, "Mechanical Properties of Quartz-added PP Based Composites Produced by High Speed Thermo-Kinetic Mixer", Acta Physica Polonica A, Volume 135, 2019
2. M. Atagur, **O. Akyuz,** K. Sever, Y. Seki, M. O. Seydibeyoglu, A. Isbilir, M. Sarikanat, L. Altay," Investigation of Thermal and Mechanical Properties of Synthetic Graphite and Recycled Carbon Fiber Filled Polypropylene Composites", Materials Research Express, Volume 6, March 2019
3. N. Kaya, **O. Akyüz,** H. Bilgili, M. Can, Ş. Demiç, "Investigation of Alumina/Graphene Mixtures Thermal and Electrical Properties into Polypropylene (PP) Matrix Based Composites", Acta Physica Polonica A, Volume 135, 2019
4. N. Kaya, M. Atagur, **O. Akyuz,** Y. Seki, M. Sarikanat, M. Sutcu, M. O. Seydibeyoglu, K. Sever, "Fabrication and characterization of olive Pomace filled PP composites", Composites Part B: Engineering, Volume 150, Pages 277-283, 1 October 2018
5. L. Altay, M. Atagur, **O. Akyuz,** Y. Seki, I. Sen, M. Sarikanat, K. Sever, "Manufacturing of Recycled Carbon Fiber Reinforced Polypropylene Composites by High Speed Thermo-Kinetic Mixing for Light Weight Applications", Polymer Composites, Volume 39, Issue 10, Pages 3656-3665, October 2018

6. Y. Karabulut, A. Canimoglu, Z. Kotan, **O. Akyuz,** E. Ekdal, "Luminescence of Dysprosium Doped Strontium Aluminate Phosphors by Codoping With Manganese Ion", Journal of Alloys and Compounds, Volume 583, Pages 91-95, 15 January 2014

7. Y. Karabulut, M. Ayvacikli, A. Canimoglu, J. Garcia Guinea, Z. Kotan, E. Ekdal, **O. Akyuz,** N. Can "Synthesis and Luminescence Properties of Trivalent Rare Earth Element-Doped Calcium Stannate Phosphors", Spectroscopy Letters, Volume 47, Issue 8, Pages 630-641, September 2014

Articles Published in Other International Refereed Journals

1. **O. Akyüz,** Z. Tek**,** Mechanical Properties of Boronized 2365 Steel by Pulsed Plasma-Electrolysis Technique, Journal of Materials Science and Engineering B, 5 (1-2) (2015) 50-57 DOI:10.17265/2161-6221/2015.1-2.005

Papers Presented at International Scientific Meetings and Published in The Proceedings Book

1. **O. Akyüz,** C. Akçay, H. Göker, "Production of Copper-Nickel 7/0.18 mm Stranded Alloy Wires For Heating Applications" International European Conference on Mathematics, Engineering, Natural&Medical Sciences, 2019, Izmir/Turkey

2. **O. Akyüz,** E. Solakoğlu, S. Elbaşı, C. Göde, H. Göker, "Production of Copper-Silver Contact Wire for High Speed Railway Catenary Systems", International European Conference on Mathematics, Engineering, Natural&Medical Sciences, 2019, Izmir/Turkey

3. M. Atagür, **O. Akyüz,** K. Sever, Y. Altay, M.Ö. Seydibeyoğlu, et al., "The Effect of Hybrid Carbon Fillers on Thermal and Mechanical Properties of PP Based Composites", The 25th Annual İnternational Conference on Composites/Nanoengineering (ICCE-25), 2017, Rome/Italy

4. M. Sarikanat, L. Altay, M. Atagür, **O. Akyüz,** Y. Seki, Y. Aycan, et al., "Utilization of Agricultural Waste Fillers in Polypropylene Based Composites", The 25th Annual İnternational Conference on Composites/Nanoengineering (ICCE-25), 2017, Rome/Italy

5. N. Kaya, **O. Akyüz**, M. Can, Ş. Demiç, "Investigation Of Thermal Conductivity And Mechanical Properties of Three Different Particles Sized 50% Silicon Carbide (SiC) Loaded Polypropylene (PP) Matrix Based Composites", 5th International Polymeric Composites Symposium and Workshops, 2017, Izmir/Turkey

6. **O. Akyuz**, N. Kaya, "Wear Behavior of Cold Sprayed Bronze Coating", 16th International Materials Syposium-IMSP, 2016, Denizli/Turkey

7. N. Kaya, M. Atagür, **O. Akyuz**, M. Sarikanat, Y. Seki, K. Sever, "Mechanical and Thermal Analysis of Different Ratios of Vermiculite-PP Composites" 16th International Materials Symposium-IMSP, 2016, Denizli/Turkey

8. K. Sever, **O. Akyuz**, M. Atagür, N. Kaya, Y. Seki, M. Sarıkanat, "Investigation of Mechanical Properties of Diatomite Filled Polypropylene Composites", 6th International Conference on Materials Science and Technologies, 2016, Bükreş/Romanya

9. N. Kaya, M. Atagur, **O. Akyuz**, Y. Seki, M. Sarikanat, Ö. Seydibeyoğlu, M. Sütçü and K. Sever, "Viscoelastic and Mechanical Properties of Olive Pomace Filled Polypropylene (PP) Composites" 3rd Thermophysical and Mechanical Properties of Advanced Materials –THERMAM, 2016, Izmir/Turkey

10. S. Dündar, **O. Akyüz,** "Titanium and Titanium Alloys Production via PTA Process" International Conference On Welding Technologies And Exhibition-ICWET, 2016, Gaziantep/Turkey

11. **O. Akyüz**, Z. Tek, "Boriding of 2344 Steel by Pulsed Plasma Electrolysis Technique" International Conference On Welding Technologies And Exhibition-ICWET, 2014, Manisa/Turkey

12. **O. Akyüz,** "Coating of Iron Boron Based Composites Powders By Using Portable Cold Spray Technique" 15th International Materials Syposium-IMSP, 2014, Denizli/Turkey

13. **O. Akyüz,** Z. Tek, "Characterization of 2365 Steel by Pulsed Plasma-Electrolysis Boronizing" 2nd International Advances in Applied Physics & Materials Science – APMAS, 2012, Antalya/Turkey

Papers Published in The Abstract Book of International Scientific Book
1. **O. Akyüz,** Ö. Tokdemir, H. Göker, "Production of Copper – Magnesium Alloy Messenger Wire For High Speed Railway Catenary Systems" 2nd Interntaional Conference on Technology and Science Techno-Science, 2019, Burdur/Turkey

2. **O. Akyüz,** G. Baykent, H. Göker, "Production of Copper – Magnesium Alloy Contact Wire For High Speed Railway Catenary Systems" 2nd Interntaional Conference on Technology and Science Techno-Science, 2019, Burdur/Turkey

CONGRESS- SYMPOSIUM- WORKSHOPS- SEMINARS
1. International European Conference on Mathematics, Engineering, Natural&Medical Sciences
2. 2nd Interntaional Conference on Technology and Science Techno-Science

3. International Advanced in Applied Physics & Materials Science Congress and Exhibiton
4. 16th International Materials Symposium IMSP'2016
5. 15th International Materials Symposium IMSP'2014

6. International Conference on Welding Technologies and Exhibition

7. International Advanced in Applied Physics & Materials Science Congress

8. Lümidoz-VI6. Lüminesans Dozimetre Kongresi

9. İzmir Yüksek Enerji Fiziği ve Uygulamaları Çalıştayı

10. Ege Üniversitesi Gateway Öğrenci Topluluğu 4. Teknoloji Zirvesi

11. Ege Üniversitesi Gateway Öğrenci Topluluğu ve Human Resources Management İzmir
12. Ege Üniversitesi Gateway Öğrenci Topluluğu Matematik-İstatistik-Fizik Oryantasyon Eğitimi
13. Ege Üniversitesi Gateway Öğrenci Topluluğu Bireysel Koçluk Eğitimi

PROJECTS (Grant Funded)

1. Yüksek Frekanslı Alternatif Akım Uygulamaları İçin Emaye Kaplı Bükülü İletken Demeti Üretimi, TÜBİTAK-TEYDEB, Project No: 3191038, 2019-, **Project Manager**
2. Aktif Brazing Yöntemi ile RMU'lar için 17,5kV Vakum Tüp Tasarımı ve Üretimi, TÜBİTAK-TEYDEB, Project No: 7150452, 2015- 2016, **Researcher**
3. SF6 Gazlı Harici Tip Yük Ayırıcısı Üretimi, KOSGEB Ar-Ge İnovasyon projesi, 2016-2017, **Project Staff**
4. Mineral Katkılı Termoplastik Kompozit Malzemelerin Üretilmesi ve Özelliklerinin İncelenmesi, Izmir Kâtip Çelebi University/Scientific Research Projects Coordinatorship, Project No: 2015-ÖDL-MÜMF-0002, 2015-2017, **Researcher**
5. Karbon Esaslı Dolgu Malzemeleri ile Termal İletken Polipropilen Kompozitlerin Üretimi ve Karakterizasyonu, Izmir Kâtip Çelebi University/Scientific Research Projects Coordinatorship, Project No: 2016-GAP-MÜMF- 0030, 2016- 2018, **Researcher**
6. New Concepts to Regenerate Worn AMC Component Surfaces by Coating and Machining, Chemnitz Teknoloji Üniversitesi-Almanya, Project No: SFB 692, 2015, **Guest Researcher**
7. PEEK Esaslı Biyopolimerin İmplant Yüzeylerine Alev Sprey ile Kaplanması, Izmir Kâtip Çelebi University/Scientific Research Projects Coordinatorship, Project No: 2013-2-FMBP-30, 2013-2016, **Researcher**
8. 2365 ile 2344 Çeliklerinin Plazma Elektroliz Tekniğiyle Borlanması ve Yüzey Özelliklerinin İncelenmesi, Yüksek Lisans Tez Projesi, Celal Bayar University/ Scientific Research Projects Coordinatorship, Project No: BAP-2011-40, 2011-2013, **Researcher**

ADDITIONAL COURSE- EDUCATION- CERTIFICATES

ISO/TS 22163 Standard Training   TÜV NORD
   2020
MSA/FMEA/SPC Training   TÜV NORD
   2020
Cost Reduction Techniques Training   Nova Akademi
   2019
ISO 19011 Internal Auditor Training   TÜV NORD
   2019
ISO 45001:2018 Information Training   TÜV NORD
   2019

OHSAS 18001-ISO 14001 Training 2019	Yalın Sigma Danışmanlık
ISO 9001 & IATF 16949 Training 2019	Yalın Sigma Danışmanlık
TEYDEB 2.0 Information Meeting 2018	İnvesta Global Danışmanlık
Ar-Ge Project Planing and Management 2018	Nova Akademi
Shimadzu LCMSMS Users Training 2016	Ant Teknik
Shimadzu XRD Users Training 2016	Ant Teknik
Shimadzu XRF Users Training 2016	Ant Teknik
Molecular and Atomic Spectroscopy Systems 2016	SEM Laboratuar Cihazları
Quality Control Training with Minitab 2015	İTÜ/Sürekli Eğitim Merkezi
Applied Entrepreneurship Training 2015	İzmir Katip Çelebi University
TA Q2000 DSC Users Training 2012	Likrom Analitik Çözümler
TA Q600 TGA/DSC Users Training 2012	Likrom Analitik Çözümler
TA DHR-3 Rheometer Users Training 2012	Likrom Analitik Çözümler

COMPUTER SKILLS

Paintshop, Origin, Gnuplot, Minitab: Good
Word, Excel, PowerPoint, Outlook: Good
SAP, NETSİS: Good

LANGUAGE SKILLS

English   Reading: Good; Writing: Good; Speaking: Good

SOCIAL ACTIVITIES

Sports, Cinema, Camping, Travel, Technology

REFERENCES

Halil Göker 4248151	Er-Bakır A.Ş.	Technical Group Manager (533)
Ceren Göde 5684555	Pamukkale Üniversitesi	Assoc. Prof. (533)
Murat Alparslan 5209501	Batel Elektromekanik	R&D Manager (533)

PERSONAL INFORMATION

Sex	**:** Male
Date of Birth	**:** 01/06/1987
Marital Status	**:** Single
Nationality	**:** T.C.
Driving Licence	**:** B (2008)
Military Service	**:** Completed